E-ISSN: 2148-6247

Turkish Journal of PHARMACEUTICAL SCIENCES

An Official Journal of the Turkish Pharmacists' Association, Academy of Pharmacy

Volume: 22 Issue: 6 December 2025

www.turkjps.org

Emerging Sources Citation Index · PubMed Central · PubMed · Scopus · TR Dizin

galenos Publishing House

Turkish Journal of
PHARMACEUTICAL SCIENCES

Turkish Journal of
PHARMACEUTICAL SCIENCES

Prof. Robert Rapoport, Ph.D.
ORCID: orcid.org/0000-0001-8554-1014
Cincinati University Faculty of Pharmacy, Department of Pharmacology and Cell Biophysics, Cincinati, USA
robertrapoport@gmail.com

Prof. Tayfun Uzbay, Ph.D.
ORCID: orcid.org/0000-0002-9784-5637
Üsküdar University Faculty of Medicine, Department of Medical Pharmacology, İstanbul, Türkiye
tayfun.uzbay@uskudar.edu.tr

Prof. Wolfgang Sadee, Ph.D.
ORCID: orcid.org/0000-0003-1894-6374
Ohio State University, Center for Pharmacogenomics, Ohio, USA
wolfgang.sadee@osumc.edu

Advisory Board

Turkish Journal of
PHARMACEUTICAL SCIENCES

Please refer to the journal's webpage (https://www.turkjps.org/) for "Editorial Policy" and "Instructions to Authors".

The editorial and publication process of the **Turkish Journal of Pharmaceutical Sciences** are shaped in accordance with the guidelines of ICMJE, WAME, CSE, COPE, EASE, and NISO. The Turkish Journal of Pharmaceutical Sciences is indexed in **PubMed, PubMed Central, Thomson Reuters / Emerging Sources Citation Index, Scopus, ULAKBİM, Türkiye Citation Index, Embase, EBSCO Host, Türk Medline, Cabi, CNK**I.

The journal is published online.

Owner: Turkish Pharmacists' Association, Academy of Pharmacy

Responsible Manager: Mesut Sancar

galenos yayınevi

Publisher Contact
Address: Molla Gürani Mah. Kaçamak Sk. No: 21/1
34093 İstanbul, Türkiye
Phone: +90 (530) 177 30 97
E-mail: info@galenos.com.tr/yayin@galenos.com.tr
Web: www.galenos.com.tr | **Publisher Certificate Number:** 14521

Publication Date: February 2026
E-ISSN: 2148-6247
International scientific journal published bimonthly.

Turkish Journal of
PHARMACEUTICAL SCIENCES

CONTENTS

Original Articles

Index

Turk J Pharm Sci 2025;22(6):357-366
DOI: 10.4274/tjps.galenos.2025.61168

ORIGINAL ARTICLE

Evaluation of Wound Healing Potential of (5-formylfuran-2-yl)Methyl Benzoates by *In Vitro* Cell Culture Studies

Mehmet KOCA[1], Fatma YEŞİLYURT[2], Hatice Şükran DURMAZ[1], Ahmet HACIMÜFTÜOĞLU[3], Neslihan ÇELEBİOĞLU[4]

[1]Atatürk University Faculty of Pharmacy, Department of Pharmaceutical Chemistry, Erzurum, Türkiye
[2]Atatürk University Health Services Vocational College, Erzurum, Türkiye
[3]Atatürk University Faculty of Medicine, Department of Medical Pharmacology, Erzurum, Türkiye
[4]Atatürk University Faculty of Science, Department of Organic Chemistry, Erzurum, Türkiye

ABSTRACT

Objectives: 5-hydroxymethylfurfural (5-HMF) derivatives, found in many natural products, exhibit various biological activities. Benzoate derivatives enhance cellular re-epithelialization without inducing cytotoxicity. This study aimed to evaluate the wound-healing potential of six benzoate derivatives of 5-HMF by usingan *in vitro* cell culture method.

Materials and Methods: Six ester derivatives of 5-HMF were synthesized, and the molecular structures were elucidated by proton-1 nuclear magnetic resonance, carbon-13 nuclear magnetic resonance, and Quadrupole time-of-flight mass spectrometry. The effects of the compounds on neuronal and fibroblast cell survival were determined *in vitro* using the 3-(4,5-dimethylthiazol-2-yl)-2,5-diphenyltetrazolium bromide (MTT) assay. The total oxidation state (TOS) and total antioxidant capacity (TAC) were measured spectrophotometrically. The effects of the lead compounds (M3 and M5) on fibroblast migratory potential were evaluated using a wound-healing scratch assay.

Results: The MTT test showed that M2, M3, M5, and M6 did not damage fibroblasts at any tested concentration (10^{-1} µM–10^{-2} µM). M3 and M5 increased fibroblast cell numbers at all tested concentrations ($p \leq 0.05$ to $p \leq 0.001$). It was observed that M2, M3, M5, and M6 at concentrations of 10^{-1} µM and 1 µM did not damage the neuronal cells. Also, M3 and M5 did not damage neuronal cells at 10 µM. M3 and M5 exhibited lower oxidant activity ($p \leq 0.001$) than other compounds in TOS tests, and showed higher antioxidant activity than other compounds in TAC tests. In the scratch test, the wound area in the M3 group was 72% on the first day and decreased to 32% on the second day ($p \leq 0.001$). On the other hand, in the M5 group, the wound area was 81% on the first day and decreased to 25% on the second day ($p \leq 0.001$).

Conclusion: M3 and M5 promote cell migration and have the highest potential for wound healing among the compounds tested.

Keywords: Ester derivatives of 5-hydroxymethylfurfural, cell viability assay, total antioxidant capacity, cell migration

INTRODUCTION

The skin acts as a barrier, protecting the body against assaults by external agents, such as chemicals, microorganisms, and physical insults. Therefore, a successful and short wound healing process is critical in practice.[1] Fibroblasts are critical for promoting normal wound healing, including the breakdown of the fibrin clot and the formation of collagen structures. Fibroblasts migrate to the skin wound and form granulation tissue.[2]

To understand the biological behavior of a substance, it is necessary to determine its toxic or non-toxic effects on cells. *In vitro* cytotoxicity assays are performed in cell culture to evaluate substances with drug-like properties or to investigate their toxic profiles.[3]

***Correspondence:** kocamehmet@atauni.edu.tr, **ORCID-ID:** orcid.org/0000-0002-8606-2039
Received: 23.07.2024, **Accepted:** 02.12.2025 **Publication Date:** 30.012026

Cite this article as: KOCA M, YEŞİLYURT F, DURMAZ HŞ, HACIMÜFTÜOĞLU A, ÇELEBİOĞLU N. Evaluation of wound healing potential of (5-formylfuran-2-yl)methyl benzoates by *in vitro* cell culture studies. Turk J Pharm Sci. 2025;22(6):357-366

Oxidative stress causes oxidative damage, which leads to tissue damage or delayed healing of damaged tissues.[4] Therefore, the total oxidation state (TOS) test is used to predict the oxidation potential of a compound in cells. Similarly, the total antioxidant capacity (TAC) test is used to assess the antioxidant potential of a compound within cells.[5]

5-hydroxymethylfurfural (5-HMF) (Figure 1) is an organic compound consisting of a furan ring with aldehyde and alcohol functional groups, and is formed from the dehydration of carbohydrates such as fructose, glucose, sucrose, cellulose, and inulin.[6] 5-HMF can be formed by the Maillard reaction when sugar-containing foods, such as honey, are heated under acidic conditions.[7] In addition, 5-HMF and its derivatives are found in many plant extracts.[8]

Some preclinical studies suggested that 5-HMF might be carcinogenic.[9] On the other hand, studies reveal aspects of 5-HMF and its derivatives that may benefit human health.[10] 5-HMF acts as an antioxidant,[11] protective against hypoxic injury,[12] anti-inflammatory,[13] tyrosinase inhibitor.[14] Antidiabetic, antiproliferative, antibacterial, antisickling, and analgesic properties of 5-HMF derivatives (ester, alkyl ether, and aryl ether) have been reported in the literature.[15-18]

Antioxidant, antifungal, antipsoriatic, and antithrombotic effects of salicylic acid and benzoic acid derivatives have been reported.[19,20] Benzoate derivatives have also been reported to improve cell re-epithelialization without cytotoxic effects.[21]

Wound healing is a complex biological process that involves hemostasis, inflammation, re-epithelialization, and tissue maturation, which are interconnected and occur sequentially. One of the most important factors affecting wound healing is oxidative stress.

This study aimed to evaluate the wound healing potential of 6 benzoate derivatives of 5-HMF by using the *in vitro* cell culture method. For this purpose, 5-HMF ester derivatives of nonsubstituted, 4-OCH3, 4-F, 4-F3C, 2-OH, and 4-CN benzoic acids were synthesized. Then, the wound-healing potential of these synthesized compounds was evaluated *in vitro* using MTT cytotoxicity tests in primary neurons and fibroblasts, and by TAC and TOS assays. In addition, the wound-healing capacities of the compounds on injured L929 fibroblasts were evaluated using an *in vitro* fibroblast migration assay.

MATERIALS AND METHODS

Chemistry

^{1}H and ^{13}C nuclear magnetic resonance (NMR) spectra were recorded on a Bruker FT-400 spectrometer (^{1}H: 400 MHz; ^{13}C: 100 MHz), using $CDCl_3$ as the solvent and tetramethyl silane as the internal standard. Coupling constants are given in hertz (Hz). Q-TOF LC-MS mass spectra were recorded on an Agilent 6530 Accurate-Mass instrument. The Melting points of the compounds were determined using an Electrothermal 9100 melting-point apparatus. All chemicals were obtained from Merck or Sigma-Aldrich.

General procedure for the synthesis of 5-HMF

One equivalent of D-fructose (3.6 g) was dissolved in dimethyl sulfoxide (DMSO) (40 mL) in a 100-mL glass bottle. After that, 0.1 equivalent of $FeCl_3{\cdot}H_2O$/activated charcoal (135 mg and 800 mg, respectively) was added to the mixture as the catalyst. The reaction mixture was heated at 90 °C in an oil bath with magnetic stirring for 5 h. Afterward, 80 mL of water was added, and the mixture was extracted three times with 30 mL portions of ethyl acetate. The organic layer was separated, and the solvent was evaporated. The product could be directly employed in the next step. Additionally, the residue was purified by column chromatography (4:1 petroleum ether/EtOAc) to obtain pure 5-HMF, completely separated from DMSO, as a brownish-yellow syrup (77% yield).[22]

General procedure for the synthesis of (5-formylfuran-2-yl) methyl benzoate derivatives

5-HMF (366 mg, 1 mmol) and benzoyl chloride derivatives (1.5 mmol) were dissolved in 8 mL of CH_2Cl_2. Afterward, the mixture was cooled to 0 °C, and trimethylamine (606 g, 2 mmol) was added slowly (Figure 1). The resultant reaction mixture was stirred at 0 °C for 30 min, then at room temperature for 15 h. Then the mixture was concentrated, extracted with CH_2Cl_2/H_2O, and the organic layer was dried over Na_2SO_4. The resultant crude oil was purified by silica gel column chromatography and eluted EtOAc/hexanes (6:4), yielding 80-93% (Figure 1).

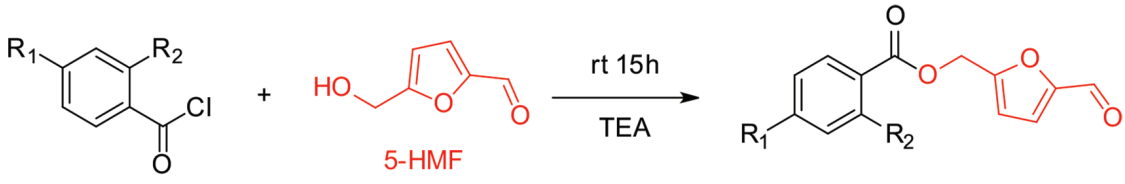

M1 (R_1:-H R_2:-H)
M2 (R_1:-OCH_3 R_2:-H)
M3 (R_1:-F R_2:-H)
M4 (R_1:-F_3C R_2:-H)
M5 (R_1:-H R_2:-OH)
M6 (R_1:-CN R_2:-H)
M7 (R_1:-H R_2:-$O(CO)CH_3$)

Figure 1. Synthesis of the target compounds
5-HMF: 5-hydroxymethylfurfural

(5-Formylfuran-2-yl)methyl benzoate (M1)

Yield: 80%, mp: 64-66 ˚C, White crystal.

^{1}H-NMR (400 MHz, $CDCl_3$) δ (ppm): 5.38 (s, 2H, CH_2), 6.68 (d, 1H, J:3.5 Hz, CH_{furan}), 7.24 (d, 1H, J:3.5 Hz, CH_{furan}), 7.45 (d, 2H, J:7.7 Hz, Ph-H), 7.58 (d, 1H, J:7.4 Hz, Ph-H), 8.34-7.85 (m, 2H, Ph-H), 9.65 (s, 1H, CHO). ^{13}C-NMR (100 MHz, $CDCl_3$) δ (ppm): 58.2, 112.84, 121.94, 128.50, 129.23, 129.84, 133.48, 152.85, 155.52, 165.94, 177.90. HRMS (Q-TOF) *m/z* Calcd for [M+H]+ 231.0579, found. 231.0651.

(5-Formylfuran-2-yl)methyl 4-methoxybenzoate (M2)

Yield: 78%, mp: 40-42 ˚C, Yellow crystal.

^{1}H-NMR (400 MHz, $CDCl_3$) δ (ppm): 3.86 (s, 3H, Ph-OCH_3), 5.35 (s, 2H, CH_2), 6.67 (d, 1H, J:3.5 Hz, CH_{furan}), 6.92 (d, 2H, J:8.9 Hz, Ph-H), 7.25 (d, 1H, J:3.5 Hz, CH_{furan}), 8.01 (d, 2H, J:8.9 Hz, Ph-H), 9.64 (s, 1H, CHO). ^{13}C-NMR (100 MHz, $CDCl_3$) δ (ppm): 58.48, 58.01, 112.70, 113.75, 121.54, 131.94, 152.78, 155.15, 155.92, 163.76, 165.73 177.98. HRMS (Q-TOF) *m/z* Calcd for [M+H]+ 261.0685, found. 261.0756.

(5-Formylfuran-2-yl)methyl 4-fluorobenzoate (M3)

Yield: 83%, Yellow liquid.

^{1}H-NMR (400 MHz, $CDCl_3$) δ (ppm): ^{1}H-NMR (400 MHz, $CDCl_3$) δ (ppm): 5.36 (s, 2H, CH_2), 6.67 (d, 1H, J:3.3 Hz, CH_{furan}), 7.10 (d, 2H, J:8.7 Hz, Ph-H), 7.23 (d, 1H, J:3.6 Hz, CH_{furan}), 8.0 (d, 2H, J:5.4 Hz, Ph-H), 9.64 (s, 1H, CHO). ^{13}C-NMR (100 MHz, $CDCl_3$) δ (ppm): 58.31, 112.91, 115.55, 115.8, 122.04, 125.51, 132.38, 132.48, 132.74, 132.84 152.87, 155.41, 164.98, 177.99. HRMS (Q-TOF) *m/z* for $[M+H]^+$, calculated: 249.0485, found: 249.0483.

(5-Formylfuran-2-yl)methyl 4-(trifluoromethyl)benzoate (M4)

Yield: 92%, mp: 79-81 ˚C, Yellow crystal.

^{1}H-NMR (400 MHz, $CDCl_3$) δ (ppm): 5.41 (s, 2H, CH_2), 6.71 (d, 1H, J:3.5 Hz, CH_{furan}), 7.25 (d, 1H, J:3.5 Hz, CH_{furan}), 7.71 (d, 2H, J:8.2 Hz, Ph-H), 8.17 (d, 2H, J: 8.1 Hz, Ph-H), 9.66 (s, 1H, CHO). ^{13}C-NMR (100 MHz, $CDCl_3$) δ (ppm): 58.61, 113.17, 121.83, 122.16, 124.87, 125.54, 125.51, 129.98, 130.26, 132.47, 154.86, 164.77, 177.88. HRMS (Q-TOF) *m/z* Calcd for [M+NH_4]+ 316.0791, found. 316.0791.

(5-Formylfuran-2-yl)methyl 2-hydroxybenzoate (M5)

Yield: 78%, mp: 67-69 ˚C, Yellow crystal.

^{1}H-NMR (400 MHz, $CDCl_3$) δ (ppm): 5.40 (s, 2H, CH_2), 6.71 (d, 1H, J:3.2 Hz, CH_{furan}), 6.88 (d, 1H, J:7.5 Hz, Ph-H), 6.98 (d, 1H, J:8.3 Hz, Ph-H), 7.25 (d, 2H, J: 3.3 Hz, Ph-H), 7.47 (d, 1H, J:7.6 Hz, Ph-H), 7.85 (d, 2H, J: 7.8 Hz, Ph-H), 9.66 (s, 1H, CHO), 10.53 (s, 1H, Ph-OH). ^{13}C-NMR (100 MHz, $CDCl_3$) δ (ppm): 58.31, 111.68, 113.29, 117.67, 119.39, 121.79, 130.09, 136.29, 152.99, 154.64, 161.78, 169.44, 177.92. HRMS (Q-TOF) *m/z* Calcd for [M+H]+ 247.0528, found. 247.0601.

(5-Formylfuran-2-yl)methyl 4-cyanobenzoate (M6)

Yield: 90%, mp: 91-93 ˚C, White crystal.

^{1}H-NMR (400 MHz, $CDCl_3$) δ (ppm): 5.43 (s, 2H, CH_2), 6.68 (d, 1H, J:3.6 Hz, CH_{furan}), 7.23 (d, 1H, J:3.2 Hz, CH_{furan}), 7.73 (d, 2H, J:8.7 Hz, Ph-H), 8.13 (d, 2H, J: 8.4 Hz, Ph-H), 9.63 (s, 1H, CHO). ^{13}C-NMR (100 M*Hz*, $CDCl_3$) δ (ppm): 58.79, 113.29, 116.85, 117.82, 121.78, 130.34, 132.31, 133.08, 153.04, 154.58, 164.34, 177.84. HRMS (Q-TOF) *m/z* Calcd for [M+Na]+ 278.0430, found. 278.0425.

Cell cultures

Since the compounds were dissolved in DMSO and applied in cell culture studies, DMSO was used as the control. The effects of doses of M1-M6 (0.1, 1, 10, and 100 µg/mL), which were identified as non-toxic in MTT tests on neuronal cell lines, were evaluated in other *in vitro* experiments (TAC, TOS, Cell Migration Test).

Primary neuron culture

Sprague-Dawley rat pups younger than 24 hours were used to obtain cortical and brain neurons. After the rats were swiftly decapitated, the excised cortices were transferred to 5 mL of Hanks' Balanced Salt solution; macro-fragmentation was performed with a scalpel, and microlysis was performed using trypsin-ethylenediaminetetraacetic acid (EDTA) (0.25% trypsin-0.02% EDTA). The cells were then centrifuged at 1200 rpm for 5 min. Fresh medium [88% Neurobasal medium, Gibco, USA, 10% fetal bovine serum (FBS, Gibco, USA), 2% B-27 supplement (ThermoFisher, Germany), 0.1% antibiotic (penicillin-streptomycin), and amphotericin B (Thermo Fisher, Germany)] was added to the cells that had settled to the bottom.[23]

L929 fibroblast culture

L929 mouse fibroblasts were obtained from the Medical Pharmacology Department, Atatürk University (Erzurum, Türkiye). Then, the cells were centrifuged at 1200 rpm for 5 min. The cells were suspended in fresh medium [89% Roswell Park Memorial Institute, 10% FBS, and 1% antibiotic (penicillin-streptomycin) and amphotericin B (ThermoFisher, Germany)]. They were grown in T-25 culture flasks until they reached 70-80% confluency. The prepared flasks were stored in an incubator with 5% CO_2 at 37 ˚C. When 80% of the flasks were covered by cells, the cells were removed from the flasks with trypsin-EDTA (0.25% trypsin-0.02% EDTA) and centrifuged. The supernatant was discarded, and the cell suspension was distributed homogeneously to 24-well tissue culture plates at 400 µL/well (40,000 cells/well). It was incubated at 5% CO_2 and 37 ˚C until the cells reached confluence.

Cell cultures MTT assay

The direct contact test was applied to determine the cytotoxicity of the materials. The evaluation was performed using the MTT reagent (Sigma Aldrich Inc., St. Louis, USA) containing 3-(4,5-dimethylthiazol-2-yl)-2,5-diphenyl tetrazolium bromide. To determine cytotoxicity by the MTT test, a mixture was prepared consisting of 1 mL of 5 mg/mL MTT solution in PBS. The outer surface was covered with aluminum foil and was kept in the refrigerator. After the culture media from the incubated cells were removed, the previously prepared samples were placed into each well and incubated again for 24 hours at 37 ˚C in a 5% CO_2 atmosphere. Thus, the cytotoxic effects of the materials were evaluated at the end of 24 hours. A total of 99.4 µL of the mixture containing DMSO, 0.6 mL HCl, and 10 g sodium lauryl sulphate was added to each well at 100 µL/well to dissolve

the formazan crystals formed following MTT application, and the plates were incubated again for 4 hours. After this process, the absorbance (optical density) was measured using a spectrophotometer (μQuant, Bad Friedrichshall, BioTek) at a wavelength of 570 nm. Data are presented graphically following SPSS analysis.[24]

TAC-TOS assay

The TOS and TAC were evaluated by spectrophotometric measurement. The cell culture medium was harvested when the experiment was complete. According to the manufacturing process, the TAC absorbance at 660 nm (Trolox equiv/mmol L-1) and the TOS absorbance at 530 nm (H_2O_2 equiv/mmol L-1) were evaluated.

At the end of the experiment, morphological changes were assessed using an inverted microscope (Leica, USA). Images of all treatment groups, exposed to the doses for the desired period, were taken at 20× magnification.

Inspections with an inverted microscope

In cell culture, the distance between wound edges in six randomly selected areas for each dose was measured in μm.

Statistical analysis

The results are presented as the mean ± standard error. Statistical comparisons between groups were calculated using one-way analysis of variance and Tukey's honestly significant difference method. All calculations were performed using SPSS version 20. $p<0.05$ and $p<0.001$ were considered statistically significant in all tests. To determine normality, the Shapiro-Wilk tests were used.

L929 cell line migration test

L929 fibroblast cells cultured in tissue culture plates had their medium renewed every three days until the cells in the wells reached 100% growth. When the desired density was achieved, wounds were created in the cell monolayers on tissue culture plates using a 100 μL pipette tip. The synthesized substances (M1-M6) were administered at concentrations of 0.1, 1, 10, and 100 μM. After the doses were administered, the experiment was terminated upon establishment of the first bridge in the wound.

Ethics

Ethics committee approval of the study was received from the Atatürk University Animal Experiments Local Ethics Committee (approval number: 49, dated: 26.02.2024) and Atatürk University Non-Interventional Research Ethics Committee (approval number: 120, dated: 29.03.2024).

RESULTS

According to the *in vitro* fibroblast MTT assay results (Figure 2), compound-treated groups exhibited higher viability rates (95-123%) than the control group ($p<0.001$). In particular, the group treated with compound M3 at 10 μM exhibited the highest viability compared with the control group ($p<0.001$).

The *in vitro* fibroblast TAC assay data for all compounds are summarized in Figure 3. The TAC levels of the compounds in fibroblast cell culture were 1.41-1.87 Trolox equivalents (mmol L-1). In particular, the groups treated with compounds M3 and M5 at 10 μM exhibited the highest antioxidant capacity compared with the control group ($p<0.001$).

The *in vitro* fibroblast TOS assay data for all compounds are summarized in Figure 4. The TOS level in the M3-treated group at 100 μM was significantly lower than that in the control group ($p<0.001$).

The *in vitro* neuronal MTT assay data for all compounds are summarized in Figure 5. In MTT tests, when the compounds were applied to neuronal cells at 0.1 μM, cell survival exceeded 90%. In MTT tests, when M1, M2, M4, and M6 were administered to neuronal cells at 10 μM, statistically significant toxic effects were observed (for M1, M2, M6 $p<0.05$ and for M4 $p<0.001$). Significant toxicity was observed only at 100 μM in the groups administered M3 and M5 ($p<0.001$).

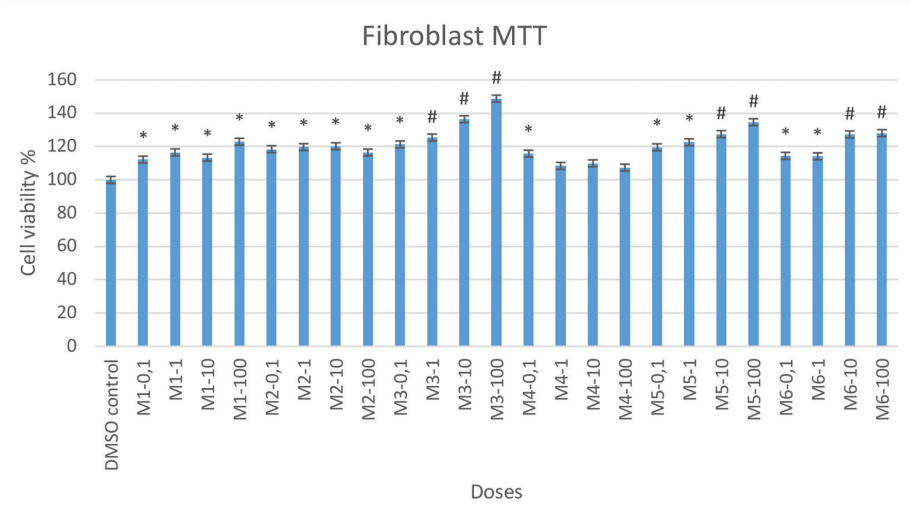

Figure 2. *In vitro* fibroblast MTT assay viability ratio of the groups (*$p<0.05$ and #$p<0.001$ compared to the control group)
DMSO: Dimethyl sulfoxide, MTT: 3-(4,5-dimethylthiazol-2-yl)-2,5-diphenyltetrazolium bromide

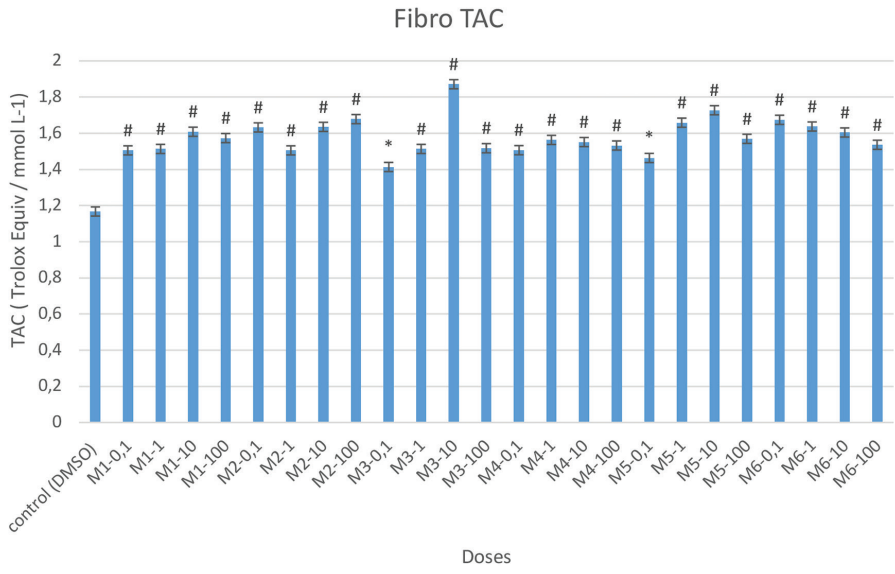

Figure 3. *In vitro* fibroblast TAC assay data (*p<0.05 and #p<0.001 compared to the control group)
DMSO: Dimethyl sulfoxide, TAC: Total antioxidant capacity

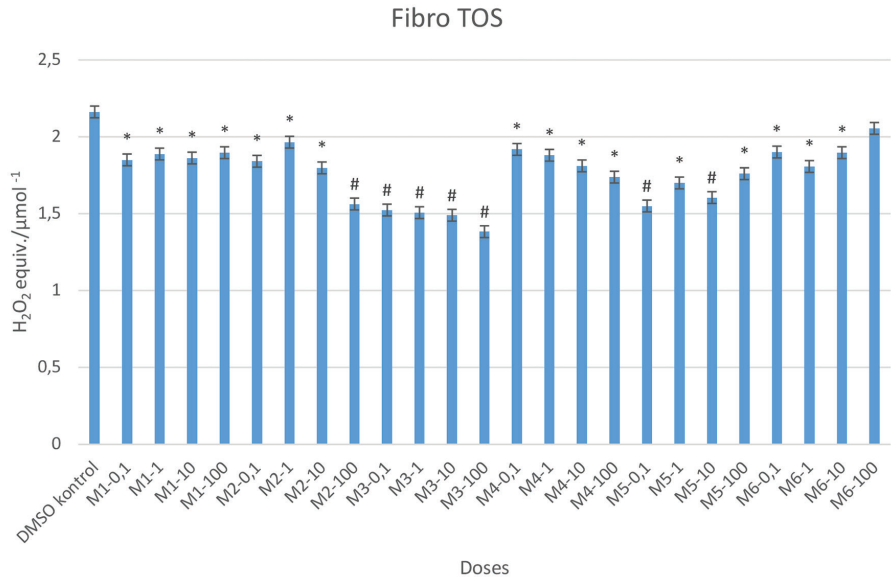

Figure 4. *In vitro* fibroblast TOS assay data (*p<0.05 and #p<0.001 compared to the control group)
DMSO: Dimethyl sulfoxide, TOS: Total oxidation state

The *in vitro* neuron TAC assay data for all compounds are summarized in Figure 6. TAC levels of compounds in neuronal cell cultures ranged from 0.66 to 2.44 Trolox equivalents (mmol L-1). In particular, the groups treated with compound M5 at concentrations of 0.1, 1, and 10 µM exhibited the highest antioxidant capacity compared to the control group (p<0.05).

The *in vitro* neuronal TOS assay data for all compounds are summarized in Figure 7. TOS levels of the compounds in neuronal cell culture were determined at a concentration of 0.1 µM and ranged between 0.79 and 1.45 H_2O_2 equivalent mmol L^{-1}. In particular, the group treated with compound M5 at 0.1 µM exhibited the lowest oxidant capacity compared with the control groups (p<0.001).

Based on TAC and TOS tests, among the compounds tested, the 4-F derivative (M3) and the 2-OH derivative (M5) were found to be the safest with respect to oxidative stress in neuronal cells in this study (Figures 3, 4, 5, and 7).

In this study, the effects of 5-HMF benzoates on wound healing were investigated at concentrations ranging from 0.1 to 100 µM. The cell migration test results for the control and the least cytotoxic compounds (M3 and M5) are summarized in Figures 8. Findings from inverted microscopy are summarized in Table 1. Statistically significant differences in wound closure were found between the groups.

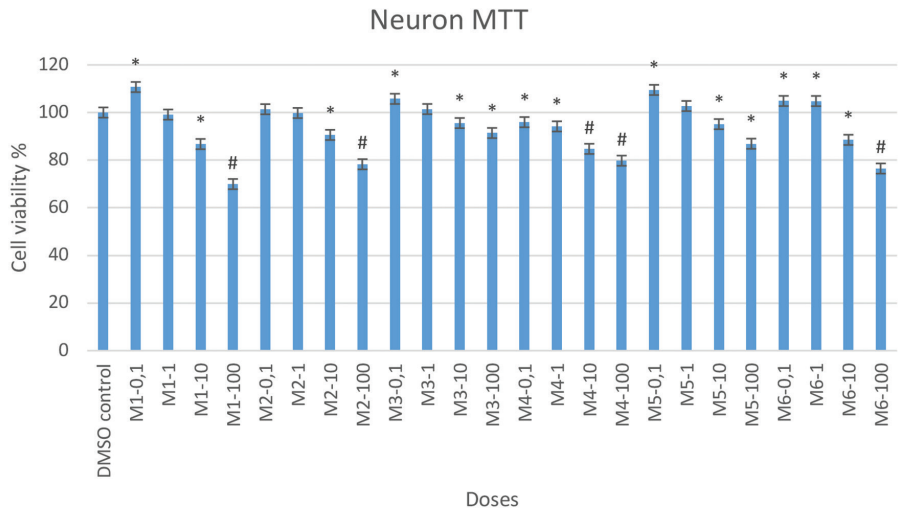

Figure 5. *In vitro* Neuron MTT assay viability ratio of the groups (*$p<0.05$ and #$p<0.001$ compared to the control group)
DMSO: Dimethyl sulfoxide, MTT: 3-(4,5-dimethylthiazol-2-yl)-2,5-diphenyltetrazolium bromide

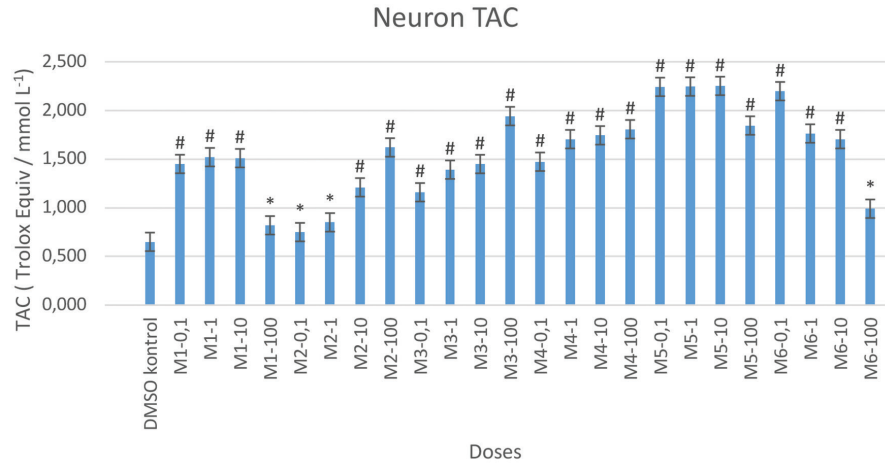

Figure 6. *In vitro* neuron TAC assay data (*$p<0.05$ and #$p<0.001$ compared to the control group)
DMSO: Dimethyl sulfoxide, TAC: Total antioxidant capacity

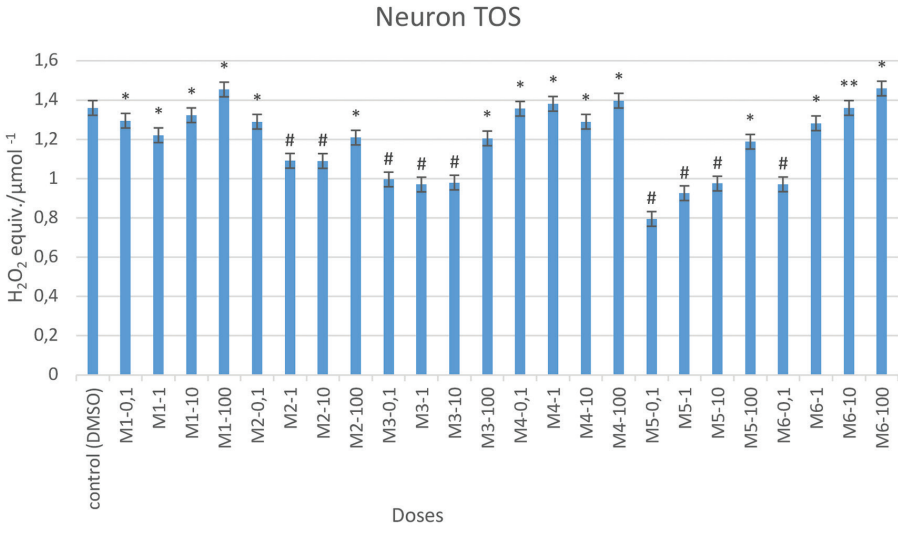

Figure 7. *In vitro* Neuron TOS assay data (*$p<0.05$ and #$p<0.001$ compared to the control group)
DMSO: Dimethyl sulfoxide, TOS: Total oxidation state

The best wound closure was achieved at a concentration of 10 μM, compared with applications of M3 and M5 across the 0.1-100 μM concentration range (Figure 8).

Table 1. Inverted microscopic findings

Groups	1st day	2nd day
Control	71.12±3.16^{a,A}	72.24±0.16^{a,A}
M3-0.1 μM	69.44±2.04^{a,A}	51.64±3.12^{b,B}
M3-1 μM	50.78±1.26^{b,A}	53.16±4.06^{b,A}
M3-10 μM	72.09±2.14^{a,A}	32.11±5.02^{c,B}
M3-100 μM	51.24±0.98^{b,A}	52.78±3.08^{b,A}
M5-0.1 μM	71.64±0.28^{a,A}	34.04±4.18^{b,B}
M5-1 μM	33.24±2.78^{b,A}	42.34±2.88^{c,b}
M5-10 μM	81.02±2.06^{c,A}	25.18±3.84^{d,B}
M5-100 μM	25.02±2.06^{d,A}	26.56±1.16^{d,A}

^{a,b,c}Shows the difference between groups in the same column (p<0.001), ^{A,B}Shows the difference between groups in the same row (p<0.001)

DISCUSSION

The first step of the reaction, the synthesis of 5-HMF, occurs at a moderate temperature in DMSO. DMSO is less toxic than other polar aprotic solvents such as dimethylformamide and dimethylacetamide.[25] The second step of the reaction (synthesis of the benzoate derivatives) occurs at room temperature in CH_2Cl_2. In summary, energy consumption in the reaction processes is low. In both cases, the products can be isolated with high yields and selectivity.

One strategy in drug development is to replace a hydrogen atom with a fluorine atom.[18,26] In drug modification, fluorine substitution changes the chemical and physical properties of the drug molecule, such as stability, solubility, molecular polarity, intramolecular hydrogen bonding, and charge-transfer capacity.[27] Thus, fluorine substitution in a drug molecule can influence pharmacokinetic, pharmacodynamic, and toxicological properties.[28] In this study, fibroblast viability was high in the group treated with the 4-fluoro derivative (M3). According to Figure 2, fibroblast viability increased as the M3 dose rose from 0.1 to 10 μM. Fibroblasts play an important role in wound healing, aggregating in the dermis at the wound margin to produce collagen.[29]

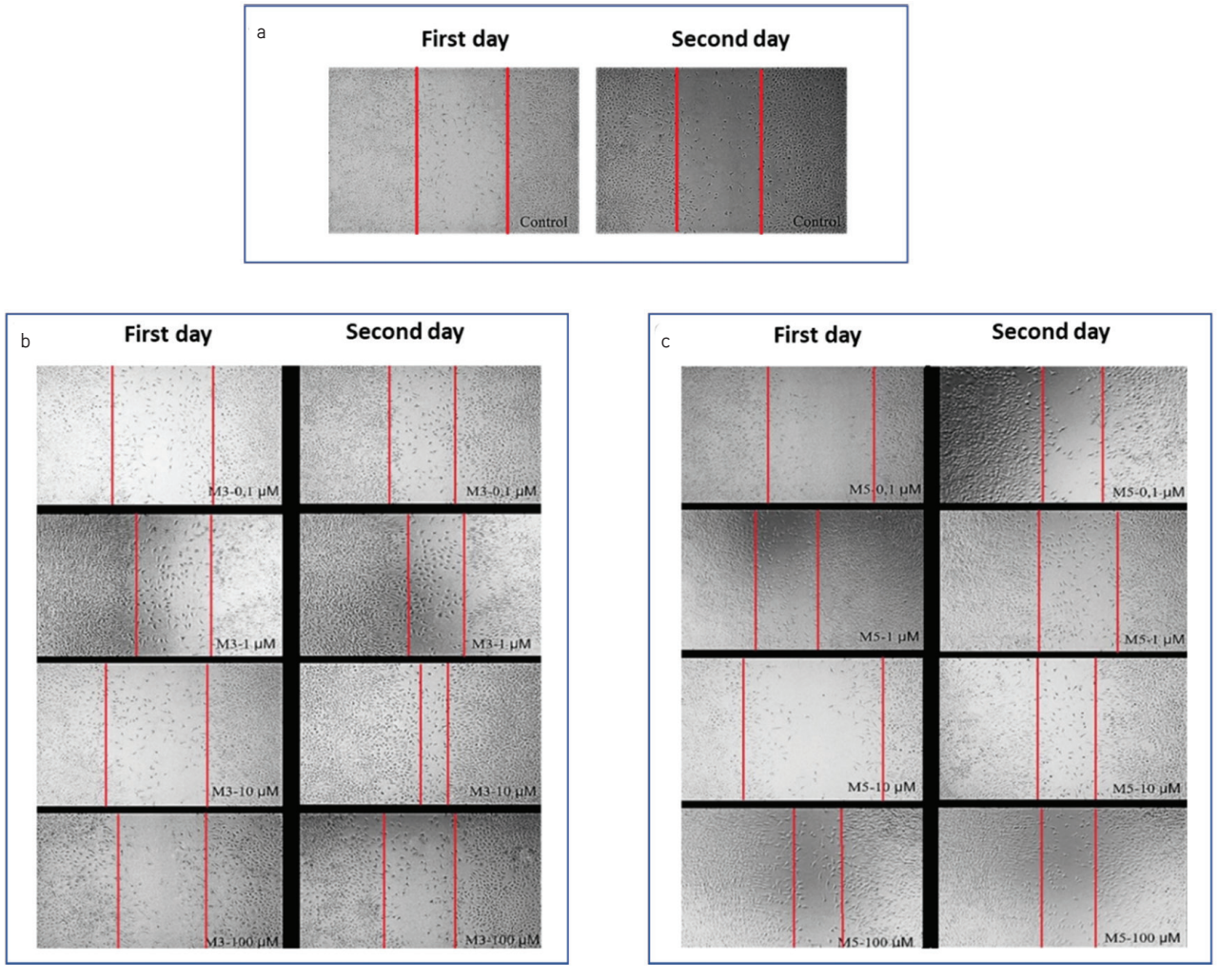

Figure 8. Cell migration test images of the groups (a) control, (b) M3 (0.1-100 μM)-treated, and (c) M5 (0.1-100 μM)-treated

A high TAC assay level and a low TOS assay level in cells indicate a safe oxidative-stress profile for the compound.[30] Among the benzoic acid derivatives (2-hydroxy, 3-hydroxy, 4-hydroxy, 2,6-dihydroxy, and 2,3-dihydroxy methyl benzoate) in the literature, the monohydroxybenzoic derivative with the hydroxyl group in the ortho position relative to the carboxylate group was found to exhibit the strongest antioxidant properties.[31] In this study, M5, a 2-hydroxybenzoate derivative, demonstrated notable antioxidant activity, as indicated by high TAC and low TOS levels.

One way to assess compound toxicity is to conduct *in vitro* studies using cells or cell lines.[32] The importance and popularity of *in vitro* experiments have increased because they are more frequently used prior to *in vivo* studies and because *in vitro* technology saves both time and money. Reproducible and reliable analyses from *in vitro* experiments can be obtained more easily and inexpensively than from *in vivo* experiments.[33] The central nervous system innervates all body regions, including cutaneous structures. Therefore, dermatological studies need to evaluate, during the early stages of drug development, whether a drug candidate damages neurons.[34] Damage to neuronal cells reduces fibroblast proliferation; therefore, synthesized molecules should both increase fibroblast numbers to promote wound healing and avoid damaging neuronal cells. Neuropathic ulcers are often observed in diabetic patients. In diabetic patients, Insulin resistance and hyperglycemia are associated with increased production of reactive oxygen species and elevated oxidative stress.[35] Increased oxidative stress in cells leads to inflammation in tissues. Inflammation in tissues also leads to dysfunction in nerve cells. Treatment of both the underlying cause of neuropathy and the ulceration is important in the management of neuropathic ulcers.[36] In this study, the groups treated with the compound exhibited higher viability of neuronal cell cultures than the control groups ($p<0.001$). According to the *in vitro* neuronal MTT test results in Figure 5, the compounds did not show cytotoxicity in neuronal cell cultures at concentrations of 0.1 and 1 µM. A reduction in cell viability was observed in neurons treated with M1 (non-substituted), M2 (4-CH_3), M4 (4-Cl), and M6 (4-CN) at 10 µM concentration, whereas no significant toxic effect was observed in neurons treated with M3 and M5 at 10 µM concentration.

In the literature, the wound-healing potential of benzyl benzoate derivatives has been evaluated using anti-inflammatory assays *in vitro* and *in vivo*, as well as with *in vivo* excision wound models. In the related study, it was reported that benzyl benzoate derivatives inhibited albumin denaturation and COX-2, and promoted wound healing more rapidly than the standard compound (nitrofurazone).[37]

Cell migration tests help assess the wound healing potential of compounds.[38] The wound healing assay is easily performed for small molecule screening[39] and drug discovery.[40] In this study, the cell migration results for the M3- and M5-treated groups were consistent with the MTT, TAC, and TOS assay results. *In vitro* cell migration assays show that the wound-healing process is accelerated as the migration rate and number of fibroblasts migrating into the scratched area increase.[41] In this study, M3 and M5 had a strong effect on both viability and wound healing at a concentration of 10 µM.

The findings obtained in this study demonstrate that compounds M3 and M5 have the potential to promote wound healing. However, to more comprehensively assess the efficacy of these compounds, it is crucial to conduct comparative studies against reference substances with well-established wound-healing effects reported in the literature. Agents such as allantoin, dexpanthenol, and silver sulfadiazine are widely used as reference compounds whose wound-healing effects have been demonstrated in both clinical and experimental studies. Comparison of compounds M3 and M5 with such references will enable further studies, particularly *in vivo* animal models, to demonstrate their therapeutic value more clearly. In this respect, our study lays the foundation for future comprehensive preclinical evaluations.

CONCLUSION

According to the MTT results, compounds M3 (4-fluoro derivative) and M5 (2-hydroxy derivative) stand out for their ability to increase cell viability. The study focused on M3 and M5 compounds because fibroblast viability was higher in the M3-treated group, whereas neuronal viability was higher in the M5-treated group. M3 and M5 did not increase oxidative stress in the TAC and TOS tests. As a result, M3 and M5 promote cell migration and have the highest potential for wound healing among the compounds tested. In further studies, the albumin-denaturation and COX-2-inhibition potentials of 5-HMF benzoates can be investigated. Secondly, the wound-healing potential of these derivatives can be investigated using *in vivo* diabetic wound models. Furthermore, nanotechnology-oriented strategies facilitate the delivery of drugs to the target site with accurate concentrations and release patterns, and often serve as bioactive carriers and therapeutic agents for the treatment of severe wounds. Therefore, in further studies, nano-formulations of M3 and M5 compounds can be prepared, and their wound-healing properties can be studied in diabetic wound models.

Ethics

Ethics Committee Approval: Ethics committee approval of the study was received from the Atatürk University Animal Experiments Local Ethics Committee (approval number: 49, dated: 26.02.2024) and Atatürk University Non-Interventional Research Ethics Committee (approval number: 120, dated: 29.03.2024).

Informed Consent: Not required.

Acknowledgements

I thank Prof. Dr. Hasan Seçen for supporting this study with laboratory facilities, knowledge, and experience. The dataset can be provided by the corresponding author.

Footnotes

Authorship Contributions

Surgical and Medical Practices: F.Y., H.Ş.D., Concept: M.K., A.H., Design: M.K., A.H., Data Collection or Processing: M.K., F.Y., H.Ş.D., Analysis or Interpretation: M.K., F.Y., H.Ş.D., A.H., N.Ç., Literature Search: M.K., Writing: M.K.

Conflict of Interest: The authors declare no conflicts of interest.

Financial Disclosure: The authors declared that this study received no financial support.

REFERENCES

1. Mani S. Wound healing and its importance: a review. Der Pharmacia Sinica. 2014;1:24.
2. Wilkinson H, Hardman M. Wound healing: cellular mechanisms and pathological outcomes. Open Biol. 2020;10:200223-200237.
3. Tokur O, Aksoy A. *In vitro* sitotoksisite testleri. Harran Univ Vet Fak Derg. 2017;6:112-118.
4. Wei J, Wang B, Wang H, Chen L, Li J, Ren F. Radiation-induced normal tissue damage: oxidative stress and epigenetic mechanisms. Oxid Med Cell Longev. 2019;2019:3010342.
5. Wu R, Feng J, Yang Y, Zhang H, Wang Y, Ye L. Significance of serum total oxidant/antioxidant status in patients with colorectal cancer. PLoS One. 2017;12:e0170003-e0170003.
6. Rosatella A, Simeonov S, Frade R, Afonso C. 5-Hydroxymethylfurfural (HMF) as a building block platform: biological properties, synthesis and synthetic applications. Green Chem. 2011;13:754-793.
7. Shapla UM, Solayman M, Alam N, Khalil MI, Gan SH. 5-Hydroxymethylfurfural (HMF) levels in honey and other food products: effects on bees and human health. Chem Cent J. 2018;12:35.
8. Arockiamary NAS, Vijayalakshmi VK. Chromatographic separation of bioactive compounds from Ipomoea batatas Lam (sweet potatoes) by column, high-performance thin layer chromatography, and gas chromatography–mass spectrum analysis techniques. Asian J Pharm Clin Res. 2014;7:4-8.
9. Svendsen C, Husøy T, Glatt H, Haugen M, Alexander J. 5-Sulfooxymethylfurfural (SMF), the metabolite of 5-hydroxymethylfurfural (HMF), increases the numbers of adenoma and aberrant crypt foci in the intestine of Min-mice. Toxicol Lett. 2007;172:S202.
10. Choudhary A, Kumar V, Kumar S, Majid I, Aggarwal P, Suri S. 5-Hydroxymethylfurfural (HMF) formation, occurrence and potential health concerns: recent developments. Toxin Rev. 2021;40:545-561.
11. Li YX, Li Y, Zhong-Ji Q, Kim MM, Kim SK. *In vitro* antioxidant activity of 5-HMF isolated from marine red alga Laurencia undulata in free radical mediated oxidative systems. J Microbiol Biotechnol. 2009;19:1319-1327.
12. Li MM, Wu LY, Zhao T, Chen GQ, Zhang L, Xu Y. The protective role of 5-HMF against hypoxic injury. Cell Stress Chaperones. 2011;16:267-273.
13. Kong F, Lee BH, Wei K. 5-Hydroxymethylfurfural mitigates lipopolysaccharide-stimulated inflammation via suppression of MAPK, NF-κB and mTOR activation in RAW 264.7 cells. Molecules. 2019;24:275.
14. Kang HS, Choi JH, Cho WK, Park JC, Choi JS. A sphingolipid and tyrosinase inhibitors from the fruiting body of Phellinus linteus. Arch Pharm Res. 2004;27:742-750.
15. Hong Won S, Soon Sung I, PSH S. 5-Membered heterocyclic derivative, preparation method therefor and pharmaceutical composition comprising same. KR2014003733W. 2016;10-30.
16. Xu GG, Pagare PP, Ghatge MS, Karthikeyan R, Mutalik S, Sangamwar A. Design, synthesis, and biological evaluation of ester and ether derivatives of antisickling agent 5-HMF for the treatment of sickle cell disease. Mol Pharm. 2017;14:3499-3511.
17. Phutdhawong W, Inpang S, Taechowisan T, Phutdhawong W. Synthesis and biological activity studies of methyl-5-(hydroxymethyl)-2-furan carboxylate and derivatives. Orient J Chem. 2019;35:1080-1085.
18. El-Naggar ME, Abdelgawad AM, Shaheen TI, El-Kholy SA, Hashem MM, Elsherbiny DA. Viable approach for preventing skin wound infections using bioactive dressing films from chitosan–furfural/α-aminophosphonate nanocomposite. Int J Biol Macromol. 2025;306:141731.
19. Amborabé BE, Fleurat-Lessard P, Chollet JF, Roblin G. Antifungal effects of salicylic acid and other benzoic acid derivatives towards Eutypa lata: structure–activity relationship. Plant Physiol Biochem. 2002;40:1051-1060.
20. Ngo T, Kim K, Bian Y, Lee Y, Park J, Kim S. Antithrombotic effect of SP-8008, a benzoic acid derivative, through the selective inhibition of shear stress–induced platelet aggregation. Br J Pharmacol. 2020;177:929-944.
21. El-Zawawy NA, Ali SS, Khalil MA, Sun J, Nouh HS. Exploring the potential of benzoic acid derived from the endophytic fungus strain Neurospora crassa SSN01 as a promising antimicrobial agent in wound healing. Microbiol Res. 2022;262:127108.
22. Ding Z, Luo X, Ma Y, Zhao X, Liang J, Zhang Y. Eco-friendly synthesis of 5-hydroxymethylfurfural (HMF) and its application to the Ferrier-rearrangement reaction. J Carbohydr Chem. 2018;37:1-13.
23. Kamalak H, Kamalak A, Taghizadehghalehjoughi A, Hacimuftuoglu A, Nalci KA. Cytotoxic and biological effects of bulk-fill composites on rat cortical neuron cells. Odontology. 2018;106:377-388.
24. Gundogdu G, Nalci KA, Ugur Kaplan AB, Demirel G, Ozkan A, Karaman M. Evaluation of the effects of nanoemulsion formulations containing boron and/or zinc on wound healing in diabetic rats. Int J Low Extrem Wounds. 2020;21:492-501.
25. Sheldon RA. The greening of solvents: towards sustainable organic synthesis. Curr Opin Green Sustain Chem. 2019;18:13-19.
26. Strunecka A, Patocka J, Connett P. Fluorine in medicine. J Appl Biomed. 2004;2:141-150.
27. Zhang Y, Dou D, Gu W. Fluorinated-antioxidant derivatives with improved pharmacological activity: a theoretical study. J Biomol Struct Dyn. 2021;39:3874-3881.
28. Wakselman C. Fluorinated organic compounds: synthesis and biological applications. Ann Pharm Fr. 1999;57:108-115.
29. Gonzalez AC de O, Costa TF, Andrade ZA, Medrado ARAP. Wound healing: a literature review. An Bras Dermatol. 2016;91:614-620.
30. Çelikezen FÇ, Hayta Ş, Özdemir Ö, Türkez H. Cytotoxic and antioxidant properties of essential oil of Centaurea behen L. *in vitro*. Cytotechnology. 2019;71:345-350.
31. Velika B, Kron I. Antioxidant properties of benzoic acid derivatives against superoxide radical. Free Radic Antioxid. 2012;2:62-67.
32. Parasuraman S. Toxicological screening. J Pharmacol Pharmacother. 2011;2:74-79.

33. Singh S, Khanna VK, Pant AB. Development of *in vitro* toxicology: a historic story. In: Dhawan A, Kwon SB, editors. Toxicology *In Vitro* Testing. Academic Press; 2018. p. 1-19.

34. Lage OM, Ramos MC, Calisto R, Almeida E, Vasconcelos V, Vicente F. Current screening methodologies in drug discovery for selected human diseases. Mar Drugs. 2018;16:279.

35. Giacco F, Brownlee M. Oxidative stress and diabetic complications. Circ Res. 2010;107:1058-1070.

36. Feldman EL, Callaghan BC, Pop-Busui R, Zochodne DW, Wright DE, Bennett DL, Bril V, Russell JW, Viswanathan V. Diabetic neuropathy. Nat Rev Dis Primers. 2019;5:41.

37. Verma E, Patil S, Gajbhiye A, Deshmukh S, Khedekar P, Patil P. Sequential analysis for identification of byproduct from N-benzylation reaction: wound healing and anti-inflammatory potential of the byproduct 4-chlorobenzyl 2-((4-chlorobenzyl)amino)benzoate. RSC Adv. 2023;13:25904-25911.

38. Furuno T, White MD, Balasubramanian N, Chan C, Weigel P, Gupta S. *In vitro* cell migration, invasion, and adhesion assays: from cell imaging to data analysis. Front Cell Dev Biol. 2019;1:107.

39. Yarrow J, Totsukawa G, Charras G, Mitchison T. Screening for cell migration inhibitors via automated microscopy reveals a Rho-kinase inhibitor. Chem Biol. 2005;12:385-395.

40. Hulkower KI, Herber RL. Cell migration and invasion assays as tools for drug discovery. Pharmaceutics. 2011;3:107-124.

41. Jonkman J, Cathcart J, Xu F, Bartolini ME, Amon JE, Stevens KM. An introduction to the wound healing assay using live-cell microscopy. Cell Adh Migr. 2014;8:440-451.

Turk J Pharm Sci 2025;22(6):367-380
DOI: 10.4274/tjps.galenos.2025.72361

ORIGINAL ARTICLE

Overcoming Intrinsic and Acquired Temozolomide Resistance in Glioblastoma: Fisetin as a Potential Strategy to Enhance Sensitivity via ZEB1 Modulation

Sena FERAH[1], Mine ÇAMLIBEL[1], Melis ERÇELİK[1], Çağla TEKİN[1], Gülçin TEZCAN[2], Melisa GÜRBÜZ[1], Ahmet BEKAR[3], Hasan KOCAELİ[3], Berrin TUNCA[1]*

[1]Bursa Uludağ University Faculty of Medicine, Department of Medical Biology, Bursa, Türkiye
[2]Bursa Uludağ University Faculty of Dentistry, Department of Fundamental Sciences, Bursa, Türkiye
[3]Bursa Uludağ University Faculty of Medicine, Department of Neurosurgery, Bursa, Türkiye

ABSTRACT

Objectives: Glioblastoma (GB) is the most aggressive type of brain tumor in adults, and the chemical agent temozolomide (TMZ) is widely used for its treatment. However, TMZ resistance can lead to therapeutic failure. The aim of this study was to investigate the effect of the bioflavonoid fisetin on GB cell growth and on overcoming TMZ resistance in TMZ-sensitive, inherited-resistant, and acquired-resistant GB cells the effect of fisetin on TMZ efficacy evaluin primary GB cells.

Materials and Methods: GB cell lines (T98G; intrinsic TMZ-resistant, A172; TMZ-sensitive, A172-R; acquired TMZ-resistant) and primary GB cells derived from patient samples were treated with effective doses of TMZ (ranging from 900 to 1000 μM), fisetin (ranging from 13.78 to 16.40 μM), or a combination of both. TMZ resistance was acquired in A172 cells through stepwise increases in TMZ concentration. Real-time cell proliferation was measured using the xCELLigence system. The migratory capacity of the cells was evaluated using a wound-healing assay. The RNA expression of the epithelial-to-mesenchymal transition (EMT)-inducing transcription factor E-box-binding homeobox 1 (ZEB1) was assessed by quantitative polymerase chain reaction. Cell assays were analyzed by analysis of variance, and ZEB1 expression was analyzed by t-test.

Results: Fisetin substantially enhanced the effect of TMZ in all the cell lines included in the present study, as evidenced by significant decreases in cell proliferation and wound-healing, and in ZEB1 expression ($p<0.0001$). In addition, TMZ+fisetin reduced ZEB1 expression in primary GB tumors but not in butterfly GB cells.

Conclusion: Fisetin alone was effective against GB; importantly, the TMZ+fisetin combination demonstrated greater efficacy than TMZ alone by enhancing sensitivity to TMZ through downregulation of ZEB1 in various resistant models, including patient-derived samples. Since ZEB1 is associated with EMT and drug resistance, fisetin may be a promising anticancer candidate to improve chemotherapeutic efficacy in resistant GB and to shed light on personalized treatments, pending further preclinical research.

Keywords: Glioblastoma, temozolomide resistance, fisetin, epithelial-to-mesenchymal transition, ZEB1

***Correspondence:** btunca@uludag.edu.tr, **ORCID-ID:** orcid.org/0000-0002-1619-6680
Received: 12.02.2024, **Accepted:** 12.12.2025 **Publication Date:** 30.012026

Cite this article as: FERAH S, ÇAMLIBEL M, ERÇELİK M, TEKİN Ç, TEZCAN G, GÜRBÜZ M, BEKAR A, KOCAELİ H, TUNCA B. Fisetin, a bioflavonoid, reduces ZEB1 and promotes temozolomide sensitivity in inherited and acquired resistant glioblastoma. Turk J Pharm Sci. 2025;22(6):367-380

INTRODUCTION

Glioblastoma (GB) is the most prevalent and aggressive brain tumor,[1] and it exhibits an alarmingly high 5-year mortality rate (up to 95%).[2] The World Health Organization statistics from the year 2020 indicate a significant burden of brain tumors, accounting for approximately 1.6% of all cancer cases and 2.5% of cancer-related deaths; incidence rates are rising, reaching up to 10 per 100,000 population.[2,3] Standard treatment for GB consists of surgical resection, radiotherapy, and chemotherapy. Despite this treatment protocol, patients have a median survival of only 12.6 months.[4]

Maximum surgical resection is an effective treatment method that prolongs the survival of patients with this disease. However, due to the invasive nature of GB, maximum resection cannot be performed in many cases, which increases the risk of recurrence.[5] Temozolomide (TMZ), an alkylating agent, is commonly used to treat GB.[6] TMZ is indispensable in the treatment of GB because it effectively crosses the blood-brain barrier (BBB), the main obstacle to GB therapy.[6] However, because these tumors are highly heterogeneous, resistance to TMZ therapy is common among GB patients [7] TMZ resistance can be mainly due to O6-methylguanine-DNA methyltransferase (MGMT) methylation[8] and alterations in other signaling pathways involved in DNA repair systems[9] and stem-like cell growth.[10] TMZ resistance can be inherited or acquired after a period of treatment.[11] Although the intrinsic factors and mechanisms affected during tumor acquisition differ, tumor aggressiveness, recurrence, and metastasis, which can result from enhanced epithelial-to-mesenchymal transition (EMT), are observed in both cases.[11] Zinc finger E-box-binding homeobox 1 (ZEB1) is a transcription factor that plays a role in the induction of EMT.[12] In addition, ZEB1 has been shown to contribute to chemotherapy resistance by promoting the acquisition of cancer stem cell properties.[13] Therefore, targeting ZEB1 may be an effective strategy to interrupt EMT and maintain stem-like cells.

To date, promising findings have been obtained from including natural compounds in research on new therapies for many cancer types, considering their antioxidant and cytotoxic effects.[14] In addition, the combined use of some natural compounds with certain chemotherapeutic agents has been shown to increase the effectiveness of these agents and reduce their side effects.[15,16] Fisetin, a flavonoid found mainly in strawberries, apples, onions, wine, and tea, is also commercially available and exhibits various bioactivities, including antioxidant, anti-inflammatory, and anticancer effects.[17] Studies have shown that fisetin can modulate key pathways implicated in GB and in drug resistance, including MSH2, ZEB1, P53, PI3K, and Bax/Bcl2, across different cancers.[18,19] Particularly, fisetin has shown inhibitory effects on ZEB1 and ZEB1-mediated invasion in melanoma, thereby enhancing sorafenib efficacy by modulating EMT.[20] Although fisetin has been investigated in other cancer models, its effects on GB and TMZ remain underexplored. While previous studies have reported the senolytic and pro-apoptotic actions of fisetin[21] and its influence on GB senescence in GB cell lines,[22] its specific role in modulating cellular aggressiveness and resistance, especially when combined with TMZ, remains unelucidated. In this study, we aimed to determine the effect of fisetin on GB cancer cell aggressiveness, TMZ response, and ZEB1 expression *in vitro*. To address varying TMZ sensitivities observed in GB, we included intrinsically TMZ-resistant T98G and TMZ-sensitive A172 cells in this study. Notably, this study is the first to investigate the effects of fisetin on cell lines that acquired resistance following long-term TMZ exposure. This study aims to investigate the therapeutic potential of fisetin in overcoming existing and acquired TMZ resistance in GB. Specifically, we evaluated the effects of fisetin, both alone and in combination with TMZ, on cell proliferation, migratory capacity, and the expression of the EMT-related transcription factor ZEB1 across various models, including TMZ-sensitive, intrinsic-resistant, and acquired-resistant GB cell lines, as well as patient-derived primary tumor samples with different pathological features. We hypothesize that fisetin enhances TMZ efficacy by modulating the EMT process, thereby providing a potential strategy to circumvent drug resistance in GB treatment.

MATERIALS AND METHODS

The experimental procedure was established to evaluate the effects of TMZ and fisetin treatments on GB cells with varied resistance profiles. TMZ-sensitive (A172) and TMZ-resistant (T98G) GB cell lines, a resistant subline (A172-R) generated by exposing A172 cells to increasing doses of TMZ for 18 months, a primary tumor culture obtained from tumor tissues removed from three GB patients at surgery, and a healthy fibroblast cell line (L929) were used to represent GB cells with varying resistance properties. Treatment of cells with various concentrations of fisetin and TMZ, assessment of cell viability using a real-time cell analyzer [xCELLigence real-time cell analyzer (RTCA)], evaluation of cell migration by a wound-healing assay, quantification of ZEB1 gene expression by real-time-quantitative polymerase chain reaction (qPCR), and statistical comparison of treatment-group differences using analysis of variance (ANOVA) and t-test were performed in this study.

Reagents

TMZ (C6H6N6O2) was obtained from Sigma–Aldrich, Inc. (St. Louis, MO, USA; Cat. no.: T2577). Fisetin (3,3′,4′,7-tetrahydroxyflavone) (≥96% purity) was obtained from Tokyo Chemical Industry Co. (TCI) (Cat no.: T0121; Tokyo, Japan). All reagents were dissolved in dimethyl sulfoxide (Sigma-Aldrich, MO, USA) and stored at -20 °C until use.

Cell lines and primary GB cells

The fibroblast-like GB cell lines, TMZ-resistant T98G[23] and TMZ-sensitive A172[24], were obtained from Dr. Tuğba Bağcı Önder, Koç University, İstanbul, Türkiye, and the healthy fibroblast line L929[25] was obtained from the American Type Culture Collection (ATCC) (Manassas, VA, USA). In addition, primary tumors from three GB patients who underwent surgery as part of their therapy were included in the study. Tumor samples

were collected during surgical procedures at the Neurosurgery Department of Bursa Uludağ University and were characterized by a pathologist. The collection of tumor samples was approved by the Uludağ University Faculty of Medicine Clinical Research Ethics Committee (approval number: 2023-3/43, dated: 14.02.2023). Written informed consent was obtained from all patients prior to their inclusion in the study. GB patients were included based on the following criteria: primary high-grade brain tumors (GB) that were surgically resected, non-metastatic, and treatment-naive (no prior chemotherapy/radiotherapy). Of all patients, those who did not meet the inclusion criteria were excluded. The primary tumor samples were cultured *in vitro* as described previously.[26] All cell lines and primary GB cells were maintained in Dulbecco's modified Eagle's medium-F12 (HyClone, UT, USA) supplemented with 10% fetal bovine serum (Gibco, MA, USA), 1% antibiotic/antimycotic solution (Capricorn, Ebsdorfergrund, Germany), 1 mM sodium pyruvate (Gibco, MA, USA), and 2 mM L-glutamine (Gibco, MA, USA) in a 5% CO_2 humidified incubator at 37 °C. All samples were stored in the cryotube at -152 °C.

Cell viability

An xCELLigence- RTCA (ACEA Biosciences, San Diego, CA, USA) was used to visualize cell proliferation. Briefly, 15×10^3 cells were seeded into an E-plate 16. After determining the log phase of the growth curve, TMZ-resistant T98G cells, TMZ-sensitive A172 cells, and noncancerous L929 fibroblasts were treated with seven concentrations of fisetin (5–200 µM) and a range of TMZ concentrations for 24–72 hours. The time-dependent half-maximal inhibitory concentration (IC_{50}) was considered the effective dose for both fisetin and TMZ. The experiments were repeated three times for each dose.

TMZ resistance acquisition

TMZ-sensitive A172 cells were exposed to seven increasing cycles of TMZ (100, 200, 350, 450, 550, 750, and 900 µmol/L) every 2-3 weeks for 18 months using a combination of methods previously described by Lee et al.[27] and St-Coeur et al.[28] After treatment with TMZ at the same concentration, the surviving cells were allowed to proliferate and were re-treated. The same cycle was repeated for 2-3 weeks, followed by a resting period in fresh medium without TMZ treatment. After the recovered cells reached 70% confluency, they were treated with increasing concentrations of TMZ. After treatment with increasing doses of TMZ for 18 months, the resulting cells were named A172-R. Cells that did not reach 70% confluence after 4 weeks were excluded from the experiment. The acquired TMZ insensitivity was assessed by measuring cell viability and wound-healing rate.

Migration assay

Cells were grown in a 6-well culture plate until they reached 70% confluency. A 10 µL pipette tip was used to vertically scratch the monolayers at three different locations, and the debris was removed. The wounded monolayers were treated with the IC_{50} concentrations of fisetin, TMZ, or TMZ+fisetin. The rate of gap closure along scratches reflected the migratory ability of the cells. The wound gap was visualized under an inverted microscope at 0, 6, 12, 18, and 24 hours and measured using NIH ImageJ software v1.52a (National Institutes of Health, Bethesda, MD, USA). Each experiment was performed with three technical replicates.

Reverse transcription PCR analysis

RNA extraction was performed following the protocol of the Zymo RNA Isolation Kit (Zymo Research; Irvine, CA, USA). The concentration and purity of the RNA samples were determined from the A260/A280 ultraviolet/visible absorbance ratio obtained with a Maestro Nano Micro-Volume spectrophotometer (Maestrogen Inc., Las Vegas, NV, USA). RNA samples with a ratio of ~1.8-2.0 were converted to complementary DNA (cDNA) using the ProtoScript® II First Strand cDNA Synthesis Kit (New England Bioscience; Ipswich, MA, USA). cDNA (200 ng) was used for real-time PCR. The expression of ZEB1 (F: AGTGTTACCAGGGAGGAGCAGTG, R: TTTCTTGCCCTTCCTTTCCTGTGTC; annealing: 55 °C)[29] was analyzed by qPCR using SYBR Green GoTaq® qPCR master mix (Madison, WI, USA). The RNA input was normalized to the housekeeping gene β-actin with primers (F: GACAGGATGCAGAAGGAGATTACT, R: TGATCCACATCTGCTGGAAGGT) and an annealing temperature of 60°C.[30] The threshold cycle (Ct) for RNA expression was determined using the StepOne real-time-qPCR System (Thermo Fisher, CA, USA). The $2-\Delta\Delta Ct$ method was used to calculate fold changes from Ct values.

Statistical analysis

In each sample, the untreated group served as the control. To evaluate the effects of fisetin and TMZ, each treatment group was analyzed in comparison to its respective control. The normality of the data was tested using the Shapiro-Wilk normality test in GraphPad Prism (v8.0). Since the data followed a normal distribution ($p>0.05$), they are presented as mean ± standard deviation (SD) and analyzed using parametric tests. One-way ANOVA and Tukey's test were used to analyze the effects of fisetin, TMZ, and TMZ+fisetin on cell viability. Two-way ANOVA was used to detect differences between sample groups in the wound healing analysis. An independent-samples t-test was used to assess differences in RNA expression levels. Statistical analyses were performed using SPSS version 20.0 (IBM SPSS Inc., Armonk, NY, USA), and the data were visualized using GraphPad Prism 8.0 (GraphPad Software Inc., San Diego, CA, USA). A *p*-value less than 0.05 was considered statistically significant at the 95% confidence level.

RESULTS

Fisetin decreased GB cell viability

The proliferation of T98G and A172 cells significantly decreased after incubation for more than 48 hours, regardless of fisetin treatment ($p<0.05$). This decline was attributed to the cells reaching maximum confluency within the E-plate wells. Therefore, data from incubation periods exceeding 48 hours were excluded from further analysis.

In T98G cells, 5 µM fisetin led to a 14.5±3.2% reduction after 24 hours and a 19.8±1.6% reduction after 48 hours. In contrast, treatment with 200 µM fisetin resulted in reductions of 75.3±0.6% and 79.1±2.2% in T98G cells after 24 and 48 hours, respectively (Figure 1a). The IC_{50} of fisetin for T98G cells was 16.40 µM at 24 hours and 12.26 µM at 48 hours ($p<0.001$) (Figure 1b).

In A172 cells, 5 µM fisetin reduced the proliferation rate by 26.3±1.0% and 23.6±1.9% at 24 and 48 hours, respectively (Figure 1c and d). A concentration of fisetin greater than 100 µM reversed the inhibitory effect on proliferation and reduced proliferative activity after 48 h. After 24 h of incubation with 75 µM fisetin, cell inhibition was 45.8±1.9%, whereas within 48 h it was 17.7±1.2%. In addition, 200 µM fisetin induced 40.0±5.0% cell inhibition at 24 hours, which decreased to 6.6±0.5% at 48 hours. The IC_{50} of fisetin was 13.78 µM at 24 hours and 10.34 µM at 48 hours in A172 cells ($p<0.001$) (Figure 1d). At concentrations between 50 µM and 75 µM—five times higher than the average IC_{50} observed in GB cell lines, fisetin did not reduce viability in the L929 fibroblast cell line and preserved 90.0±1.0% cell viability (Figure 1e and f). These findings demonstrated the safety of fisetin in noncancerous cells at the IC_{50} values determined for T98G and A172 cells. Therefore, T98G and A172 cells were treated with 16.40 µM and 13.78 µM fisetin, respectively, for 24 hours.

A172 cells gradually became resistant to the IC_{50} of TMZ

The IC_{50} of TMZ was determined to be 900 µM in A172 cells in our previous study.[25] Therefore, A172-R cells, resistant to 900 µM TMZ, exhibited morphological changes (Figure 2c) and were used in all analyses. To generate a 900 µM TMZ-resistant cell series, A172 cells were gradually exposed to increasing concentrations of TMZ (350, 450, 550, 750, and 900 µM). A decrease in TMZ sensitivity of A172-R cells (A172-350-R to A172-900-R) is shown in Figure 2a and 2b. Ultimately, 900 µM TMZ reduced the viability of the A172-900-R (A172-R) cells by 35%, whereas it reduced the parental A172 cells by 63% ($p<0.001$) (Figure 2a and b). Figure 2c shows the morphology of cells that became resistant to TMZ; these cells are characterized by increased aggressiveness and enhanced cell-cell interactions.

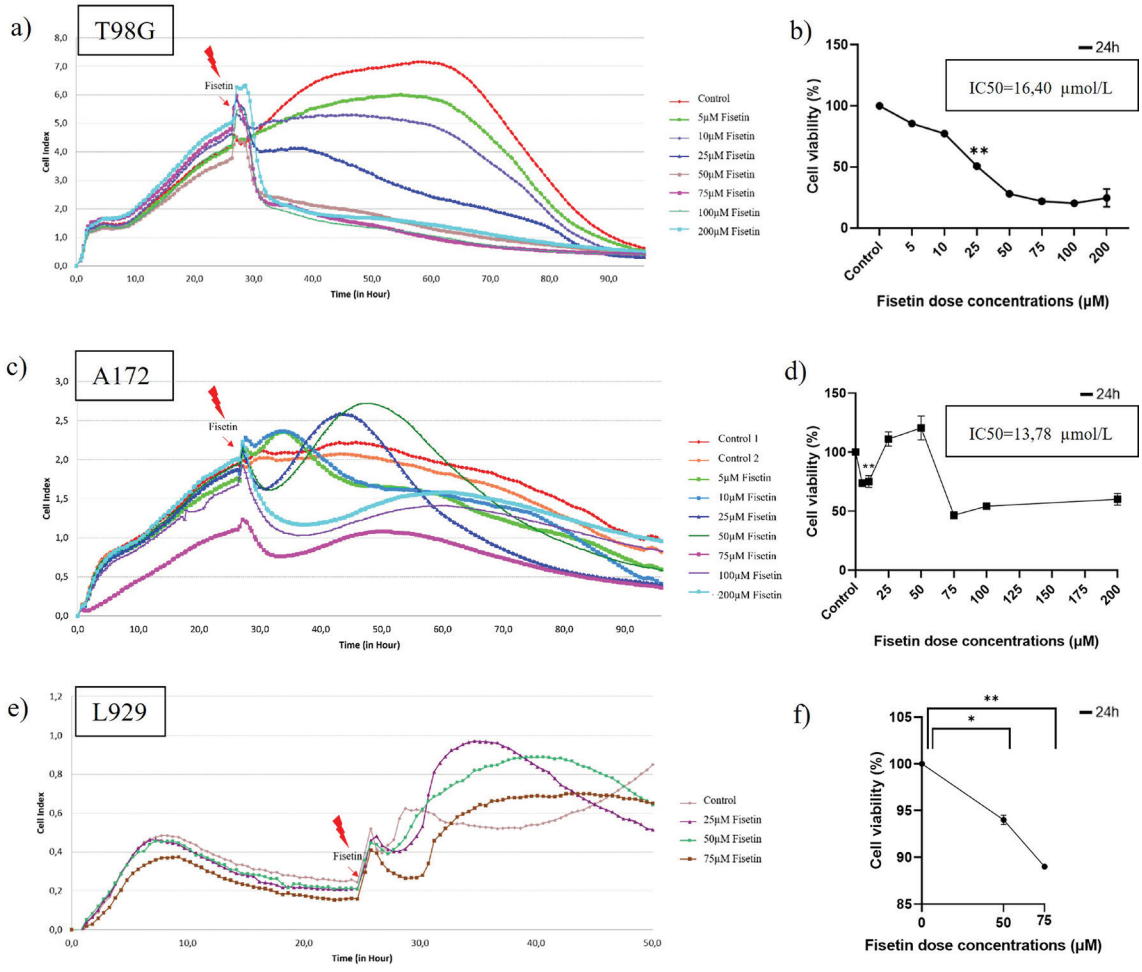

Figure 1. Effect of fisetin on GB cell proliferation. The effect of different doses of fisetin on real-time proliferation and its IC_{50} on cell viability in (a, b) T98G, (c, d) A172, and (e, f) L929 cells. *p* values were calculated using one-way ANOVA. The experiment was performed in three biological replicates. *$p<0.05$, **$p<0.0001$. Bars represent the mean ± standard deviation

ANOVA: Analysis of variance, IC: Inhibitory concentration

Fisetin additionally affects TMZ in GB cell lines

In our previous study, the IC_{50} values of TMZ were 1000 µM for T98G cells and 900 µM for A172 cells, respectively.[25] Accordingly, we treated T98G, A172, and A172-R cells with TMZ and with fisetin at their respective ICs_{50} to analyze the potential contribution of fisetin to TMZ therapy. Compared with TMZ alone, fisetin did not increase TMZ-mediated cell inhibition in T98G cells (Figure 3a and b). In contrast, combined treatment with TMZ + fisetin reinforced TMZ-mediated inhibition of A172 and A172-R cells (p<0.0001) (Figure 3c and f).

Fisetin cotreatment suppressed the migration ability of GB cell lines treated with TMZ via different resistance mechanisms.

The wound closure rate was 78.74% after 24 hours in untreated T98G cells. After TMZ treatment, the wound closure rate exceeded 72%. In addition, compared with no treatment, fisetin treatment decreased the wound area by up to 90.07%. In contrast, the inhibitory effect of TMZ + fisetin on migration was greater than that of TMZ alone (p<0.001) (Figure 4a).

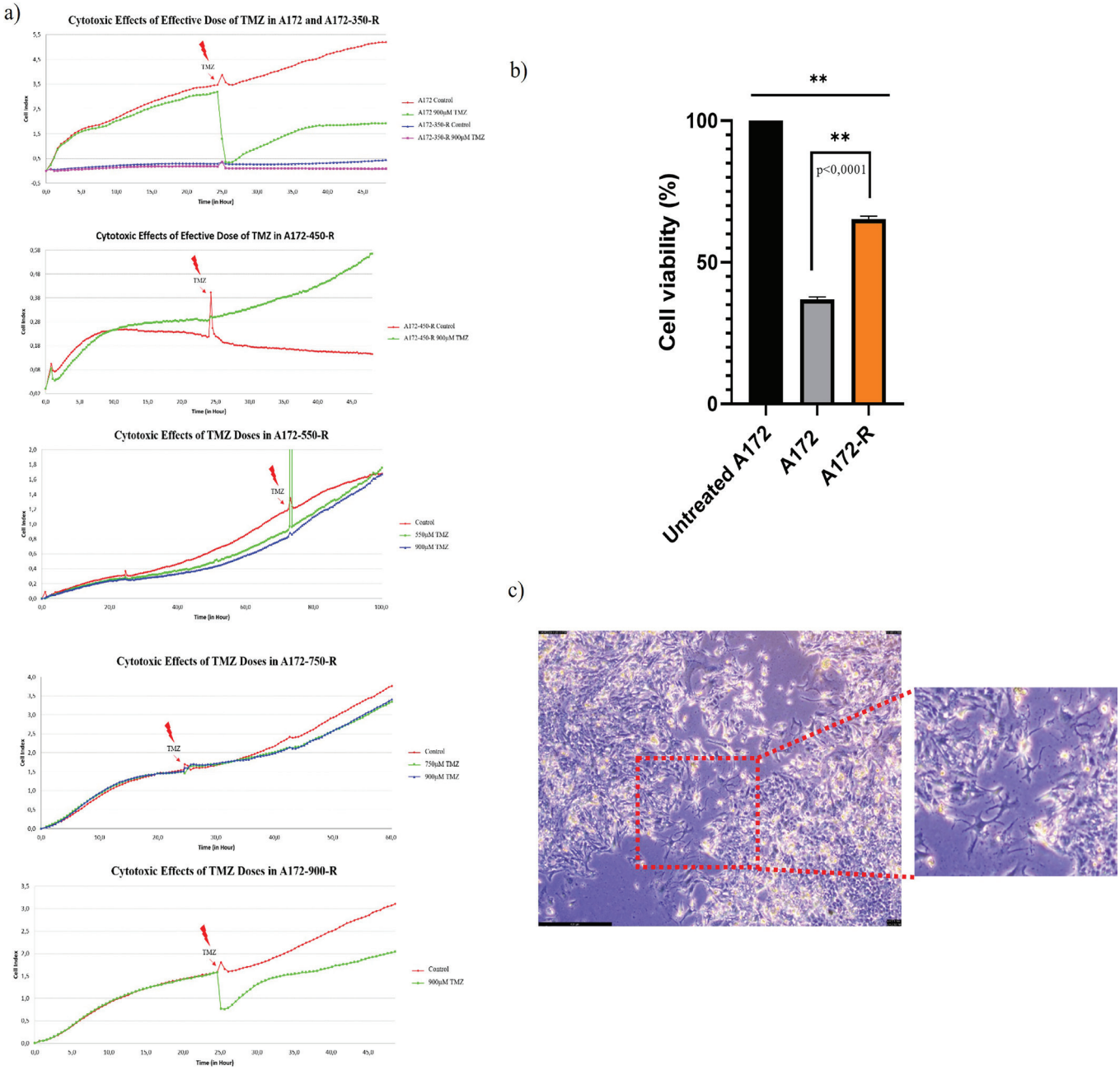

Figure 2. Effect of TMZ concentration on A172-R cells. (a) The representation of the gradually increasing TMZ resistance of A172-R cells during the acquisition of TMZ resistance. (b) The relative change in the viability of A172 and A172-R cells treated with 900 µmol/L TMZ. Each column represents the inhibitory effect of TMZ on cell viability compared with that of the corresponding untreated cell lines. Untreated A172 cells served as the negative control. (c) Microscopic representation of the morphology of acquired TMZ-resistant A172-R cells and cell-to-cell connections under a 4X objective (scale bar: 620 µm)

TMZ: Temozolomide

In untreated A172 cells, 73% of the wounded area was closed within 24 hours. Compared with no treatment, TMZ led to only a 32% decrease in wound-area recovery in A172 cells (p<0.001). Fisetin treatment of A172 cells resulted in a 27% recovery of the wound area (p<0.001). TMZ+fisetin treatment reduced wound recovery of A172 cells by 41.49% compared with cells treated with TMZ alone (p<0.001) (Figure 4b), indicating that fisetin enhances the efficacy of TMZ in A172 cells.

In untreated A172-R cells, wound-area closure was 69.49% after 24 h of treatment. After TMZ-only treatment, wound-area recovery in A172-R cells was 39.44%, which was lower than in the untreated group (Figure 4c and d). The attenuation of the wound-healing rate observed in TMZ-treated A172-R cells compared with A172 cells (p<0.001) was considered indicative of acquired TMZ resistance in A172-R cells (Figure 4d). The A172-R cells recovered 31.54% of the wounded area after fisetin-only treatment. In addition, after combined treatment with TMZ and fisetin in A172-R cells, 13.23% of the wound area healed compared with untreated cells (p<0.001). Notably, TMZ+fisetin had a significantly greater suppressive effect on TMZ alone (p<0.001) (Figure 4b-d).

Combination treatment with fisetin reduced TMZ-induced expression of ZEB1 in both intrinsic and acquired TMZ-resistant cells.

TMZ reduced ZEB1 gene expression in T98G cells (p<0.001) (Figure 5a) and A172 cells (p<0.0001) (Figure 5b). In contrast, TMZ induced ZEB1 expression in A172-R cells (p<0.0001) (Figure 5c). Fisetin reduced ZEB1 expression only in T98G cells (p<0.001), had no effect on ZEB1 in A172 cells, and increased ZEB1 expression in A172-R cells (p<0.001) compared with untreated cells. In T98G cells, TMZ-fisetin-induced ZEB1 expression was lower than TMZ-only-induced ZEB1 expression (p<0.001) (Figure 5a). However, compared with TMZ, TMZ+fisetin did not affect ZEB1 levels in A172 or A172-R cells (Figure 5b and c).

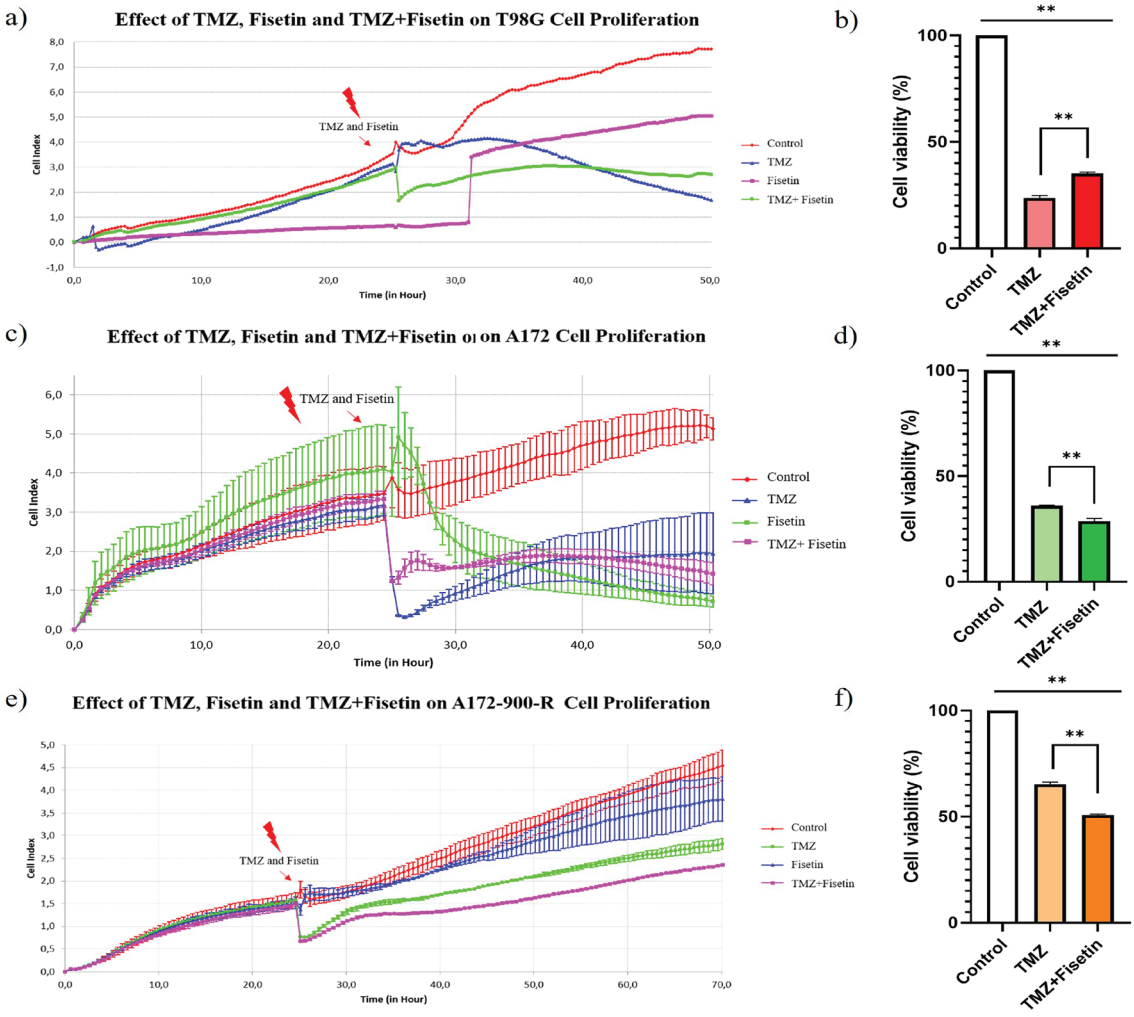

Figure 3. Effect of TMZ, fisetin, and TMZ+fisetin on the proliferation and viability of (a, b) T98G, (c, d) A172, and (e, f) A172-R cells. p values were calculated by one-way ANOVA. All experiments were performed in three biological replicates. *p<0.05, **p<0.0001. Bars represent the mean ± standard deviation

ANOVA: Analysis of variance

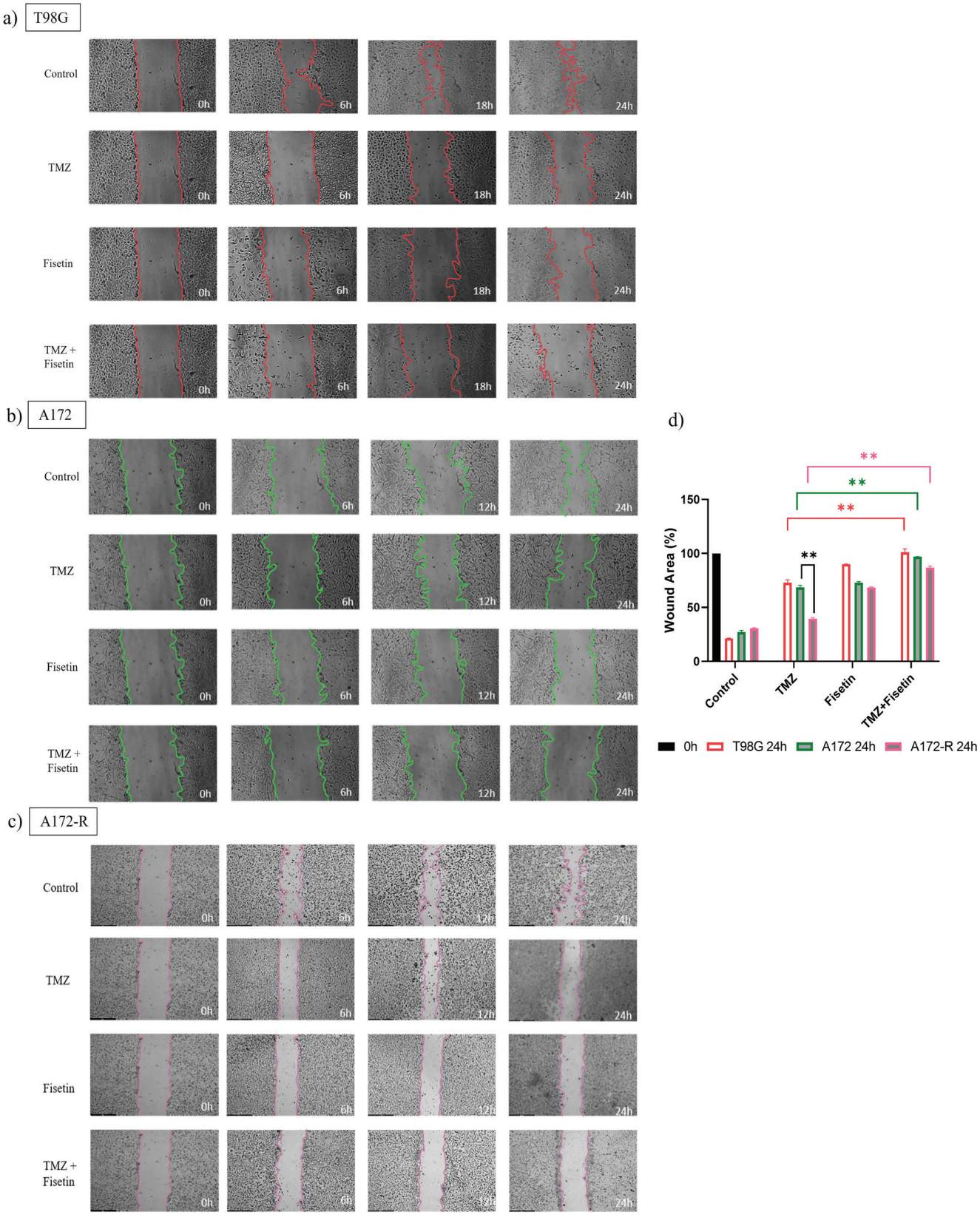

Figure 4. Representative images of the effect of TMZ, fisetin, and TMZ+fisetin on cell migration in the wound healing assay in the (a) T98G, (b) A172, and (c) A172-R cell lines (scale bar: 620 µm). (d) Comparative analysis of cells in terms of treatments. *P* values were calculated using two-way ANOVA. All experiments were performed in three biological replicates. ***p*<0.0001.

TMZ: Temozolomide, ANOVA: Analysis of variance

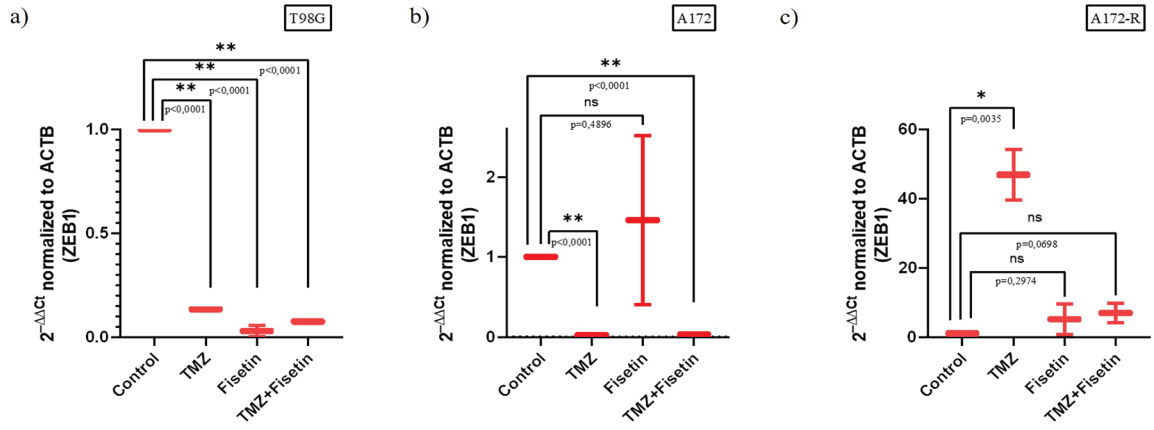

Figure 5. Effect of TMZ, fisetin, and TMZ+fisetin on the RNA expression of ZEB1 in the (a) T98G, (b) A172, and (c) A172-R cell lines. *P* values were calculated using independent-samples t-tests. All experiments were performed in three biological replicates. *$p<0.05$, **$p<0.0001$

TMZ: Temozolomide, ANOVA: Analysis of variance

Breaking of TMZ resistance by fisetin was confirmed in cancer cells collected from primary GB tumors

Three cell lineages derived from primary tumors of GB patients were included in the present study. Patient 1 had a tumor that was intracranially located in the left frontal lobe. Patient 2 was diagnosed with a butterfly GB and multiple primary tumors in the right frontal lobe. Patient 3 experienced postoperative recurrence of the cancer (Figure 6). According to the histopathological analysis, all GB tumors were positive for glial fibrillary acidic protein, Olig-2, NFP, NeuN, and H3K27me3, while they were negative for isocitrate dehydrogenase 1 (IDH-1) and ATRX. In addition, the Ki-67 index was at least 30% in all patients. After surgical tumor resection, all patients received identical postoperative concurrent radiotherapy (40 Gy/15 fx) and chemotherapy (TMZ) as part of the standard care regimen, and they were followed for their clinical status and survival until they died. The disease-free interval of patient 1 was 4 months, while it was 6.5 months and 3.5 months for patients 2 and 3, respectively. These findings indicate differences among the tumor samples included in the study in terms of molecular patterns and aggressiveness.

The effect of TMZ on ZEB1 expression varied across GB tumor-derived cell lineages (Figure 7). While TMZ reduced ZEB1 expression in patients 1 and 2, it was ineffective in patient 3. Conversely, TMZ+fisetin substantially reduced ZEB1 in patients 1 and 3, but was ineffective in patient 2 compared with TMZ alone (Figure 7).

DISCUSSION

GB is a stage IV brain tumor for which even the most aggressive treatments can be rendered ineffective by resistance, and patient survival remains limited to 12.6 months.[4,31] The response to the chemotherapeutic agent TMZ, long established as standard therapy, may vary according to GB characterization. Due to their distinct characteristics, GB patients may exhibit resistance to chemotherapy resulting from genetic and epigenetic changes and from treatment-induced acquired resistance and therefore do not respond well to treatment. Although the methylation status of MGMT was one of the first changes detected in patients and associated with TMZ response, it does not constitute a direct link.[32] The multifaceted mechanisms underlying treatment resistance and the pronounced intratumoral heterogeneity observed in GB suggest that relying on MGMT promoter methylation as a single predictive biomarker for TMZ response is insufficient for guiding clinical decision-making.[33] Supporting this notion, prior studies have demonstrated that, although p53 status may have a greater impact than MGMT on determining TMZ responsiveness, it nonetheless fails to serve as a standalone predictor, underscoring the urgent need to identify additional biomarkers associated with resistance mechanisms.[34] MGMT-methylated GB cells, such as T98G, may still express the MGMT protein and exhibit resistance to TMZ.[23] Conversely, other evidence indicates that resistance may primarily stem from the expression of alternative DNA repair enzymes, such as alkylpurine-DNA-N-glycosylase (APNG), rather than from the expression of MGMT itself. Moreover, certain TMZ-resistant GB cell lines (e.g., CCF-STTG1) do not express MGMT protein, highlighting the existence of MGMT-independent resistance mechanisms.[23] These findings underscore the complexity of TMZ resistance and the limitation of MGMT methylation status in fully capturing tumor behavior. Furthermore, while IDH mutation status plays a pivotal role in the molecular classification of GB—differentiating primary (IDH wild-type) from secondary (IDH mutant) forms—it is clear that MGMT methylation alone is insufficient to predict therapeutic response in this molecularly heterogeneous disease, characterized by genetic and epigenetic alterations.[35]

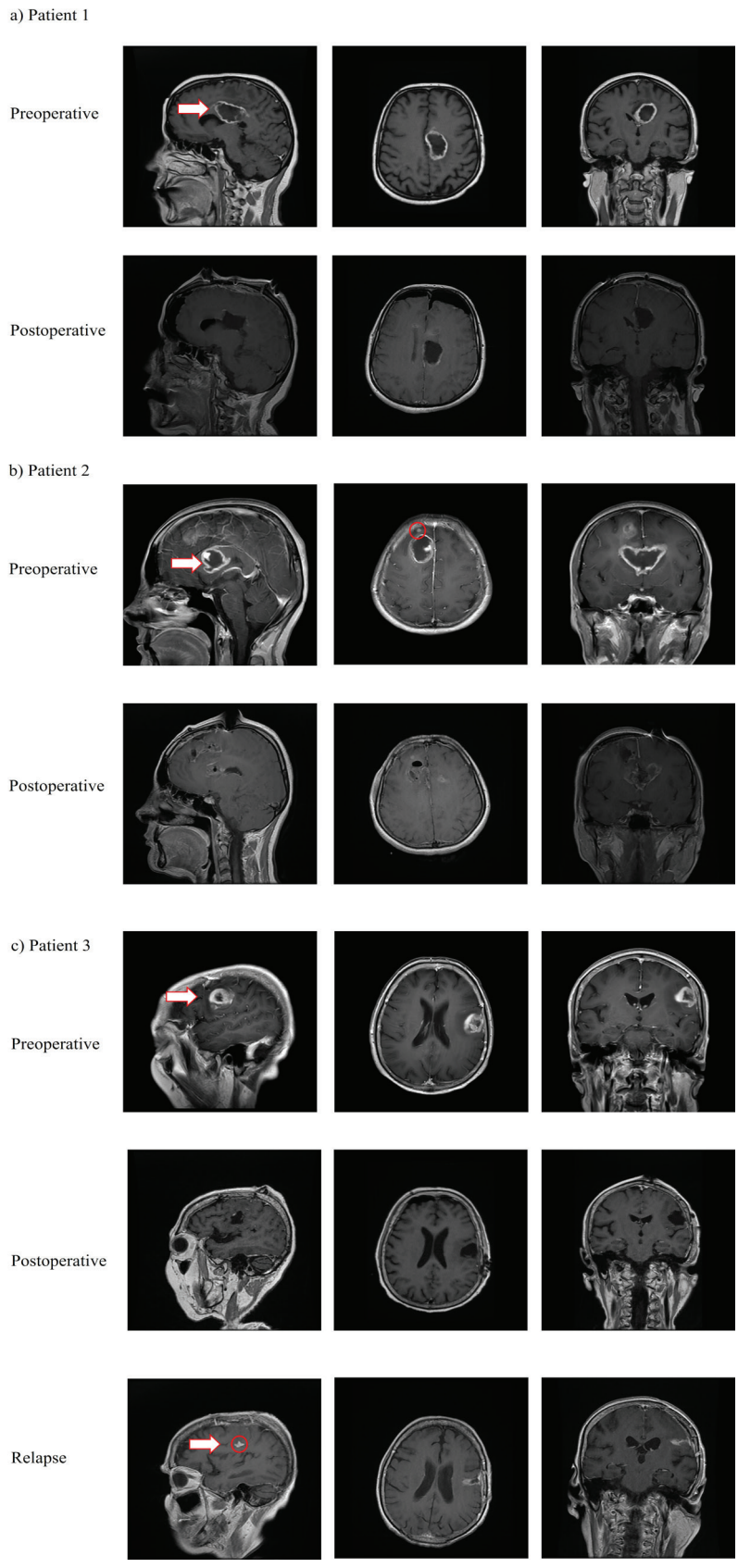

Figure 6. MRI images of GB patient tumors before and after surgery: (a) Patient 1; (b) Patient 2; (c) Patient 3
MRI: Magnetic resonance imaging, GB: Glioblastoma

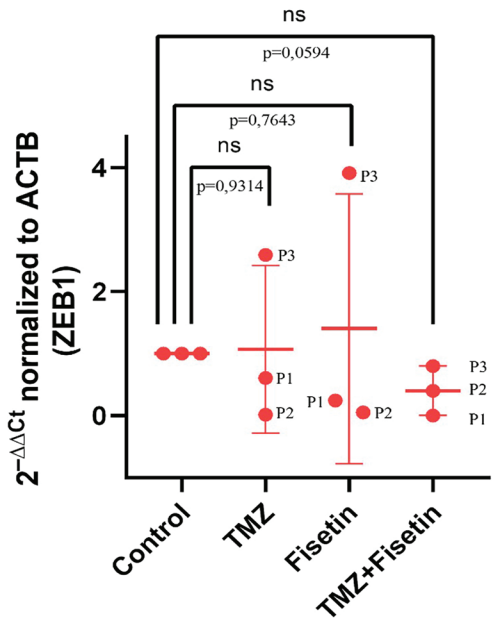

Figure 7. Graphical representation of the effect of the combination of TMZ, fisetin, and TMZ+fisetin on ZEB1 gene expression in the GB patient population. Each round represents a different GB patient (P1 = Patient 1; P2 = Patient 2; P3 = Patient 3)

TMZ: Temozolomide, GB: Glioblastoma, EMT: Epithelial-to-mesenchymal transition, ZEB1: Zinc finger E-box-binding homeobox 1, BBB: Blood-brain barrier, MGMT: O6-methylguanine-DNA methyltransferase, IC_{50}: The time-dependent half-maximal inhibitory concentration, qPCR: Real-time-quantitative polymerase chain reaction, cDNA: Complementary DNA, APNG: Alkylpurine-DNA-N-glycosylase

Indeed, there is an urgent need to evaluate new biomarkers as potential predictive and prognostic markers of patient response and resistance to treatment.[36] Accordingly, this study first investigated invasion and the regulation of the EMT transcription marker ZEB1 in non-resistant, intrinsically resistant, and acquired-resistant GB cell lines and in cancer cells obtained from primary GB tumors. Second, the effects of the natural flavonoid fisetin and its combination with TMZ on cancer cell aggressiveness were analyzed, and ZEB1 expression levels were investigated in these cells *in vitro*.

The selective cytotoxicity of fisetin is a critical finding in the context of GB therapy. Our observations indicate that fisetin possesses a favorable therapeutic window, as it effectively reduces the viability of both TMZ-sensitive and TMZ-resistant GB cells while exhibiting minimal impact on non-tumorigenic fibroblasts. This differential response suggests that fisetin may specifically target tumor-specific signaling pathways, sparing healthy cells even at concentrations well above those required for GB growth inhibition. While fisetin demonstrated a potent anti-proliferative effect independently, its combination with TMZ did not interfere with the known cytotoxic profile of the latter. These findings highlight fisetin's potential as a safe adjunctive agent that suppresses GB cell growth without inducing adverse systemic cytotoxicity, further supporting its role in enhancing the management of drug-resistant brain tumors. Several studies have investigated the safety profile of fisetin in both *in vitro* and *in vivo* models. However, it is important to note that a previous study reported cytotoxic effects in BEAS-2B cells—a normal human bronchial epithelial cell line—only at a significantly higher concentration (270 µmol/L) than its effective dose.[21] This underscores the importance of considering both cell-type-specific responses and concentration-dependent toxicity. *In vivo* studies suggest that fisetin exhibits generally low toxicity in animal models. Guo and Feng[37] reported IC_{50} values ranging from 200 mg/kg (intravenous) to 1700 mg/kg (oral) in rats, depending on the route of administration. Seal et al.[38] further demonstrated that fisetin complexed with metal ions had an IC_{50} of 500 mg/kg in mice, without inducing mortality. While no genotoxic potential was observed, some alterations in hematological and serum biochemical parameters were noted at doses of 400 mg/kg; these alterations may be attributable to enhanced activity resulting from organometallic complex formation. These findings warrant further investigation to clarify the mechanisms underlying such effects. Additionally, fisetin has been shown to possess neuroprotective properties, with minimal toxic symptoms or organ-specific toxicity reported in animal studies.[39] Despite its commercial availability as a dietary supplement, clinical trials remain ongoing to evaluate its therapeutic potential, particularly in cancer treatment (ClinicalTrials.gov.).[40]

Notably, fisetin has been reported to cross the BBB in mice.[41] This pharmacokinetic property enhances the clinical relevance of our findings, which demonstrate its antitumor effects *in vitro* against GB cells. Given its low molecular weight, natural origin, BBB permeability, relatively low toxicity, antitumor activity, and multi-targeted mechanism of action—including modulation of EMT and ZEB1—fisetin emerges as a promising candidate to augment existing therapies such as TMZ. In conclusion, the pharmacokinetic characteristics of fisetin and its demonstrated antitumor effects *in vitro* support further investigation into its potential clinical translation for GB therapy. Nevertheless, practical clinical implementation will require comprehensive pharmacokinetic studies, with a focus on optimizing dosage, improving solubility, and developing effective delivery systems to enhance bioavailability while minimizing off-target effects.

Chemoresistance can be inherited or acquired as a result of long-term exposure to chemotherapeutic drugs.[42] T98G cells are intrinsically resistant to TMZ because of the high expression of MGMT and, particularly, APNG, which are involved in DNA repair.[23] Although A172 cells exhibit a low level of MGMT expression, any of the mismatch repair complex, P-glycoprotein, or the presence of cancer stem cells could promote acquired resistance to TMZ after long-term exposure.[43] Differences in the molecular regulatory patterns of intrinsic and acquired TMZ resistance may lead to different outcomes of therapeutic approaches.[44] For this reason, we compared the effects of fisetin alone and in combination with TMZ on intrinsically TMZ-resistant T98G cells and on acquired TMZ-resistant A172-R cells. Previous studies have shown that a mutated p53 protein fails to reduce ZEB1 expression.[45] Therefore, suppressing

ZEB1 might contribute to the development of an effective therapeutic strategy.[46] T98G cells harbor mutated p53, while A172 cells express wild-type p53.[23] Therefore, TMZ could modestly suppress ZEB1 expression during proliferation in p53-mutant T98G cells. In contrast, TMZ significantly suppressed ZEB1 expression in A172 cells, which express wild-type p53 ($p<0.0001$). Although A172-R cells were more resistant to TMZ than the parental A172 cells, they did not have an inherited p53 mutation, unlike the parental cells. TMZ led to excessive ZEB1 expression in A172-R cells, similar to T98G cells with inherited p53 mutations. Understanding the regulatory mechanism of ZEB1 in GB cells with acquired TMZ resistance requires further investigation. However, fisetin reduced acquired resistance when used in combination with TMZ in both T98G and A172-R cells, regardless of p53 mutation status. Our findings in primary GB cells from patients 1 and 3 confirmed this phenomenon. TMZ increased ZEB1 expression to varying degrees in primary tumor cells from GB patients who developed TMZ resistance across different histopathological patterns. Notably, the tumor of patient 2, a butterfly GB, was not responsive to fisetin. The butterfly GB is known to infiltrate the corpus callosum unilaterally, and it has been associated with more aggressive migratory behavior than other GB subtypes, which have a propensity to invade both hemispheres.[47,48] The lack of ZEB1 suppression by TMZ+fisetin in butterfly GB cells, in contrast to primary GB tumors, may be attributed to intrinsic mesenchymal transition and invasive characteristics of this subtype, which may contribute to resistance to ZEB1 downregulation by the drug combination. Although these patients typically have poor prognoses, the molecular basis of these features remains poorly defined. Given the poorer survival of butterfly GB, these outcomes may be attributable to higher basal ZEB1 expression, consistent with the association between high ZEB1 levels and poor prognosis in GB. Thus, butterfly GB appeared to respond more favorably to aggressive therapeutic approaches.[47] Additionally, the distinct tumor microenvironment and cellular heterogeneity prevalent in butterfly GB may influence the differential response to the therapeutic intervention and highlight the importance of personalized therapy. Therefore, because we were able to enroll only a single butterfly GB primary tumor in the study, our understanding of the basis for fisetin's failure in this tumor is insufficient. However, based on current findings from cell lines and primary GB cells, fisetin may be beneficial for non-butterfly GB tumors.

A previous study reported that fisetin has the potential to overcome cisplatin resistance in lung adenocarcinoma cells.[49] Researchers have shown that this effect of fisetin could be achieved by inducing apoptotic caspase cascades.[49] Our study is the first to demonstrate that fisetin disrupts chemoresistance in both inherited and acquired TMZ-resistant GB cells. One of the key mechanisms that promotes TMZ resistance in GB cells is EMT.[50] The ability of fisetin to simultaneously modulate multiple pathways and exert antitumor effects across various GB cell lines with distinct resistance mechanisms represents a significant therapeutic advantage. Given that ZEB1 is a known target of fisetin and was suppressed by our combined TMZ and fisetin treatment, it is plausible that ZEB1 contributes to TMZ resistance through additional regulatory pathways. Notably, ZEB1 inhibition has been reported to reduce expression of the stemness-related marker SOX2, which has also been implicated in TMZ resistance,[10] particularly in prostate cancer models.[51] One of the upstream signaling pathways influencing ZEB1—and thus TMZ resistance—is the PI3K/Akt pathway.[52] Fisetin has been shown to downregulate the PI3K/Akt pathway in laryngeal cancer[19] and to suppress EMT via modulation of PI3K/Akt signaling in triple-negative breast cancer.[53] In addition, Fisetin was shown to induce p53 protein expression in the human renal cancer cell line Caki.[54] p53 was shown to inhibit the EMT process by reducing expression of the transcription factor ZEB1.[45] In line with this, the decrease in the EMT effect by fisetin, when it was used in combination with sorafenib in BRAF-mutated melanoma cells, was linked to its reduction of ZEB1 expression.[20] Similarly, our findings demonstrated that fisetin reduced ZEB1 expression in both TMZ-resistant T98G and A172-R cell lines. Moreover, fisetin in combination with TMZ decreased TMZ-mediated ZEB1 expression in both non-resistant A172 cells and p53-mutant intrinsically resistant models, suggesting that it may circumvent resistance pathways associated with both p53 dysfunction and ZEB1 overexpression. Interestingly, in acquired TMZ-resistant A172-R cells, treatment with TMZ alone paradoxically increased ZEB1 expression. However, the combination of TMZ and fisetin reversed this effect, leading to a reduction in both ZEB1 expression and resistance. This suppression of ZEB1 by fisetin is likely tied to its ability to inhibit EMT, a process strongly associated with therapy resistance and tumor progression. Therefore, the capacity of fisetin to modulate ZEB1 and EMT pathways may underlie its effectiveness against intrinsic and acquired TMZ resistance in GB.

Furthermore, the decrease in the wound-healing rate of T98G, A172, and A172-R cells confirmed that fisetin inhibits the migratory features of these cells by interrupting the EMT process through suppression of ZEB1. Moreover, fisetin enhanced the inhibitory effect of TMZ on metastasis, which could be explained by the considerable reduction in ZEB1 expression following combined TMZ and fisetin treatment. These findings may provide insight into the effects of fisetin, an anti-migratory agent, on EMT in TMZ-resistant and non-resistant GB cells. Further studies will clarify the exact underlying mechanism.

The efforts to augment the effectiveness of Food and Drug Administration-approved drugs are of paramount importance for GB patients, who continue to face poor survival outcomes. Our current findings suggest that fisetin has the potential to enhance the efficacy of TMZ in GB cells exhibiting both inherent and acquired resistance. New insights have been gained from both established cell-line models and primary patient samples regarding how flavonoids like fisetin—currently under clinical evaluation—can impact adjunctive chemotherapeutic strategies. Specifically, the observed downregulation of ZEB1 and the subsequent inhibition of the EMT process suggest that

fisetin could reduce TMZ resistance by targeting the crosstalk between these molecular pathways. Furthermore, examining dysregulated biomarkers in resistant versus non-resistant lineages is crucial for guiding personalized therapeutic approaches. By considering a patient's specific predisposition to drug resistance, such adjunctive treatments could aid in the selection of more effective, tailored clinical interventions. These results support the clinical relevance of fisetin as a promising candidate for drug development, particularly in the context of personalized therapy.

Study Limitations

However, several limitations must be acknowledged. The study was limited by the small number of patient-derived samples analyzed, which may not fully capture the heterogeneity of GB. Moreover, the scope of resistance mechanisms investigated was relatively narrow. In particular, further research is needed to elucidate the role of fisetin in modulating chemotherapy-related side effects and explore the involvement of ZEB1-associated pathways, such as DNA repair processes, in TMZ resistance. These aspects are critical for a more comprehensive understanding of the therapeutic potential of fisetin and its mechanisms of action.

CONCLUSION

In summary, the dietary flavonoid fisetin inhibits GB cell proliferation and migration, potentially by interrupting EMT by suppressing ZEB1 expression. In addition, fisetin increased the response of GB cells to TMZ regardless of whether chemoresistance was inherited or acquired. Therefore, our findings suggest that fisetin could be a candidate for drug development to support the therapeutic efficacy of TMZ. Understanding the mechanism by which fisetin targets ZEB1 and its biosafety in clinical settings requires further investigation.

Ethics

Ethics Committee Approval: The collection of tumor samples was approved by the Uludağ University Faculty of Medicine Clinical Research Ethics Committee (approval number: 2023-3/43, dated: 14.02.2023).

Informed Consent: Written informed consent was obtained from all patients prior to their inclusion in the study.

Footnotes

Authorship Contributions

Surgical and Medical Practices: A.B., H.K., Concept: S.F., B.T., Design: S.F., M.E., Ç.T., Data Collection or Processing: S.F., M.Ç., M.G., Analysis or Interpretation: S.F., M.Ç., G.T., B.T., Literature Search: S.F., Writing: S.F., G.T., B.T.

Conflict of Interest: The authors declare no conflicts of interest.

Financial Disclosure: The authors declared that this study received no financial support.

REFERENCES

1. Wen PY, Kesari S. Malignant gliomas in adults. N Engl J Med. 2008;359:492-507.
2. Bijalwan G, Shrivastav AK, Mallik S, Dubey MK. Glioblastoma multiforme - a rare type of cancer: A narrative review. Cancer Res Stat Treat. 2024;340-351.
3. Sung H, Ferlay J, Siegel RL, Laversanne M, Soerjomataram I, Jemal A, Bray F. Global Cancer Statistics 2020: GLOBOCAN estimates of incidence and mortality worldwide for 36 cancers in 185 countries. CA Cancer J Clin. 2021;71:209-249.
4. Van Gool SW, Makalowski J, Bitar M, Vliet PV, Schirrmacher V, Stuecker W. Synergy between TMZ and individualized multimodal immunotherapy to improve overall survival of IDH1 wild-type MGMT promoter-unmethylated GBM patients. Genes Immun. 2022;23:255-259.
5. Stupp R, Hegi ME, Mason WP, van den Bent MJ, Taphoorn MJ, Janzer RC, Ludwin SK, Allgeier A, Fisher B, Belanger K, Hau P, Brandes AA, Gijtenbeek J, Marosi C, Vecht CJ, Mokhtari K, Wesseling P, Villa S, Eisenhauer E, Gorlia T, Weller M, Lacombe D, Cairncross JG, Mirimanoff RO; European Organisation for Research and Treatment of Cancer Brain Tumour and Radiation Oncology Groups; National Cancer Institute of Canada Clinical Trials Group. Effects of radiotherapy with concomitant and adjuvant temozolomide versus radiotherapy alone on survival in glioblastoma in a randomised phase III study: 5-year analysis of the EORTC-NCIC trial. Lancet Oncol. 2009;10:459-466.
6. Schreck KC, Grossman SA. Role of temozolomide in the treatment of cancers involving the central nervous system. Oncology (Williston Park). 2018;32:555-560.
7. Ortiz R, Perazzoli G, Cabeza L, Jiménez-Luna C, Luque R, Prados J, Melguizo C. Temozolomide: An updated overview of resistance mechanisms, nanotechnology advances and clinical applications. Curr Neuropharmacol. 2021;19:513-537.
8. Butler M, Pongor L, Su YT, Xi L, Raffeld M, Quezado M, Trepel J, Aldape K, Pommier Y, Wu J. MGMT Status as a clinical biomarker in glioblastoma. Trends Cancer. 2020;6:380-391.
9. Caccese M, Ius T, Simonelli M, Fassan M, Cesselli D, Dipasquale A, Cavallin F, Padovan M, Salvalaggio A, Gardiman MP, Skrap M, Zagonel V, Lombardi G. Mismatch-repair protein expression in high-grade gliomas: A large retrospective multicenter study. Int J Mol Sci. 2020;21:6716.
10. Garnier D, Meehan B, Kislinger T, Daniel P, Sinha A, Abdulkarim B, Nakano I, Rak J. Divergent evolution of temozolomide resistance in glioblastoma stem cells is reflected in extracellular vesicles and coupled with radiosensitization. Neuro Oncol. 2018;20:236-248.
11. Daniel P, Sabri S, Chaddad A, Meehan B, Jean-Claude B, Rak J, Abdulkarim BS. Temozolomide ınduced hypermutation in glioma: Evolutionary mechanisms and therapeutic opportunities. Front Oncol. 2019;9:41.
12. Wu K, Fan J, Zhang L, Ning Z, Zeng J, Zhou J, Li L, Chen Y, Zhang T, Wang X, Hsieh JT, He D. PI3K/Akt to GSK3β/β-catenin signaling cascade coordinates cell colonization for bladder cancer bone metastasis through regulating ZEB1 transcription. Cell Signal. 2012;24:2273-2282.
13. Zhang P, Sun Y, Ma L. ZEB1: at the crossroads of epithelial-mesenchymal transition, metastasis and therapy resistance. Cell Cycle. 2015;14:481-487.

14. Kammerud SC, Metge BJ, Elhamamsy AR, Weeks SE, Alsheikh HA, Mattheyses AL, Shevde LA, Samant RS. Novel role of the dietary flavonoid fisetin in suppressing rRNA biogenesis. Lab Invest. 2021;101:1439-1448.

15. Cragg GM, Newman DJ. Plants as a source of anti-cancer agents. J Ethnopharmacol. 2005;100:72-79.

16. Li J, Liu H, Ramachandran S, Waypa GB, Yin JJ, Li CQ, Han M, Huang HH, Sillard WW, Vanden Hoek TL, Shao ZH. Grape seed proanthocyanidins ameliorate Doxorubicin-induced cardiotoxicity. Am J Chin Med. 2010;38:569-584.

17. Imran M, Saeed F, Gilani SA, Shariati MA, Imran A, Afzaal M, Atif M, Tufail T, Anjum FM. Fisetin: An anticancer perspective. Food Sci Nutr. 2020;9:3-16.

18. Singh N, Miner A, Hennis L, Mittal S. Mechanisms of temozolomide resistance in glioblastoma- a comprehensive review. Cancer Drug Resist. 2021;4:17-43.

19. Zhang XJ, Jia SS. Fisetin inhibits laryngeal carcinoma through regulation of AKT/NF-κB/mTOR and ERK1/2 signaling pathways. Biomed Pharmacother. 2016;83:1164-1174.

20. Pal HC, Diamond AC, Strickland LR, Kappes JC, Katiyar SK, Elmets CA, Athar M, Afaq F. Fisetin, a dietary flavonoid, augments the anti-invasive and anti-metastatic potential of sorafenib in melanoma. Oncotarget. 2016;7:1227-1241.

21. Pak F, Oztopcu-Vatan P. Fisetin effects on cell proliferation and apoptosis in glioma cells. Z Naturforsch C J Biosci. 2019;74:295-302.

22. Beltzig L, Christmann M, Kaina B. Abrogation of cellular senescence ınduced by temozolomide in glioblastoma cells: Search for senolytics. Cells. 2022;11:2588.

23. Lee SY. Temozolomide resistance in glioblastoma multiforme. Genes Dis. 2016;3:198-210.

24. Soni V, Adhikari M, Lin L, Sherman JH, Keidar M. Theranostic potential of adaptive cold atmospheric plasma with temozolomide to checkmate glioblastoma: An *in vitro* study. Cancers (Basel). 2022;14:3116.

25. Ercelik M, Tekin C, Tezcan G, Ak Aksoy S, Bekar A, Kocaeli H, Taskapilioglu MO, Eser P, Tunca B. Olea europaea leaf phenolics oleuropein, hydroxytyrosol, tyrosol, and rutin induce apoptosis and additionally affect temozolomide against glioblastoma: In particular, oleuropein inhibits spheroid growth by attenuating stem-like cell phenotype. Life (Basel). 2023;13:470.

26. Tezcan G, Tunca B, Bekar A, Preusser M, Berghoff AS, Egeli U, Cecener G, Ricken G, Budak F, Taskapılıoglu MO, Kocaeli H, Tolunay S. microRNA expression pattern modulates temozolomide response in GBM tumors with cancer stem cells. Cell Mol Neurobiol. 2014;34:679-92.

27. Lee ES, Ko KK, Joe YA, Kang SG, Hong YK. Inhibition of STAT3 reverses drug resistance acquired in temozolomide-resistant human glioma cells. Oncol Lett. 2011;2:115-121.

28. St-Coeur PD, Poitras JJ, Cuperlovic-Culf M, Touaibia M, Morin P Jr. Investigating a signature of temozolomide resistance in GBM cell lines using metabolomics. J Neurooncol. 2015;125:91-102.

29. Chen B, Li X, Wu L, Zhou D, Song Y, Zhang L, Wu Q, He Q, Wang G, Liu X, Hu H, Zhou W. Quercetin suppresses human glioblastoma migration and invasion via GSK3β/β-catenin/ZEB1 signaling pathway. Front Pharmacol. 2022;13:963614.

30. Pérès EA, Gérault AN, Valable S, Roussel S, Toutain J, Divoux D, Guillamo JS, Sanson M, Bernaudin M, Petit E. Silencing erythropoietin receptor on glioma cells reinforces efficacy of temozolomide and X-rays through senescence and mitotic catastrophe. Oncotarget. 2015;6:2101-2119.

31. Mesfin FB, Al-Dhahir MA. Gliomas. In: StatPearls [Internet]. Treasure Island (FL): StatPearls Publishing; 2023.

32. Hegi ME, Liu L, Herman JG, Stupp R, Wick W, Weller M, Mehta MP, Gilbert MR. Correlation of O6-methylguanine methyltransferase (MGMT) promoter methylation with clinical outcomes in glioblastoma and clinical strategies to modulate MGMT activity. J Clin Oncol. 2008;26:4189-4199.

33. Parker NR, Hudson AL, Khong P, Parkinson JF, Dwight T, Ikin RJ, Zhu Y, Cheng ZJ, Vafaee F, Chen J, Wheeler HR, Howell VM. Intratumoral heterogeneity identified at the epigenetic, genetic and transcriptional level in glioblastoma. Sci Rep. 2016;6:22477.

34. Bocangel DB, Finkelstein S, Schold SC, Bhakat KK, Mitra S, Kokkinakis DM. Multifaceted resistance of gliomas to temozolomide. Clin Cancer Res. 2002;8:2725-2734.

35. Alves ALV, Gomes INF, Carloni AC, Rosa MN, da Silva LS, Evangelista AF, Reis RM, Silva VAO. Role of glioblastoma stem cells in cancer therapeutic resistance: a perspective on antineoplastic agents from natural sources and chemical derivatives. Stem Cell Res Ther. 2021;12:206.

36. Wick W, Weller M, van den Bent M, Sanson M, Weiler M, von Deimling A, Plass C, Hegi M, Platten M, Reifenberger G. MGMT testing—the challenges for biomarker-based glioma treatment. Nat Rev Neurol. 2014;10:372-385.

37. Guo P, Feng YY. Anti-inflammatory effects of kaempferol, myricetin, fisetin and ibuprofen in neonatal rats. Trop J Pharm Res. 2017;16:1819-1826.

38. Seal I, Sil S, Das A, Roy S. Assessment of toxicity and genotoxic safety profile of novel fisetin ruthenium-p-cymene complex in mice. Toxicol Res. 2022;39:213-229.

39. Hassan SSU, Samanta S, Dash R, Karpiński TM, Habibi E, Sadiq A, Ahmadi A, Bunagu S. The neuroprotective effects of fisetin, a natural flavonoid in neurodegenerative diseases: Focus on the role of oxidative stress. Front Pharmacol. 2022;13:1015835.

40. Sari EN, Soysal Y. Molecular and therapeutic effects of fisetin flavonoid in diseases. J Basic Clin Health Sci. 2020;4:190-196.

41. Krasieva TB, Ehren J, O'Sullivan T, Tromberg BJ, Maher P. Cell and brain tissue imaging of the flavonoid fisetin using label-free two-photon microscopy. Neurochem Int. 2015;89:243-248.

42. Zheng HC. The molecular mechanisms of chemoresistance in cancers. Oncotarget. 2017;8:59950-59964.

43. Perazzoli G, Prados J, Ortiz R, Caba O, Cabeza L, Berdasco M, Gónzalez B, Melguizo C. Temozolomide resistance in glioblastoma cell lines: Implication of MGMT, MMR, P-glycoprotein and CD133 expression. PLoS One. 2015;10:e0140131.

44. Teraiya M, Perreault H, Chen VC. An overview of glioblastoma multiforme and temozolomide resistance: can LC-MS-based proteomics reveal the fundamental mechanism of temozolomide resistance? Front Oncol. 2023;13:1166207.

45. Kim T, Veronese A, Pichiorri F, Lee TJ, Jeon YJ, Volinia S, Pineau P, Marchio A, Palatini J, Suh SS, Alder H, Liu CG, Dejean A, Croce CM. p53 regulates epithelial-mesenchymal transition through microRNAs targeting ZEB1 and ZEB2. J Exp Med. 2011;208:875-883.

46. Edwards LA, Kim S, Madany M, Nuno M, Thomas T, Li A, Berel D, Lee BS, Liu M, Black KL, Fan X, Zhang W, Yu JS. ZEB1 is a transcription factor that is prognostic and predictive in diffuse gliomas. Front Neurol. 2019;9:1199.

47. Bjorland LS, Dæhli Kurz K, Fluge Ø, Gilje B, Mahesparan R, Sætran H, Ushakova A, Farbu E. Butterfly glioblastoma: Clinical characteristics, treatment strategies and outcomes in a population-based cohort. Neurooncol Adv. 2022;4:vdac102.

48. Sinha S, Avnon A, Perera A, Lavrador JP, Ashkan K. Butterfly gliomas: a time for stratified management? Neurosurg Rev. 2023;46:223.

49. Zhuo W, Zhang L, Zhu Y, Zhu B, Chen Z. Fisetin, a dietary bioflavonoid, reverses acquired cisplatin-resistance of lung adenocarcinoma cells through MAPK/survivin/caspase pathway. Am J Transl Res. 2015;7:2045-2052.

50. Kahlert UD, Maciaczyk D, Doostkam S, Orr BA, Simons B, Bogiel T, Reithmeier T, Prinz M, Schubert J, Niedermann G, Brabletz T, Eberhart CG, Nikkhah G, Maciaczyk J. Activation of canonical WNT/β-catenin signaling enhances *in vitro* motility of glioblastoma cells by activation of ZEB1 and other activators of epithelial-to-mesenchymal transition. Cancer Lett. 2012;325:42-53.

51. Pérez G, López-Moncada F, Indo S, Torres MJ, Castellón EA, Contreras HR. Knockdown of ZEB1 reverses cancer stem cell properties in prostate cancer cells. Oncol Rep. 2021;45:58.

52. Zhang Y, Wang X, Li A, Guan Y, Shen P, Ni Y, Han X. PP2A regulates metastasis and vasculogenic mimicry formation via PI3K/AKT/ZEB1 axis in non-small cell lung cancers. J Pharmacol Sci. 2022;150:56-66.

53. Li J, Gong X, Jiang R, Lin D, Zhou T, Zhang A, Li H, Zhang X, Wan J, Kuang G, Li H. Fisetin inhibited growth and metastasis of triple-negative breast cancer by reversing epithelial-to-mesenchymal transition via PTEN/Akt/GSK3β signal pathway. Front Pharmacol. 2018;9:772.

54. Min KJ, Nam JO, Kwon TK. Fisetin Induces Apoptosis Through p53-Mediated Up-Regulation of DR5 expression in human renal carcinoma caki cells. Molecules. 2017;22:1285.

Turk J Pharm Sci 2025;22(6):381-392
DOI: 10.4274/tjps.galenos.2025.57455

ORIGINAL ARTICLE

Development and Optimization of Electrospun Poly(vinyl alcohol) Nanofibers for Vaginal Drug Delivery Using Design of Experiments Approach

Sinem SAAR, Fatmanur TUĞCU-DEMİRÖZ*, Füsun ACARTÜRK

Gazi University Faculty of Pharmacy, Department of Pharmaceutical Technology, Ankara, Türkiye

ABSTRACT

Objectives: Vaginal nanofibers with high surface area and tunable porosity are a promising platform for vaginal administration. Poly(vinyl alcohol) (PVA) is a widely used polymer in the pharmaceutical field due to its hydrophilic, biodegradable, non-toxic, and mucoadhesive properties. This study aimed to optimize PVA-based electrospun nanofibers for vaginal drug delivery by evaluating polymer concentration, solvent system, and collector rotation speed using a design of experiments-based approach.

Materials and Methods: PVA was dissolved in distilled water (DW) at 90 °C to prepare polymer solutions; then N, N-dimethylformamide (DMF) or ethanol was added. The surface tension, viscosity, and conductivity of the polymer solutions were evaluated. For the production of nanofibers via electrospinning, the parameters selected were PVA concentrations of 7.5% and 15%, collector rotation speed of 100 and 1000 rpm, and two solvent systems (DMF: DW and ethanol: DW). Mechanical and mucoadhesive properties of nanofibers were evaluated using a texture analyzer.

Results: Viscosity and conductivity increased as polymer concentration increased. An increase in PVA concentration resulted in increased tensile strength of the nanofibers, from 1.41±0.07 to 3.92±0.14 MPa (p<0.0001). Nanofiber diameters ranged from 196±41 nm to 1721±114 nm (p<0.0001). All formulations exhibited complete wettability with contact angles of 0°. *Ex vivo* mucoadhesion studies revealed that collector rotation speed influenced the work of adhesion, with the highest mucoadhesion observed for the R3 formulation produced at 1000 rpm.

Conclusion: The solvent system and collector rotation speed were found to influence the morphological structure of the fibers. R3 (7.5% PVA, ethanol/DW, 1000 rpm) formulation was found to be more suitable than other formulations based on its mechanical and mucoadhesive properties. It was concluded that in the production of PVA nanofibers, the rotating speed of the collector, the polymer concentration, and the solvent system directly affect the mechanical and mucoadhesive properties of the nanofibers.

Keywords: Design of experiments, electrospinning, nanofiber, poly(vinyl alcohol), vaginal drug delivery

INTRODUCTION

The vaginal route offers several advantages, including a large specific surface area with rich vascularization and perfusion; convenient self-administration; suitability for both local and systemic therapy; and circumvention of the hepatic first-pass metabolism, thereby potentially reducing hepatic exposure and limiting adverse effects associated with oral dosing.[1-8] A critical consideration in the development of vaginally administered products is user preference and acceptability. The acceptability of such products depends on multiple factors, including ease of use, mode of administration, therapeutic efficacy, and potential adverse effects.[9] Factors such as formulation design, applicator type, and packaging are also critical to ensuring user adherence. The biocompatibility and tolerability of excipients warrant particular consideration, especially when the vaginal mucosa is compromised or the product is intended to treat mucosal lesions associated with microbial or viral pathologies.[10]

***Correspondence:** fatmanur@gazi.edu.tr, **ORCID-ID:** orcid.org/0000-0002-9468-3329
Received: 23.08.2025, **Accepted:** 19.12.2025 **Publication Date:** 30.012026

Cite this article as: SAAR S, TUĞCU-DEMİRÖZ F, ACARTÜRK F. Development and optimization of electrospun poly(vinyl alcohol) nanofibers for vaginal drug delivery using design of experiments approach. Turk J Pharm Sci. 2025;22(6):381-392

The pursuit of controlled drug release, targeted delivery, and improved drug stability has intensified interest in nanotechnology-based drug delivery systems.[11] Among various nanocarriers, nanofibers offer unique advantages in multiple applications owing to their porous structure, which closely resembles that of natural biological tissues.[12] Nanofibers have been extensively investigated for use in drug delivery systems, filtration media, face masks, tissue engineering scaffolds, and wound dressings. High surface-area-to-volume ratio, porosity, tunable pore size, adjustable surface characteristics, and favorable mechanical properties of nanofibers provide significant benefits for diverse biomedical applications.[13] Production of nanofibers from synthetic or natural polymers, or their blends, offers versatility in composition, enabling optimization for specific drug delivery applications.[14,15]

Vaginally administered dosage forms include gels, creams, films, rings, tablets, sponges, and suppositories. Semi-solid and liquid vaginal dosage forms, such as gels, creams, and solutions, may suffer from drawbacks including leakage, messiness, and limited residence time at the site of application, which can negatively impact patient compliance and therapeutic efficacy.[16] Nanofibers are a solid dosage form that can mitigate spillage and leakage associated with liquid- or gel-based formulations. Nanofibers can be integrated into composite drug carriers and combined with other dosage forms, such as films, sponges, and 3D-printed scaffolds.[17]

Nanofibers can be produced using various techniques, including electrospinning, template synthesis, phase separation, polymerization, and melt blowing. Among these, electrospinning is the simplest and most suitable method, employing electrostatic forces as the driving mechanism for fiber formation. It is a versatile and scalable technique capable of producing polymeric nanofibers with diameters ranging from nanometers to micrometers.[18] The electrospinning method relies on generating electrostatic charges in a polymer solution by applying a high voltage.[19] Multiple parameters influence the electrospinning process: solution variables (polymer concentration, viscosity, surface tension, conductivity), process variables (applied voltage, flow rate, tip-to-collector distance), collector variables (stationary or rotating collectors, rotation speed), nozzle variables (uniaxial, coaxial, triaxial, needleless), and environmental factors (temperature, humidity). These parameters directly affect the production of smooth, bead-free fibers. By appropriately controlling these factors, fibers with desired morphologies and diameters can be obtained.[20]

Vaginal drug delivery systems are commonly formulated with polymeric carriers to enhance efficacy and prolong absorption and retention in vaginal mucosal cells.[21] Poly(vinyl alcohol) (PVA) is a synthetic, semicrystalline polymer that is highly hydrophilic, non-toxic, and biocompatible with excellent properties, including durability, water solubility, gas permeability, mechanical properties, and thermal stability.[22-24] PVA is a versatile polymer widely employed in oral, buccal, and vaginal drug delivery applications. PVA nanofibers have been reported as fish-oil-encapsulated formulations produced by emulsion electrospinning for oral administration; doxorubicin-loaded PVA/polycaprolactone (PCL) coaxial fibers for cervical cancer treatment; and PEGylated paclitaxel nanocrystal-loaded PVA fibers for cervical cancer treatment via vaginal administration.[25-28] Using PVA as a surface stabilizer or modifying its surface with polyethylene glycol (PEG) chains contributes to vaginal adhesion and enhances binding to the hydrophobic domains of mucin, thereby facilitating rapid diffusion through the cervicovaginal mucus.[29] Sharma et al.[30] developed fluconazole-loaded PVA nanofibers for the treatment of vaginal candidiasis. Beyond pharmaceutical applications, PVA nanofibers have been used in sensors, catalysis, and filtration technologies.[31-33] The properties of PVA-based nanofibers vary markedly with the chosen fabrication technique and associated process parameters.[34]

Despite extensive research on electrospun systems for mucosal delivery, there remains a need for systematically optimized, mechanically robust, and mucoadhesive nanofiber platforms designed for vaginal delivery. Most studies focus on drug-loaded systems without fully characterizing the mechanical integrity, wettability, and bioadhesion of nanofibers; formulation variables are key determinants of the applicability of vaginal products. Quality by Design (QbD) is a systematic approach to product and process development in which objectives are predefined and a comprehensive understanding of critical quality attributes and process parameters is prioritized. This strategy enables the formulation and manufacturing of products in compliance with required safety, efficacy, and quality standards, and the consistent analysis of products with the necessary accuracy and precision.[35] In nanofiber production, testing the influence of every parameter by random selection and measurement would be time-consuming and impractical; therefore, the design of experiments (DoE) approach was employed. In this context, the target product profile of the system was defined to include mechanical strength greater than 1 MPa, elongation at break exceeding 50%, and suitability for vaginal administration. DoE-guided optimization of PVA nanofibers provides a critical foundation for developing next-generation vaginal dosage forms with predictable performance, scalable manufacturing processes, and improved user acceptance.[35]

In this study, we aimed to develop and optimize PVA electrospun nanofiber formulations for vaginal drug delivery using a DoE approach. The effects of polymer concentration, solvent system, and collector rotation speed on the mechanical and mucoadhesive properties of the nanofibers were systematically investigated to identify the optimal formulation for potential vaginal application. This study employs a quantitative approach based on DoE to elucidate the relationships among polymer concentration, solvent system, and process parameters in PVA-based vaginal nanofibers. This evaluation provides a predictive design framework for vaginal PVA nanofibers, representing a quantitative structure-performance relationship that has not previously been demonstrated.

MATERIALS AND METHODS

Material

Polyviol 13/140 (49.000 Da) was purchased from Wacker Chemie AG. N, N-dimethylformamide (DMF) and ethanol were purchased from Sigma-Aldrich. All chemicals were of analytical grade. Distilled water (DW) was used for all studies.

Preparation of the polymer solutions

For solution preparation, PVA was first dispersed in the aqueous phase and heated to 90 °C under magnetic stirring at 500 rpm to ensure complete dissolution. After the polymer was fully solubilized, either ethanol or DMF was added to obtain a homogeneous solution. In all formulations, ethanol/DW and DMF/DW solvent systems were used at a 1:1 ratio. For nanofiber formulations, tensile strength values greater than 1 MPa and elongation at break exceeding 50% are generally desirable. In the present study, polymer concentration, collector rotation speed, and solvent system were selected as independent variables for the DoE model. Considering these parameters, a 2^3 factorial experimental design was applied using Design Expert® 13 software (Stat-Ease Inc., Minneapolis, MN, USA). The Tensile strength and elongation at break of the nanofiber formulations were chosen as dependent variables to determine the optimal formulation. Table 1 summarizes the design parameters and the corresponding nanofiber formulations.

Characterization of electrospinning solutions

Polymer solutions were characterized for electrospinning by measuring viscosity, conductivity, and surface tension. In electrospinning, the transfer of electric charge from the electrode to the polymer droplet requires a minimum electrical conductivity of the solution. Conductivity measurements were performed using a Seven2Go Cond meter S3 (Mettler Toledo, UK) by immersing the probe in the polymer solution. All measurements were carried out at room temperature and were expressed in µS/cm.[36]

Surface tension plays a critical role in the electrospinning process.[37] During nanofiber formation by electrospinning, jet initiation occurs when the polymer solution exhibits sufficient surface tension. In this study, surface tension measurements were performed using the pendant drop method (Attension-Theta Lite, Biolin Scientific, Finland). In this method, an image of a droplet of the polymer mixture suspended from the tip of a syringe needle is captured by the instrument. The droplet remains suspended due to the balance between gravitational forces and the liquid's surface tension; this equilibrium configuration was analyzed to determine the surface tension. Surface tensions were calculated using the Young-Laplace equation.[38]

In the electrospinning process, solution flow and fiber production are impeded when viscosity is high, whereas continuous, uniform fibers from polymer solutions with low viscosity cannot be formed. The viscosities of the polymer solutions were measured using a cone-plate viscometer (Brookfield, DV-III Rheometer with spindle type CPE-41, USA). Experiments were performed using 0.5 mL of the sample. All measurements were conducted at room temperature using spindle 52 at a constant shear rate of $100s^{-1}$.[39]

Electrospinning method

The polymer solutions were electrospun using an NE300 electrospinning apparatus equipped with a rotating drum collector. Electrospinning was carried out using a standard uniaxial stainless-steel needle connected to the high-voltage power supply. The solutions were loaded into 10-mL syringes, and voltages of 15-25 kV were tested for jet formation. The tip-to-collector distance was adjusted between 10 and 20 cm, depending on the solvent system, to ensure adequate solvent evaporation. The collector collector rotation speed was set to between 100 and 1,000 rpm, according to the formulation. After optimizing the distance and collector rotation speed, different feed rates were tested according to polymer concentration to produce fibers (Table 2).

Morphological studies

The fiber morphology of the formulations was characterized by scanning electron microscopy (SEM) (FEI Company, Quanta 400 F, USA). Diameters of the electrospun nanofibers were measured from SEM images using ImageJ software (National Institutes of Health, USA).[40] After importing the images into the software, fiber diameters were measured using the image scale. For each sample, 100 individual fibers were measured

Table 1. DoE parameters and content of nanofiber formulations

Formulations	Polymer concentration (X_1)	Solvent system (X_2)	Collector rotation speed (X_3)
R1	7.5%	Ethanol/DW	100 rpm
R2	7.5%	DMF/DW	100 rpm
R3	7.5%	Ethanol/DW	1000 rpm
R4	15%	DMF/DW	1000 rpm
R5	15%	Ethanol/DW	1000 rpm
R6	15%	DMF/DW	100 rpm
R7	7.5%	DMF/DW	1000 rpm
R8	15%	Ethanol/DW	100 rpm

DoE: Design of experiments, DW: Distilled water, DMF: N,N-dimethylformamide

Table 2. Process parameters used in the electrospinning of nanofiber formulations

Formulation code	Voltage (kV)	Feed rate (mL/h)	Distance (mm)	Rotating speed (rpm)
R1	19.5	1.3	110	100
R2	20	1	100	100
R3	18.5	1	110	1000
R4	19	0.8	130	1000
R5	18	0.8	130	1000
R6	17.5	0.7	110	100
R7	19.5	0.9	105	1000
R8	17.5	0.5	120	100

to calculate the mean diameter and examine the fiber size distribution. Diameter distribution histograms were generated using OriginPro® (Origin Lab, USA). For porosity analyses, SEM images were converted to binary (black-and-white) format, and the percentage of void area relative to the total image area was calculated using ImageJ software.

Mechanical properties of nanofibers

The mechanical properties of the nanofibers were evaluated using a Texture Analyser TA-XT equipped with a mini tensile grip. Nanofiber samples were cut into strips measuring 3×1 cm and clamped between the grips. While the lower grip remained stationary, the upper grip moved upward at a crosshead speed of 5 mm/min. The elongation at break and tensile strength were calculated using the instrument's software. On stress-strain curves, the maximum value on the x-axis represents elongation at break, while the maximum value on the y-axis corresponds to tensile strength. All measurements were performed in triplicate.[41]

Contact angle measurements

An optical tensiometer was used for contact angle measurements (Attension-Theta Lite, Biolin Scientific, Finland). Contact angle measurements were performed by placing a droplet of liquid on the material surface and monitoring changes in droplet shape and dimensions over time using optical imaging systems. During the measurements, a 5 µL droplet of DW was deposited onto the nanofiber surface, and changes in the contact angle were monitored. A convex sample holder was used to ensure a smooth and uniform nanofiber surface for accurate imaging.[42] All measurements were performed in triplicate for each nanofiber formulation.

Ex vivo mucoadhesion studies

The mucoadhesive properties of the nanofibers were evaluated using a Texture Analyser TA-XT. Cow vaginal tissue was selected for experiments because of its large surface area and was stored at -20 °C until use. The mucoadhesion study was conducted under previously validated test conditions.[43] Nanofiber samples were cut and affixed to the upper probe. The cow's vaginal tissue was placed at the bottom. The probe was moved at a predetermined speed to make contact with the vaginal tissue. The software calculated the mucoadhesion work value from the distance-force curve.[44] For each measurement, fresh tissue was used, and all tests were performed in triplicate. The TA.XT.Plus Texture Analyser software calculated the work of adhesion (expressed in N·mm). The work of mucoadhesion was calculated using the following equation:

$$\text{Work of mucoadhesion} = \frac{AUC}{\pi r^2} \quad (1)$$

AUC: Area under the curve

πr^2: Area in contact with the formulation and tissue (1,1304 cm^2)

Statistical analysis

GraphPad Prism version 7.0 (GraphPad Software Inc., San Diego, CA, USA) was used for all statistical analyses. Data were expressed as mean ± standard deviation. Parametric tests were applied throughout the study. Comparisons between two groups were conducted using the unpaired t-test, whereas differences among more than two groups were assessed by one-way analysis of variance (ANOVA). Following ANOVA, Dunnett's T3 test was used for comparisons against a control group, and Tukey's HSD test was employed for pairwise post hoc analyses when appropriate. A 95% confidence interval was adopted, and p-values <0.05 were considered statistically significant. Statistical significance levels were indicated as: ns ($p \geq 0.05$), *$p<0.05$, **$p<0.01$, ***$p<0.001$, and ****$p<0.0001$).

RESULTS

Characterization of polymer solutions

Characterization results for the polymer solutions prepared for the nanofiber formulations are presented in Table 3. Viscosity values increased with increasing polymer concentration, with the highest viscosity observed in formulations containing 15% PVA. Surface tension values varied with the solvent system; ethanol-DW mixtures exhibited lower values than DMF-DW mixtures. Conductivity was also influenced by solvent composition: DMF-DW systems showed higher conductivity than ethanol-DW systems. These characterization results were used to guide the selection of electrospinning process parameters. R1/R3, R2/R7, R4/R6, and R5/R8 share the same formulation; only the electrospinning processing parameters differ. Consequently, viscosity, conductivity, and surface tension are shared values within each pair.

Table 3. Characterization results of polymer solutions (n=3, mean ± SD)

Formulation code		Viscosity (cP.s)	Conductivity (µS/cm)	Surface tension ($mN.m^{-1}$)
R1	R3	395±26	149.8±1.2	30.98±0.15
R2	R7	219±0	158.4±0.4	42.34±0.10
R4	R6	2497±0	226.2±0.7	41.97±0.07
R5	R8	2672±0	212.2±0.8	32.97±0.15

SD: Standard deviation

Morphological studies

SEM imaging revealed that electrospun PVA nanofiber formulations exhibited continuous, bead-free fiber structures with smooth surfaces (Figure 1). Fiber diameters varied among the formulations, with finer and more uniform fibers observed in formulations containing lower polymer concentrations and a DMF-DW solvent system. In contrast, higher polymer concentrations and ethanol-DW systems tended to produce thicker fibers with a broader diameter distribution. Images at 10,000× magnification confirmed the absence of morphological defects and enabled clear visualization of the fiber surface texture.

The mean fiber diameters obtained from SEM image analysis are presented in Table 4. The smallest average diameter was observed for R2 (196±41 nm), formulated with 7.5% PVA in DMF-DW, whereas the largest diameter was recorded for R5 (1721±114 nm), formulated with 15% PVA in ethanol-DW. Formulations prepared with DMF-DW generally produced finer fibers (196-529 nm) compared to those with ethanol-DW (310-1721 nm). Lower polymer concentration (7.5%) tended to produce more uniform fibers, while higher concentration (15%) resulted in thicker fibers and broader diameter distributions. Porosity values ranged from 57.18% (R5) to 88.01% (R1), with higher porosity generally associated with smaller fiber diameters. These results indicate that both polymer concentration and the solvent system play critical roles in determining fiber morphology and porosity.

Mechanical properties of nanofibers

The tensile strength and elongation at break values of the PVA nanofiber formulations are presented in Figure 2. Tensile strength ranged from 1.41±0.07 MPa (R1) to 3.92±0.14 MPa (R6) ($p<0.0001$). Formulations with higher polymer concentration generally exhibited higher tensile strength than those with lower concentration. Elongation at break values varied widely among the formulations, with the highest values observed in R8 (124.77±9.78%) and R7 (121.73±21.96%), and the lowest in R2 (23.95±2.12%). Higher elongation values were typically associated with higher polymer concentrations. This effect was more evident in formulations prepared with ethanol-DW solvent systems, indicating a relationship between solvent composition and fiber flexibility. These findings indicate that polymer concentration, solvent system, and collector rotation speed collectively influence the mechanical performance of electrospun PVA nanofibers.

The findings determined using the DoE approach on the influence of process parameters on nanofiber properties are presented in Table 5. A 2^3 (two-level, three-factor) factorial design was implemented using Design Expert software to identify the optimal processing parameters, resulting in eight formulations. Tensile strength and elongation at break values obtained from these formulations were statistically analyzed to evaluate the effects of the independent variables on the mechanical properties of the nanofibers. 3D surface plots are presented in Figure 3. Based on the factorial-design analysis, the tensile strength of PVA nanofibers was described by the following equation: tensile strength = 2.563875 + 0.971875 × A (concentration). Similarly, elongation at break was expressed as 0.991000 + 7.20723 × A (concentration). These results demonstrate that polymer concentration (factor A) had a measurable influence on both the tensile strength and the elongation at break of the PVA nanofiber formulations.

Contact angle measurements

In the PVA nanofiber formulations, the contact angles were measured at 0° for all samples. This complete wettability is attributed to the highly hydrophilic nature of PVA, which facilitates immediate spreading of the water droplet upon contact with the fiber surface. The instantaneous absorption of the droplet into the nanofibers indicates strong surface affinity for aqueous media, suggesting that these formulations can rapidly interact with vaginal mucosal fluids, thereby promoting intimate contact and enhancing mucoadhesion.

Ex vivo mucoadhesion studies

The mucoadhesive properties of the PVA nanofiber formulations are presented in Figure 4. The work of mucoadhesion ranged from 0.014±0.010 mJ/cm^2 (R1) to 0.194±0.060 mJ/cm^2 (R3) ($p<0.0001$). Formulations containing a lower polymer concentration of 7.5% PVA and a higher collector rotation speed (1000 rpm) generally exhibited greater mucoadhesion than formulations produced at lower collector rotation speeds. The highest mucoadhesion value was observed in R3, while the lowest was found in R1. These results indicate that, in addition to polymer concentration, processing parameters such as collector rotation speed can markedly influence the mucoadhesive performance of PVA nanofibers.

The influence of processing parameters, particularly the collector rotation speed, on mucoadhesion can be attributed to their effects on fiber alignment and exposed surface area.

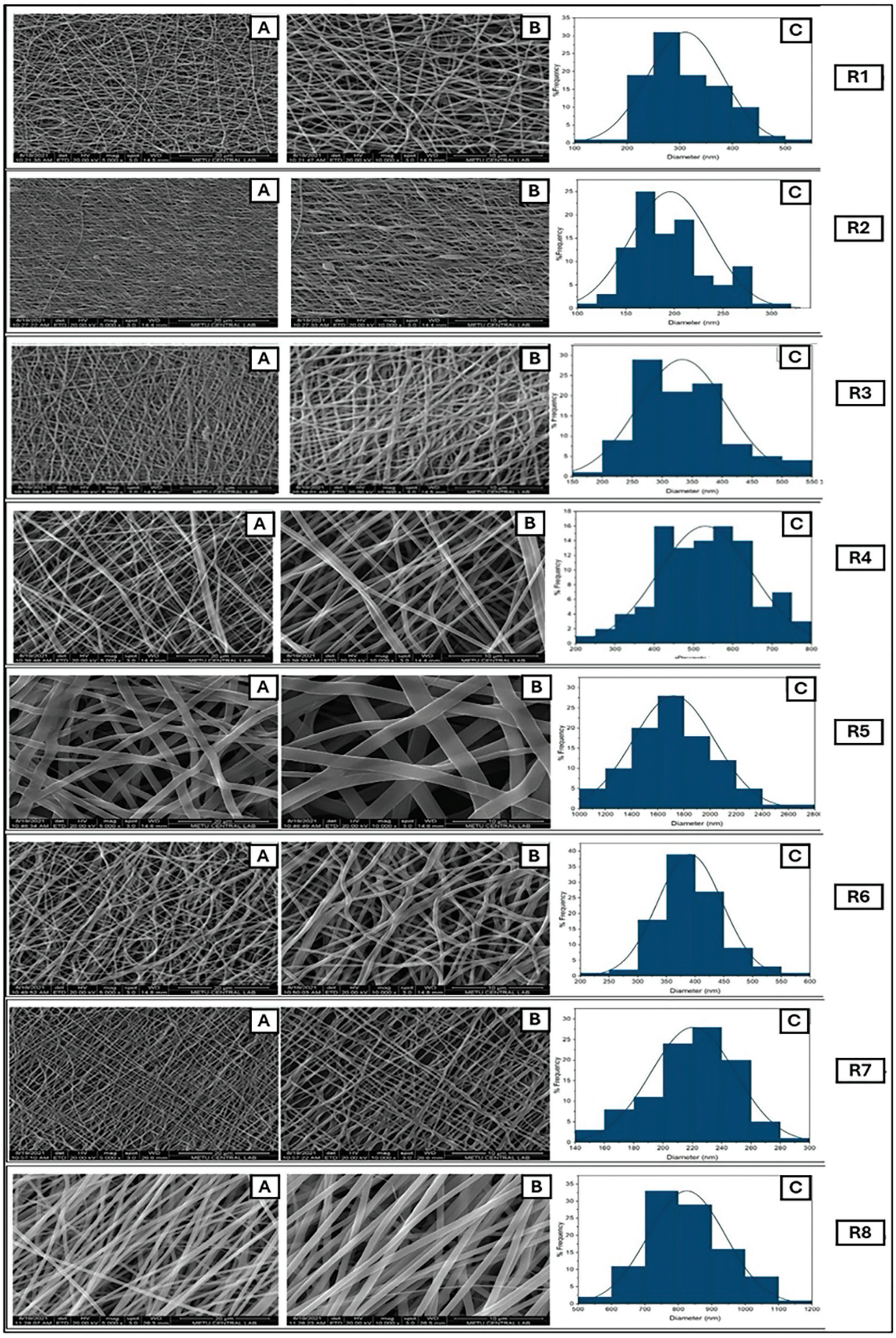

Figure 1. SEM images (a: 5000x magnification, b: 10,000x magnification) and fiber diameter distribution (c) of PVA nanofibers
SEM: Scanning electron microscopy, PVA: Poly(vinyl alcohol)

Higher rotation speeds tend to produce more uniformly aligned fibers, which may enhance the effective contact area with the mucosal surface and facilitate interfacial interactions between the hydrophilic PVA chains and mucin. This improved surface contact likely increases adhesive forces, thereby elevating the measured mucoadhesion work values. Moreover, higher rotation speeds tended to produce finer fibers. Finer fibers increase the specific surface area available for interaction with the mucosal surface.

DISCUSSION

The physicochemical characteristics of polymer solutions are critical determinants of spinnability and the morphological quality of electrospun nanofibers. Viscosity increased significantly with increasing polymer concentration ($p<0.05$). Haider and colleagues reported that increasing the concentration of the polymeric solution would increase the viscosity, which in turn would increase polymer chain entanglement.[19] This chain entanglement overcomes surface tension, resulting in homogeneous, bead-free electrospun nanofibers. In our study, as expected, viscosity increased with PVA concentration. Hameed et al.[45] developed cephalexin-loaded core-shell nanofibers from PVA-based biopolymers using emulsion electrospinning and reported fiber diameters in the range of 270-526 nm. Larger fiber diameters are associated with increased viscosity of the emulsion's oil phase.[45] In our study, the fiber diameters obtained with formulations R1 and R3, for 7.5% (*w/v*) polymer solutions prepared in the ethanol/DMF solvent system, were 310±71 nm and 334±74 nm, respectively ($p\geq0.05$). When the same solvent system was used, larger diameters of 1721±114 nm and 825±116 nm were obtained for formulations R5 and R8, respectively, at 15% concentration ($p<0.0001$). The increase in fiber diameter is due to the higher viscosity of the solution. These findings further confirm that viscosity influences jet stability and fiber thinning during electrospinning, and that solution rheology affects the final nanofiber morphology.

Table 4. Fiber diameter and porosity values of PVA nanofibers

Formulation code	Nanofiber diameter (mean ± SD)	Porosity (%)
R1	310±71	88.01
R2	196±41	73.92
R3	334±74	61.57
R4	529±119	65.45
R5	1721±114	57.18
R6	391±57	68.76
R7	220±29	75.98
R8	825±116	78.61

SD: Standard deviation, PVA: Poly(vinyl alcohol)

Table 5. Comparison of the effect of process parameters on the tensile strength of PVA nanofiber formulations based on ANOVA test.

Tensile strength				
Source	Sum of squares	Mean square	*f* value	*p* value
Model	7.56	7.56	168.5	<0.0001
A- Concentration	7.56	7.56	168.5	
Elongation at break				
Model	5843.72	5843.72	7.65	0.0326
A- Concentration	5843.72	5843.72	7.65	

ANOVA: Analysis of variance, PVA: Poly(vinyl alcohol)

Surface tension varied among formulations; ethanol-DW mixtures exhibited significantly lower surface tension than DMF-DW systems ($p<0.05$). Bonakdar and Rodrigue[46] stated that high surface tension can hinder the electrospinning process, causing instability, an increased tendency for jet breakup, and consequently the formation of beaded fibers. Lower surface tension facilitates electrostatic forces that support jet-based nanofiber formation, preventing bead formation and other defects, and resulting in a smoother, more homogeneous fiber morphology. Conversely, high surface tension in DMF-water mixtures can further inhibit jet formation and lead to defective fiber morphology. In the DMF-water formulation (R2), a few beads were observed, likely due to the higher surface tension, but the low frequency of beads in SEM images indicates that spinning was nearly stable. Khattab et al.[47] measured the surface tension of water-ethanol mixtures prepared by mixing the solvents in volumetric proportions. Varying the solvent composition altered surface tension. In our study, different surface values were obtained for water-ethanol and water-DMF mixtures. Solvent systems with lower surface tension promote more stable Taylor cone formation and continuous jet elongation, thereby improving nanofiber uniformity and reducing morphological defects.

Conductivity measurements revealed significantly higher values for DMF-DW formulations (R2/R7 and R4/R6) than for ethanol-DW formulations ($p<0.05$). Ergin et al.[48] showed that conductivity measurements in DMF-water mixtures increased with increasing DMF weight percentage. Spivey et al.[49] reported

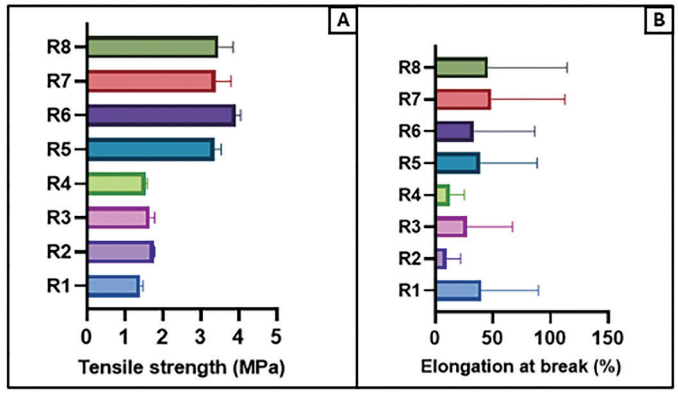

Figure 2. Tensile strength (a) and elongation at break values (b) of PVA nanofiber formulations (n=3, mean ± SD)

SD: Standard deviation, PVA: Poly(vinyl alcohol)

that increasing the ethanol concentration in water decreases the conductivity of various electrolyte solutions. These findings indicate that polymer concentration and solvent system have a measurable effect on the physicochemical properties of the electrospinning solutions. In the study conducted by Ge et al.,[50] increasing the PVA concentration caused an increase in conductivity values. In this study, it was 485.8±1.92 µS/cm at 8% PVA and 663.8±5.89 µS/cm at 15% PVA. Similarly, in our study, for 7.5% concentrations prepared using ethanol and DW, values of 149.8±1.2 µS/cm were obtained for R1 and R3, whereas values of 212.2±0.8 µS/cm were obtained for R5 and R8. At 7.5% concentration, prepared in DMF and DW, values of 158.4±0.4 µS/cm were obtained for R2 and R7, whereas values of 226.2±0.7 µS/cm were obtained for R4 and R6. Increasing concentration led to higher conductivity. These results demonstrate that both the solvent composition and the polymer concentration modulate the charge-carrying capacity of the electrospinning solution, thereby influencing jet stability and fiber formation; higher conductivity mixtures promote more efficient charge transfer.

One of the advantages of SEM is its high depth of field, which provides information on structures at various distances.[51] SEM is a valuable technique for evaluating the fundamental characteristics of nanofibers, such as fiber diameter, and for examining the effects that arise during the electrospinning process and that depend on factors such as polymer concentration and solution conductivity. Analysis of fiber diameter revealed significant differences among the formulations ($p<0.05$). The significant increase in fiber diameter observed with higher PVA concentration is consistent with previous studies, which showed that increased solution viscosity reduces jet stretching and produces thicker fibers. Zhang et al.[52] showed that increasing the concentration and viscosity of the PVA solution suppressed bead formation but increased fiber diameter. Similarly, the smaller fiber diameters obtained from DMF-DW systems are consistent with reports that higher-conductivity solvents enhance charge-carrying capacity, resulting in greater elongational forces on the jet and, consequently, finer fibers.[53] Electrospun nanofibers with small fiber diameters can be obtained from the solution with the highest conductivity. In contrast, ethanol-DW systems, with lower conductivity and higher surface tension, tend to produce thicker fibers, as observed in our R5 and R8 formulations. These results confirm that optimizing both polymer concentration and solvent system is crucial. The R3 formulation demonstrated improved performance by providing both the optimum fiber diameter and a bead-free morphology. In nanofiber production, fiber morphology varies depending on the applied voltage, flow

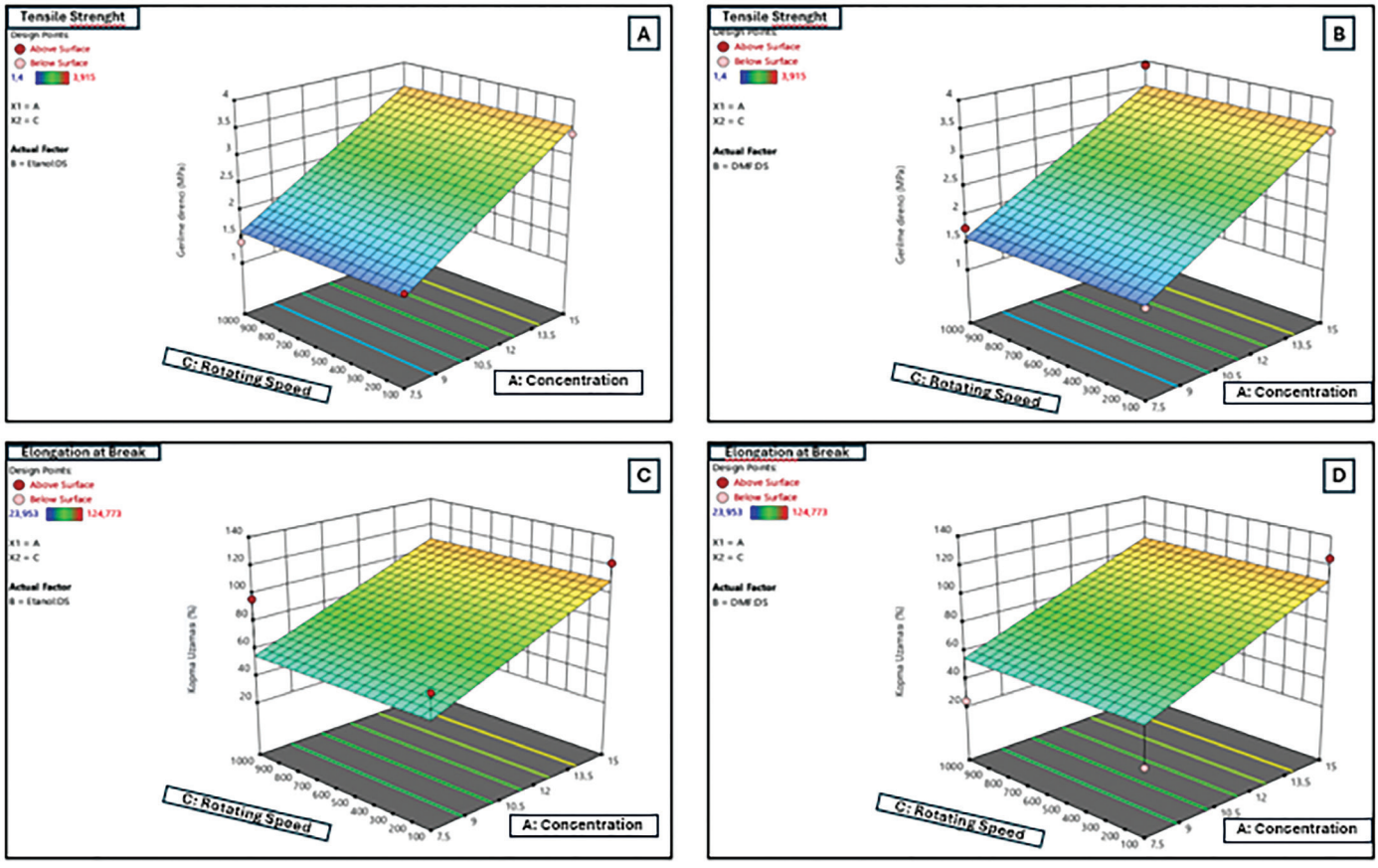

Figure 3. Three-dimensional surface plots illustrating the effect of process parameters on tensile strength and elongation at break of PVA nanofiber formulations prepared with ethanol-DW (a, c) and DMF-DW (b, d) solvent systems

DW: Distilled water, DMF: N,N-dimethylformamide, PVA: Poly(vinyl alcohol)

rate, and tip-to-collector distance. Environmental parameters such as relative humidity and ambient temperature, although not the focus of this study, are known to influence solvent evaporation rates and fiber morphology and may explain minor variations observed among replicate samples.[54]

The production parameters directly influence the morphology and mechanical properties of the nanofibers. The mechanical properties of nanofibers depend on the polymer type, crystallization rate, and crystallinity level.[55] The arrangement of the fibers on the collector during the production process, the interaction between the fibers, and excessive porosity affect the mechanical properties of the nanofibers. Our findings also indicate that collector rotation speed plays a critical role in determining fiber morphology; higher rotation speeds improve fiber alignment and reduce mean fiber diameter through enhanced mechanical stretching during deposition. Collector rotation speed emerged as another critical factor influencing mechanical performance. Higher rotation speeds promote fiber alignment, which is known to improve tensile strength. In the study by Wong et al.,[56] the tensile strength of electrospun PCL nanofiber was increased by decreasing the fiber diameter. They determined that reducing the fiber diameter improves crystallinity and molecular orientation, which explains the enhanced tensile properties of smaller-diameter fibers. In the study by Habeeb et al.,[57] nanofibers collected at high collector rotation speed exhibited greater tensile strength than those collected at low collector rotation speed. Similarly, in our study, formulations spun at 1000 rpm showed markedly higher elongation-at-break values, suggesting that improved fiber alignment not only enhances strength but also increases flexibility. Additionally, the influence of the solvent system on mechanical behavior can be indirectly explained by its effects on fiber morphology. DMF-water systems with higher conductivity likely produced fibers with fewer structural defects, thereby improving tensile properties. Ethanol-water systems, on the other hand, tend to produce thicker and less aligned fibers, explaining the relatively lower tensile strengths despite similar polymer content. Among the tested formulations, R3 demonstrated a favorable balance between tensile strength and elongation-at-break values, attributable to its smaller average fiber diameter and a high degree of fiber alignment achieved at 1000 rpm. For example, R3 exhibited a tensile strength of 1.657±0.133 MPa and an elongation at break of 73.12±6.15% with an average fiber diameter of 334±74 nm, while R1 showed a similar fiber diameter of 310±71 nm but a lower tensile strength of 1.412±0.065 MPa and a higher elongation at break of 96.20±21.50%, suggesting that alignment, rather than diameter alone, influences mechanical performance. These parameters suggest that R3 not only meets the mechanical strength required for the intended application but also maintains flexibility, making it a strong candidate for further development. These relationships emphasize that mechanical optimization in electrospun PVA systems should simultaneously consider solution composition, fiber alignment (*i.e.*, collector rotation speed), and the resulting morphological features.

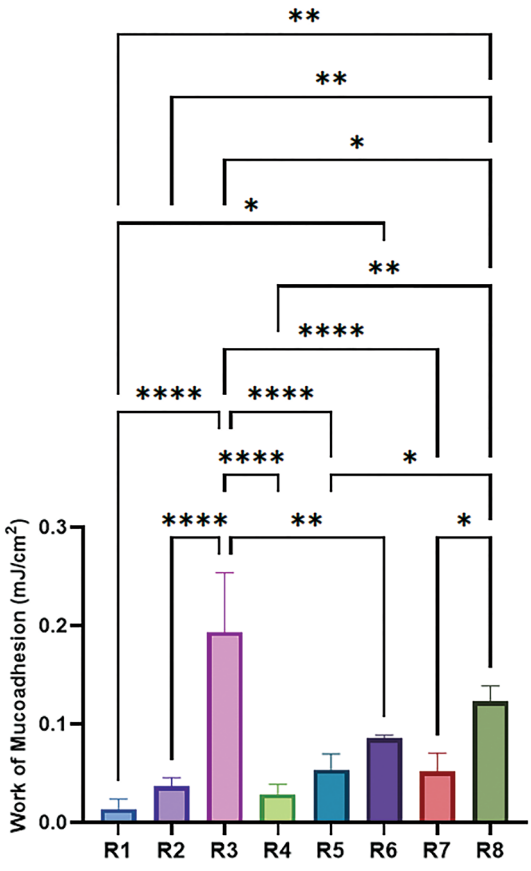

Figure 4. Work of Mucoadhesion of PVA nanofiber formulations measured on cow vaginal tissue (n=3, mean ± SD, p≥0.05, *p<0.05, **p<0.01, ***p<0.001, and ****p<0.0001)

SD: Standard deviation, PVA: Poly(vinyl alcohol)

Production parameters influenced the adhesive performance of PVA nanofibers. Formulations containing 7.5% PVA produced at a higher collector rotation speed (1000 rpm) exhibited significantly higher mucoadhesion compared to their lower-speed counterparts. This may be attributed to the reduced fiber diameter observed in these formulations, which increases the total surface area available for polymer-mucin interactions. Smaller fiber diameters increase the intimate contact with the mucosal surface, thereby supporting stronger adhesive forces. Dehydration theory proposes that the polymer absorbs water from the mucosa, creating a tighter contact with the mucosa and resulting in stronger adhesion. This effect allows the fibers to bond more strongly with the mucosa.[58] Furthermore, the solvent system influenced mucoadhesive strength. DMF-DW systems, which produced thinner fibers due to higher conductivity, generally exhibited superior mucoadhesion compared with ethanol-DW systems. R3 exhibited the highest work of mucoadhesion among all tested formulations, a result linked to its smaller fiber diameter, which increases the available surface area for polymer-mucin interactions. This suggests that solvents with higher conductivity promote electrostatic tension during spinning, creating thinner fibers that can more effectively penetrate the mucus layer. For instance, R3 achieved a work of mucoadhesion of 0.194±0.060 mJ/cm² with an average fiber diameter of 334±74 nm, whereas R1 exhibited only 0.014±0.010

mJ/cm² with an average fiber diameter of 310±71 nm. Similarly, among the 15% PVA formulations, R8 reached 0.123±0.016 mJ/cm² and had fiber diameters of 825±116 nm, compared to R5, which exhibited a lower mucoadhesion of 0.054±0.016 mJ/cm² despite having the thickest fibers. These data clearly demonstrate that finer fiber diameters, regardless of polymer concentration, correlate with enhanced mucoadhesive performance. Tuğcu-Demiröz et al.[59] obtained higher mucoadhesion values at higher concentrations of metronidazole-loaded PVP nanofibers. Similarly, in our study, increasing PVA concentration resulted in higher mucoadhesion values: R1 (7.5%), 0.014±0.010 mJ/cm^2; R8 (15%), 0.123±0.016 mJ/cm^2. Lower values were obtained for R3 (7.5%) were obtained for R3 (7.5%) and R5 (15%): 0.194±0.060 mJ/cm^2 and 0.054±0.016 mJ/cm^2, respectively. This suggests that mucoadhesion values depend not only on concentration but also on fiber diameter, porosity, and other properties that may affect them. These findings suggest that optimizing polymer concentration, collector rotation speed, and solvent conductivity can synergistically enhance the work of mucoadhesion, which is critical for achieving long-term retention in vaginal drug delivery systems. Mucoadhesion results revealed that both polymer concentration and processing parameters affect nanofiber properties.

Thanks to their thin and flexible architecture, nanofiber-based systems facilitate easy insertion, exhibit rapid hydration upon contact with vaginal fluids, and conform effectively to the mucosal surface, thereby reducing friction and irritation while enhancing comfort and overall patient tolerability.

Study limitations

This study focused on optimizing blank PVA-based electrospun nanofibers without active pharmaceutical ingredients; therefore, drug-polymer interactions, drug-loading efficiency, and drug-release profiles were not evaluated. Moreover, the experimental scope was limited to mechanical and mucoadhesive characterization; several critical performance parameters relevant to vaginal application, such as *in vitro* drug release and permeation, stability under simulated vaginal conditions, cytotoxicity, and *in vivo* retention, were not investigated. The absence of permeability studies on *ex vivo* or cell-based vaginal models limits the estimation of mucosal transport, while the lack of cytotoxicity testing prevents an initial assessment of biocompatibility. Stability under simulated vaginal conditions was also not examined, although such data are critical for understanding the behavior of PVA-based systems in the presence of vaginal fluids and under variable pH conditions. In addition, the *in vitro* mucoadhesion results were not supported by *in vivo* retention studies, which would be necessary to confirm prolonged residence under physiological conditions. These evaluations were beyond the scope of the present work. Future studies will incorporate model drugs or clinically relevant active compounds, followed by comprehensive *in vitro* and *in vivo* evaluations to fully characterize the therapeutic performance, safety profile, and biological applicability of the optimized nanofiber formulation.

CONCLUSION

Electrospun nanofibers offer practical advantages for vaginal administration: their thin, flexible, and conformable structure facilitates comfortable insertion and intimate contact with the mucosal surface. Their solid, sheet-like architecture minimizes leakage and improves handling compared with semi-solid formulations, thereby enhancing patient acceptability and adherence. Moreover, the ability to control nanofiber dimensions, mechanical softness, and folding characteristics provides a clinically relevant platform that can be optimized for ease of use and reproducible administration.

This study developed and optimized PVA electrospun nanofiber formulations for vaginal drug delivery using DoE. Polymer concentration, solvent system, and collector rotation speed were identified as critical determinants of both the physicochemical properties of polymer solutions and the mechanical and mucoadhesive performance of the resulting nanofibers. The optimized formulation exhibited desirable tensile strength (>1 MPa), elongation at break (>50%), and mucoadhesive performance, along with uniform, defect-free fiber morphology. These findings underscore the potential of PVA-based electrospun nanofibers as an advanced platform for vaginal drug delivery, offering enhanced retention and improved patient compliance compared to conventional semi-solid and liquid dosage forms. Future work will focus on drug incorporation, release kinetics, and comprehensive *in vitro* and *in vivo* evaluations to assess their translational and clinical applicability.

Ethics

Ethics Committee Approval: Not required.

Informed Consent: Not required.

Footnotes

Authorship Contributions

Concept: S.S., F.T.-D., F.A., Design: S.S., F.T.-D., F.A., Data Collection or Processing: S.S., F.T.-D., F.A., Analysis or Interpretation: S.S., F.T.-D., F.A., Literature Search: S.S., F.T.-D., F.A., Writing: S.S., F.T.-D., F.A.

Conflict of Interest: The authors declare no conflicts of interest.

Financial Disclosure: This study was supported by Gazi University Scientific Research Projects Coordination Unit under grant number 02/2020-17.

REFERENCES

1. Bonferoni MC, Sandri G, Rossi S, Ferrari F, Gibin S, Caramella C. Chitosan citrate as multifunctional polymer for vaginal delivery: evaluation of penetration enhancement and peptidase inhibition properties. Eur J Pharm Sci. 2008;33:166-176.
2. El-Hammadi MM, Arias JL. Nanomedicine for vaginal drug delivery. In: Arias JL, editor. Theory Appl Nonparenteral Nanomed. Amsterdam: Elsevier; 2021. p. 235-257.
3. Tho I, Škalko-Basnet N. Cell-based *in vitro* models for vaginal permeability studies. In: Thelen M, editor. Concepts, Models, Drug Permeability Stud. Amsterdam: Elsevier; 2024. p. 169-186.

4. Layek B, Das S. Chitosan-based nanomaterials in drug delivery applications. In: Grumezescu AM, editor. Biopolymer-Based Nanomater Drug Deliv Biomed Appl. Amsterdam: Elsevier; 2021. p. 185-219.
5. Chore S, Dighade S. A review on mucoadhesive vaginal drug delivery system. J Drug Deliv Ther. 2020;10:181-188.
6. de Araujo Pereira RR, Bruschi ML. Vaginal mucoadhesive drug delivery systems. Drug Dev Ind Pharm. 2012;38:643-652.
7. Bilensoy E, Abdur Rouf M, Vural I, Šen M, Atilla Hincal A. Mucoadhesive, thermosensitive, prolonged-release vaginal gel for clotrimazole: -cyclodextrin complex. AAPS PharmSciTech. 2006;7:E54-E60.
8. Bilensoy E, Çırpanlı Y, Şen M, Doğan AL, Çalış S. Thermosensitive mucoadhesive gel formulation loaded with 5-FU: cyclodextrin complex for HPV-induced cervical cancer. J Incl Phenom Macrocycl Chem. 2007;57:363-370.
9. Yang Z, Wu X, Wang H, Zhou J, Lin X, Yang P. Vagina, a promising route for drug delivery. J Drug Deliv Sci Technol. 2024;83:105397.
10. Caramella CM, Rossi S, Ferrari F, Bonferoni MC, Sandri G. Mucoadhesive and thermogelling systems for vaginal drug delivery. Adv Drug Deliv Rev. 2015;92:39-52.
11. Palmeira-De-Oliveira R, Palmeira-De-Oliveira A, Martinez-De-Oliveira J. New strategies for local treatment of vaginal infections. Adv Drug Deliv Rev. 2015;92:105-122.
12. Leung V, Ko F. Biomedical applications of nanofibers. Polym Adv Technol. 2011;22:350-365.
13. Rüzgar Özemre G, Kara AA, Pezik E, Tort S, Vural İ, Acartürk F. Preparation of nanodelivery systems for oral administration of low molecular weight heparin. J Drug Deliv Sci Technol. 2023;79:104068.
14. Bhardwaj N, Kundu SC. Electrospinning: a fascinating fiber fabrication technique. Biotechnol Adv. 2010;28:325-347.
15. Esentürk İ, Balkan T, Özhan G, Döşler S, Güngör S, Erdal MS, Sarac AS. Voriconazole incorporated nanofiber formulations for topical application: preparation, characterization and antifungal activity studies against *Candida* species. Pharm Dev Technol. 2020;25:440-453.
16. Baloglu E, Bernkop-Schnürch A, Karavana SY, Senyigit ZA. Strategies to prolong the intravaginal residence time of drug delivery systems. J Pharm Pharm Sci. 2009;12:312-336.
17. Kuang G, Lin X, Li J, Sun W, Zhang Q, Zhao Y. Electrospun nanofibers-derived functional scaffolds for cancer therapy. Chem Eng J. 2024;489:151253.
18. Kalantari K, Afifi AM, Jahangirian H, Webster TJ. Biomedical applications of chitosan electrospun nanofibers as a green polymer: review. Carbohydr Polym. 2019;207:588-600.
19. Haider A, Haider S, Kang IK. A comprehensive review summarizing the effect of electrospinning parameters and potential applications of nanofibers in biomedical and biotechnology. Arab J Chem. 2018;11:1165-1188.
20. Vellayappan M, Venugopal J, Ramakrishna S, Ray S, Ismail AF, Mandal M. Electrospinning applications from diagnosis to treatment of diabetes. RSC Adv. 2016;6:83638-83655.
21. Braga PC, Dal Sasso M, Spallino A, Sturla C, Culici M. Vaginal gel adsorption and retention by human vaginal cells: visual analysis by means of inorganic and organic markers. Int J Pharm. 2009;373:10-15.
22. Park JC, Ito T, Kim KO, Kim KW, Kim BS, Khil MS. Electrospun poly(vinyl alcohol) nanofibers: effects of degree of hydrolysis and enhanced water stability. Polym J. 2010;42:273-276.
23. Kusumawati D, Istiqomah K, Husnia I, Fathurin N. Synthesis of nanofiber polyvinyl alcohol (PVA) with electrospinning method. J Phys Conf Ser. 2021;1918:012042.
24. Teixeira MA, Amorim MTP, Felgueiras HP. Poly(vinyl alcohol)-based nanofibrous electrospun scaffolds for tissue engineering applications. Polymers (Basel). 2019;12:7.
25. García-Moreno PJ, Stephansen K, van der Kruijs J, Guadix A, Guadix EM, Chronakis IS, Jacobsen C. Encapsulation of fish oil in nanofibers by emulsion electrospinning: physical characterization and oxidative stability. J Food Eng. 2016;183:39-49.
26. Camerlo A, Vebert-Nardin C, Rossi RM, Popa AM. Fragrance encapsulation in polymeric matrices by emulsion electrospinning. Eur Polym J. 2013;49:3806-3813.
27. Duan H, Chen H, Qi C, Lv F, Wang J, Liu Y, Zhang Y, Liu Z. A novel electrospun nanofiber system with PEGylated paclitaxel nanocrystals enhancing the transmucus permeability and *in situ* retention for an efficient cervicovaginal cancer therapy. Int J Pharm. 2024;650:123660.
28. Yan E, Jiang J, Yang X, Fan L, Wang Y, An Q, Li Z. pH-sensitive core-shell electrospun nanofibers based on polyvinyl alcohol/polycaprolactone as a potential drug delivery system for chemotherapy against cervical cancer. J Drug Deliv Sci Technol. 2020;55:101455.
29. Chindamo G, Sapino S, Peira E, Chirio D, Gallarate M. Recent advances in nanosystems and strategies for vaginal delivery of antimicrobials. Nanomaterials (Basel). 2021;11:311.
30. Sharma R, Garg T, Goyal AK, Rath G. Development, optimization and evaluation of polymeric electrospun nanofiber: a tool for local delivery of fluconazole for management of vaginal candidiasis. Artif Cells Nanomed Biotechnol. 2016;44:524-531.
31. Liu Y, Hao M, Chen Z, Liu L, Liu Y, Yang W, Ramakrishna S. A review on recent advances in application of electrospun nanofiber materials as biosensors. Curr Opin Biomed Eng. 2020;13:174-189.
32. Ghorbani-Choghamarani A, Taherinia Z. Eco-friendly synthesis of 3-aminoimidazo[1,2-a]pyridines via a one-pot three-component reaction in PEG catalyzed by peptide nanofibers as hydrogen-bonding organocatalyst. J Iran Chem Soc. 2020;17:59-65.
33. Yilmaz OE, Erdem R. Evaluating hydrogen detection performance of an electrospun $CuZnFe_2O_4$ nanofiber sensor. Int J Hydrogen Energy. 2020;45:26402-26412.
34. Türkoğlu GC, Khomarloo N, Mohsenzadeh E, Gospodinova DN, Neznakomova M, Salaün F. PVA-based electrospun materials: a promising route to designing nanofiber mats with desired morphological shape. Int J Mol Sci. 2024;25:1668.
35. Nazari K, Mehta P, Arshad MS, Ahmed S, Andriotis EG, Singh N, Forbes B, Scurr DJ, Topham PD, Conway BR. Quality by design micro-engineering optimisation of NSAID-loaded electrospun fibrous patches. Pharmaceutics. 2019;12:2.
36. Birer M, Acartürk F. Telmisartan loaded polycaprolactone/gelatin-based electrospun vascular scaffolds. Int J Polym Mater Polym Biomater. 2022;71:858-873.
37. Okutan N, Terzi P, Altay F. Affecting parameters on electrospinning process and characterization of electrospun gelatin nanofibers. Food Hydrocoll. 2014;39:19-26.
38. Gajewski A. A couple of new ways of surface tension determination. Int J Heat Mass Transf. 2017;115:909-917.

39. Turanlı Y, Tort S, Acartürk F. Development and characterization of methylprednisolone-loaded delayed release nanofibers. J Drug Deliv Sci Technol. 2019;49:58-65.

40. Tyo KM, Vuong HR, Malik DA, Sims LB, Alatassi H, Duan J, Holt J, Teller RS, Neupane K, Shankarappa SA, Clark MR. Multipurpose tenofovir disoproxil fumarate electrospun fibers for the prevention of HIV-1 and HSV-2 infections in vitro. Int J Pharm. 2017;531:118-133.

41. Saar S, Demiröz FNT. Evaluation of mechanical and mucoadhesive properties of polyvinyl alcohol nanofibers as vaginal drug delivery system. FABAD J Pharm Sci. 2023;48:219-230.

42. Tort S, Acartürk F, Beşikci A. Evaluation of three-layered doxycycline-collagen loaded nanofiber wound dressing. Int J Pharm. 2017;529:642-653.

43. Tuğcu-Demiröz F, Acartürk F, Erdoğan D. Development of long-acting bioadhesive vaginal gels of oxybutynin: formulation, *in vitro* and *in vivo* evaluations. Int J Pharm. 2013;457:25-39.

44. Tort S, Acartürk F. Preparation and characterization of electrospun nanofibers containing glutamine. Carbohydr Polym. 2016;152:802-814.

45. Abdul Hameed MM, Mohamed Khan SAP, Thamer BM, Al-Enizi A, Aldalbahi A, El-Hamshary H, El-Newehy MH. Core-shell nanofibers from poly(vinyl alcohol)-based biopolymers using emulsion electrospinning as drug delivery system for cephalexin drug. J Macromol Sci A. 2021;58:130-144.

46. Ahmadi Bonakdar M, Rodrigue D. Electrospinning: processes, structures, and materials. Macromol. 2024;4:58-103.

47. Khattab IS, Bandarkar F, Fakhree MAA, Jouyban A. Density, viscosity, and surface tension of water-ethanol mixtures from 293 to 323 K. Korean J Chem Eng. 2012;29:812-817.

48. Ergin SP. The effect of temperature on association constants and conductivities of ferrous chloride and ferric chloride in DMF-water mixtures. Eur J Chem. 2012;3:399-403.

49. Spivey HO, Shedlovsky T. Studies of electrolytic conductance in alcohol-water mixtures. I. Hydrochloric acid, sodium chloride, and sodium acetate at 0, 25, and 35 degrees in ethanol-water mixtures. J Phys Chem. 1967;71:2165-2171.

50. Ge JC, Wu G, Yoon SK, Kim MS, Choi NJ. Study on the preparation and lipophilic properties of polyvinyl alcohol (PVA) nanofiber membranes via green electrospinning. Nanomaterials (Basel). 2021;11:2514.

51. Širc J, Hobzová R, Kostina N, Munzarová M, Juklíčková M, Lhotka M, Dvořáková J, Hampl A. Morphological characterization of nanofibers: methods and application in practice. J Nanomater. 2012;2012:1-14.

52. Zhang C, Yuan X, Wu L, Han Y, Sheng J. Study on morphology of electrospun poly(vinyl alcohol) mats. Eur Polym J. 2005;41:423-432.

53. Angammana CJ, Jayaram SH. Analysis of the effects of solution conductivity on electrospinning process and fiber morphology. IEEE Trans Ind Appl. 2011;47:1109-1117.

54. De Vrieze S, Van Camp T, Nelvig A, Hagström B, Westbroek P, De Clerck K. The effect of temperature and humidity on electrospinning. J Mater Sci. 2009;44:1357-1362.

55. Sanchaniya JV, Lasenko I, Kanukuntala SP, Smogor H, Viluma-Gudmona A, Krasnikovs A, Sanchaniya A. Mechanical and thermal characterization of annealed oriented PAN nanofibers. Polymers (Basel). 2023;15:3287.

56. Wong SC, Baji A, Leng S. Effect of fiber diameter on tensile properties of electrospun poly(ε-caprolactone). Polymer. 2008;49:4713-4722.

57. Habeeb S, Rajabi L, Dabirian F. Comparing two electrospinning methods in producing polyacrylonitrile nanofibrous tubular structures with enhanced properties. Iran J Chem Chem Eng. 2019;38:23-42.

58. Mortazavi SA, Smart JD. An investigation into the role of water movement and mucus gel dehydration in mucoadhesion. J Control Release. 1993;25:197-203.

59. Tuğcu-Demiröz F, Saar S, Tort S, Acartürk F. Electrospun metronidazole-loaded nanofibers for vaginal drug delivery. Drug Dev Ind Pharm. 2020;46:1015-1025.

Turk J Pharm Sci 2025;22(6):393-399
DOI: 10.4274/tjps.galenos.2025.51282

ORIGINAL ARTICLE

Perspectives and Experiences of Community Pharmacists on Vaccine and Cold Chain: A Qualitative Study

Hilal İLBARS[1]*, Berna TERZİOĞLU BEBİTOĞLU[2], Seyhan HIDIROĞLU[3], Fatma Burcu DOĞANÇ[3], Yeliz TUĞLU[4], Deniz Kerem ÇUHADAROĞLU[4], Hatice SARI[4]

[1]Başkent University Faculty of Pharmacy, Ankara, Türkiye
[2]Marmara University Faculty of Medicine, Department of Medical Pharmacology, İstanbul, Türkiye
[3]Marmara University School of Medicine, Department of Public Health, İstanbul, Türkiye
[4]Marmara University School of Medicine, Internship Medical Student Study Group, İstanbul, Türkiye

ABSTRACT

Objectives: Vaccination is a cornerstone of public health, and maintaining the vaccine cold chain within a temperature range of 2–8 °C is essential to preserve vaccine efficacy and prevent wastage. Community pharmacists are highly accessible healthcare professionals who play a crucial role in vaccine supply, storage, and public education. The aim of this study was to qualitatively assess vaccination and cold-chain practices in community pharmacies within Türkiye's primary healthcare system.

Materials and Methods: A qualitative study was conducted with 15 community pharmacists in Ankara, Türkiye, using semi-structured face-to-face interviews carried out between September 15 and 30, 2024. Participants were recruited through snowball sampling until thematic saturation was achieved. All interviews were audio-recorded, transcribed verbatim, and analyzed using Braun and Clarke's seven-phase thematic analysis. Data management was performed using ATLAS.ti version 24.0, and reporting adhered to the COREQ checklist.

Results: Three main themes emerged: vaccination practices, vaccine logistics and cold-chain management, and vaccine hesitancy. Pharmacists reported frequent patient inquiries, particularly regarding influenza, human papillomavirus, and childhood vaccines. Participants demonstrated a high level of awareness of cold-chain protocols, including the use of dedicated refrigerators and continuous temperature monitoring systems. Vaccine hesitancy, especially toward Coronavirus Disease 2019 vaccines, was primarily attributed to misinformation, with pharmacists emphasizing the importance of evidence-based and empathetic communication.

Conclusion: Community pharmacists possess substantial technical knowledge in vaccine logistics and play a critical role in patient counseling. Strengthening regulatory frameworks, professional training, and communication skills may further enhance pharmacists' contributions to immunization efforts and vaccine confidence.

Keywords: Vaccine, cold chain, hesitancy, pharmacy, pharmacist role

INTRODUCTION

Vaccination is a key public health intervention that prevents the spread of infectious diseases. Although global immunization efforts have led to major successes, such as the eradication of smallpox, maintaining vaccine efficacy continues to pose challenges. In developing countries, issues such as unreliable electricity and limited refrigeration disrupt the vaccine cold chain. Surprisingly, similar problems have been observed in developed settings, where improper storage remains a concern.[1] The cold chain, which maintains vaccines at 2-8 °C, is essential

***Correspondence:** hilalilbars@gmail.com, **ORCID-ID:** orcid.org/0000-0002-7832-4158
Received: 30.08.2025, **Accepted:** 13.01.2026 **Publication Date:** 30.012026

Cite this article as: İLBARS H, TERZİOĞLU BEBİTOĞLU B, HIDIROĞLU S, DOĞANÇ FB, TUĞLU Y, ÇUHADAROĞLU DK, SARI H. Perspectives and experiences of community pharmacists on vaccine and cold chain: A qualitative study. Turk J Pharm Sci. 2025;22(6):393-399

to preserving potency and preventing waste.[2] Failures in the cold chain are a major cause of vaccine wastage.[3,4]

Pharmacists serve as accessible healthcare professionals who play a central role in public education. In Türkiye, pharmacies are among the first points of contact for patients seeking vaccine information.[5] However, they are not legally permitted to administer vaccines. Despite this, pharmacists contribute significantly to vaccine access and public awareness. This study aims to qualitatively assess vaccination practices and cold chain management in community pharmacies in Ankara, while exploring pharmacists' perspectives on vaccine hesitancy and professional responsibilities.

MATERIALS AND METHODS

This qualitative study was conducted among 15 community pharmacists in Ankara, Türkiye, using a snowball sampling method. The first participant was recruited through one of the researchers, who is also a pharmacist. The remaining participants were reached using snowball sampling. Data saturation was considered achieved by the 13th interview; two additional interviews were conducted to confirm it.

Face-to-face semi-structured interviews were held between September 15 and 30, 2024. Semi-structured interviews with the participants were conducted in the pharmacists' offices during their available hours, specifically at times when there were patients or clients or when their numbers were minimal. The semi-structured interview guide was developed by the researchers based on a review of the current literature. The questions were asked in a general-to-specific order, allowing flexibility according to the participants' responses. The semi-structured interviews were conducted by two researchers. During the interviews, one researcher posed questions while the other took notes. The semi-structured interview guide included questions designed to explore pharmacists' experiences and perspectives on vaccination practices, the logistical aspects of vaccine delivery and cold-chain management in pharmacies, and their approaches to addressing vaccine hesitancy among patients. Prior to the interviews, the participants were informed about the purpose of the study, and permission was obtained to record the sessions. All participants provided consent for audio recording. The audio files were stored on a password-protected digital storage device accessible only to the researchers. Each session lasted 10-15 minutes.

For this study, ethics approval was obtained from the Marmara University Faculty of Medicine Clinical Research Ethics Committee (approval number: 09.2024.286, dated: 09.02.2024), and informed consent was obtained from all participants.

Statistical analysis

The data were analyzed using the seven-phase thematic analysis approach developed by Braun and Clarke:[6] (1) familiarization with the data, (2) generating initial codes, (3) searching for themes, (4) reviewing themes, (5) defining and naming themes, (6) writing the thematic map or story, (7) producing the report. After the interviews were transcribed in digital format, thematic content analysis was performed by the researchers to generate initial codes. Following the coding process, a meeting was held to develop a set of common codes, which were then used by the researchers to construct subthemes and overarching themes. The analysis was carried out using ATLAS.ti 24.0 (Scientific Software Development GmbH), which is appropriate for analyzing qualitative research data. Codes and themes were derived inductively, and participant quotes were used to illustrate key points. The article has been written in accordance with the COREQ checklist.[7]

RESULTS

Fifteen pharmacists participated in the study; their ages ranged from 23 to 60 years (mean, 38.1 years). Their sociodemographic characteristics are presented in Table 1. Most participants were female and had more than 15 years of experience.

Key themes were (1) vaccination practices, (2) cold-chain management, and (3) vaccine hesitancy.

The main themes and subthemes are presented in Table 2.

Table 3 summarizes pharmacists' observations regarding vaccine-related inquiries, patient trust, and opinions on providing vaccination services in community pharmacies.

Pharmacists reported frequent patient inquiries regarding vaccine types, schedules, side effects, and payment. Influenza vaccines were most commonly requested, particularly during peak seasons. Pharmacies also stocked vaccines against human papillomavirus (HPV), rotavirus, meningitis, hepatitis, and tetanus.

Highlights of pharmacists' logistical handling of vaccines, including cold-chain adherence from supply to storage and common stock in pharmacies, are presented in Table 4.

With respect to logistics, participants demonstrated a high level of awareness of cold-chain protocols and actively maintained appropriate temperature controls. They expressed confidence in their ability to manage vaccines safely, although they acknowledged room for improvement in infrastructure.

Regarding vaccine hesitancy, pharmacists noted particular concerns about Coronavirus Disease 2019 (COVID-19) vaccines. While many patients trusted pharmacists' advice, hesitancy persisted due to misinformation. Pharmacists emphasized the importance of clear, evidence-based communication in addressing public doubts.

Table 5 details pharmacists' observations on public attitudes toward vaccination and outlines the communication strategies employed to address vaccine hesitancy.

DISCUSSION

The study illustrates the pivotal role pharmacists play in vaccine accessibility and public education. The seasonal availability of the influenza vaccine is crucial for protecting public health, and increasing access to these vaccines through pharmacies can improve vaccination coverage.[8] Despite legal barriers, pharmacists in Türkiye serve as reliable sources of information and of vaccine supply. Their involvement, especially with influenza and HPV vaccines, supports greater public trust and immunization coverage.[9]

Table 1. Sociodemographic characteristics of pharmacists

Pharmacist number	Gender	Age	Years of experience	Owns pharmacy	Pharmacy location
1	Female	50	28	Yes	Near the hospital
2	Male	23	<1	No	Across FHC
3	Female	40	15	Yes	District pharmacy
4	Male	33	8	Yes	District pharmacy
5	Female	34	5	Yes	Across the FHC
6	Male	23	<1	No	Across the FHC
7	Female	60	38	Yes	Close to FHC
8	Female	54	28	Yes	District pharmacy
9	Male	46	16	Yes	Near the FHC
10	Female	54	30	Yes	Across the FHC
11	Female	24	1	No	Near the hospital
12	Female	24	<1	No	Near the hospital
13	Male	40	17	Yes	Across the training and research hospital
14	Male	32	4	Yes	Across the hospital emergency
15	Male	35	15	Yes	In the vicinity of hospital

FHC: Family Health Center

Table 2. Main themes and subthemes

Main theme	Subtheme
1. Vaccination Processes and Practices	1.1. Patient Education 1.2. Trust of Patients in Pharmacists 1.3. Vaccination Services in Pharmacies
2. Vaccine Logistics and Cold Chain Management	2.1. Current Vaccines in Pharmacies 2.2. Pharmacists' Cold Chain Practices 2.3. Monitoring the Cold Chain in Pharmacies
3. Vaccine Hesitancy and Pharmacists' Approaches	3.1. Vaccine Hesitancy 3.2. Pharmacists' Approaches Against Vaccine Hesitancy

Table 3. Overview of vaccination practices in pharmacies

Subtheme	Key findings	Illustrative quotes
Patient education	Patients frequently inquire about vaccine types, administration, dosage, side effects, and cost. Flu, HPV, meningitis, and rotavirus vaccines are the most frequently mentioned.	"They ask questions like: is this the children's dose, the adult dose, or I have a certain disease, will the state cover it? Or if I get this, will it harm me or benefit me?...I'm going to the hospital, but can I get the vaccine here?" (Pharm 3, female, 40 years)
Trust in pharmacists	While many patients trust pharmacists, some express skepticism, particularly regarding product recommendations, such as vitamins.	"When we say it's necessary, they trust us and get vaccinated." (Pharm 5, female, 34 years) "In our profession, there has been growing distrust of our recommendations, even for vitamins." (Pharm 8, female, 54)
Vaccination services in pharmacies	Most pharmacists oppose in-pharmacy vaccinations due to legal and safety concerns (e.g., anaphylaxis), lack of medical staff, and insufficient training. Some administer subcutaneous vaccines, such as the influenza vaccine.	"We do not receive training in this. Professionals are available for this purpose." (Pharm 6, male, 23)

HPV: Human papillomavirus

Table 4. Cold chain management and vaccine availability

Subtheme	Key findings	Illustrative quotes
Available vaccines	Pharmacies commonly stock vaccines for influenza, tetanus, hepatitis, meningitis, HPV, and rotavirus. Influenza vaccines are produced seasonally, whereas other vaccines are stocked according to demand.	"We have flu vaccines available because it's the influenza season. Tetanus vaccines are widely available. Hepatitis B vaccines are regularly available." (Pharm 2, male, 23)
Cold chain practices	Vaccines are ordered from suppliers and stored immediately in dedicated refrigerators with ice packs. Cold chain protocols are carefully followed.	"Vaccines are transported in portable refrigerators. We place them on ice packs and store them immediately." (Pharm 5, female, 34)
Cold chain monitoring	Pharmacies employ automated temperature- and humidity-monitoring devices that send alerts via SMS or e-mail when readings fall outside predefined ranges. Cold-chain refrigerators are used exclusively for medical products.	"We have a 24/7 monitoring device. If the temperature exceeds the desired level, we receive a message." (Pharm 7, female, 60)

HPV: Human papillomavirus

Table 5. Pharmacists' perspectives on vaccine hesitancy

Subtheme	Key findings	Illustrative quotes
Vaccine hesitancy	Hesitancy has increased in the post-COVID period, driven by misinformation and concerns about adverse effects. Some pharmacists report no hesitancy.	"Most patients became more toward vaccines after receiving the COVID vaccine." (Pharm 6, male, 23) "I've encountered many individuals who wish to be vaccinated." (Pharm 12, female, 24)
Pharmacists' approach	Pharmacists attempt to mitigate hesitancy by providing education and emphasizing vaccine necessity, especially for high-risk groups.	"We explain what a vaccine is and why it's necessary. It is part of our professional responsibility." (Pharm 8, female, 54)

COVID: Coronavirus Disease

The literature emphasizes that vaccination training for pharmacists is critical to the safety and effectiveness of vaccination services.[10] Mandatory training in emergency management, such as allergic reactions and anaphylaxis, is essential, especially since pharmacists may have limited capacity to intervene in these situations. Additionally, raising pharmacists' awareness of patient safety is crucial, as this will enhance both patient satisfaction and the effectiveness of the vaccine.[11]

A study that explored community pharmacy service users' attitudes and opinions towards vaccination programs in pharmacies, found that more than half of respondents believe that providing vaccination services in pharmacies could increase vaccination rates for seasonal illnesses, but only if these services are free or covered by national health insurance.[12]

Community pharmacists in Saudi Arabia generally hold positive attitudes toward vaccination services; however, reported barriers include a lack of support staff, adequate equipment, and certification. In their study, they also mentioned that the service will add extra workload and that there is a lack of formal certification in pharmacy-based immunization delivery. Pharmacists' clinical knowledge of vaccines should be improved.[13]

Pharmacists also reported barriers to vaccine service provision, including regulation, training, remuneration, and storage, which may consequently limit service expansion.[14]

Our findings align with global research showing increased vaccination rates where pharmacists are authorized to administer vaccines, such as in Canada and the U.S.[15] However, Turkish law limits pharmacy involvement to distribution and counseling. Current legal regulations in Türkiye restrict pharmacies from offering vaccination services. Therefore, it is essential to revise the legal framework and improve the education levels of pharmacists.[16] Regulatory change, paired with professional training, could enable pharmacists to administer vaccines safely and effectively. It is crucial to distinguish between the pharmacists' clinical aspirations and the current regulatory framework in Türkiye. Although this study explores the potential for expanded immunization services, vaccine administration by pharmacists is currently not legally permitted under existing health regulations. Consequently, the "vaccination practices" identified in our findings do not imply the physical act of injection, but rather encompass the pharmacists' rigorous oversight of cold chain integrity, inventory management, and evidence-based patient counseling. Operating beyond these defined legal boundaries

poses significant professional and legal risks, including potential malpractice liability and disciplinary actions by regulatory bodies. However, the high level of competence demonstrated by participants in cold-chain logistics suggests that the profession is technically prepared to assume broader responsibilities. As demonstrated by various global examples in which pharmacist-led vaccination has successfully increased immunization rates, a comparable transition in the local context would require a robust legal realignment and specialized clinical certification to mitigate professional risks and ensure patient safety. Thus, while our participants advocate for a larger role, these insights should be viewed as a professional perspective on the evolution of pharmacy practice rather than an endorsement of unauthorized clinical activities.

Furthermore, pharmacists should be provided with detailed information about post-vaccination side effects, allergy risks, and vaccination schedules. Participants in our study raised questions about vaccine dosages, available vaccines, and payment methods. This increases the importance of the pharmacists' role in patient education. Pharmacists should take a more active role in raising public awareness of and providing information about vaccination services.

The COVID-19 pandemic has contributed to an increase in concerns about vaccine hesitancy. In our study, participants expressed hesitancy and concerns about COVID-19 vaccines because of their rapid introduction to the market. International literature indicates that vaccine hesitancy increased during the COVID-19 pandemic and had negative effects on public health.[17] To address vaccine hesitancy, pharmacists must engage in accurate communication and persuasive dialogue with patients.[18]

The active role of pharmacists in informing patients about the benefits of vaccines is crucial to increasing herd immunity. The growing demand for childhood and HPV vaccines underscores the need for pharmacists to provide more information about these vaccines. Vaccine hesitancy is often caused by insufficient information, and pharmacists' efforts to educate the public can help reduce vaccine hesitancy.[19]

Vaccine hesitancy, intensified during the COVID-19 pandemic, remains a challenge. Pharmacists report difficulties in countering misinformation. This highlights the need for communication skills training focused on persuasive, empathetic dialogue.

In a meta-analysis, the overall prevalence of adequate knowledge of vaccine cold chain management among health professionals was found to be significantly below the expected standard in Ethiopia.[20] They reported that years of experience, availability of guidelines at the health facility, being a nurse, and receiving on-the-job training in cold chain management were important predictors of health professionals' good knowledge of vaccine cold chain management. Given that family physicians, nurses, and pharmacists play a crucial role in delivering preventive health services, their professional attitudes and beliefs about vaccination can exert significant influence on the community. Cold chain practices performed carefully in pharmacies ensure that vaccines are stored within the correct temperature ranges. The use of temperature monitoring systems during vaccine transportation and storage is vital for maintaining vaccine effectiveness.[21] Proper management of these processes is critical to the safety of both pharmacists and patients. Devices such as ice packs and temperature monitoring systems used during transportation and storage contribute to the safe storage of vaccines and help maintain their efficacy.[22]

Cold chain management was well understood among participants. Most used appropriate monitoring tools and storage practices. These practices are essential to prevent spoilage and ensure vaccine efficacy. However, global studies suggest that cold chain knowledge varies by profession and region, reinforcing the need for continuous training.[20]

It was reported that vaccination administered by pharmacists would relieve the burden on medical staff and the healthcare system.[23] Multiple systematic reviews and meta-analyses show that pharmacist involvement (as immunizers or advocates) significantly increases vaccination rates (risk ratios approximately 1.1-1.6), resulting in fewer infections, hospitalizations, and downstream healthcare utilization.[24,25]

Improving pharmacists' roles in vaccination requires integrated policies, certification programs, and emergency response readiness. Community pharmacies, if supported by adequate resources and appropriate regulation, can significantly enhance vaccination coverage and reduce the burden on healthcare systems.

Study limitations

The findings of this study should be interpreted within the context of several limitations. First, the use of snowball sampling may have introduced selection bias, as participants might have referred colleagues with similar professional backgrounds or viewpoints, potentially limiting the diversity of perspectives. Consequently, the results may not fully represent the entire spectrum of community pharmacists' attitudes. Second, the localized setting and relatively small sample size (n=15) restrict the generalizability of the findings to a national or international level. While the sample size was determined based on reaching thematic saturation, further quantitative research with a larger and more geographically diverse population is required to validate these results and explore regional differences. Third, the data relied on self-reports, which are susceptible to social desirability bias or recall inaccuracies. Although the interviews were conducted in a focused, semi-structured format, their duration (10-15 minutes) may have limited the depth of exploration into complex socio-legal issues compared to longer ethnographic studies. Finally, pharmacist-led vaccination is currently not legally permitted in the study's jurisdiction. Therefore, the participants' responses regarding "practices" primarily reflect their roles in cold-chain management, supply management, and patient counseling rather than clinical administration. The suggestions for legislative changes provided in this study are intended as preliminary insights to inform future policy discussions rather than definitive calls for regulatory reform.

CONCLUSION

Pharmacists are highly accessible and trusted healthcare professionals who hold significant potential to enhance public vaccine access and awareness. Currently, Turkish regulations define their role primarily through supply chain management and patient counseling. This study highlights that, while pharmacists are well-equipped with technical knowledge, particularly in cold chain management and temperature logistics, there is a clear opportunity to further integrate them into the national immunization framework.

Our findings suggest that the community pharmacist's role in combating vaccine hesitancy has become increasingly vital in the post-COVID-19 era. To fully leverage this potential, there is a need for structured support systems and continuous professional development programs focused on advanced communication strategies. Such support would enable pharmacists to more effectively address public concerns and provide evidence-based education.

Regarding the expansion of their clinical roles, the insights gained from this participant group suggest that future policy discussions could explore the feasibility of pharmacist-led immunization services. However, such a transition would necessitate comprehensive legal frameworks, standardized clinical training, and necessary emergency equipment to ensure patient safety and professional accountability.

While this study is limited by its sample size and qualitative nature, it serves as a preliminary rationale for further large-scale research. Empowering pharmacists, through legal, educational, and systemic advancements, could eventually help reduce the burden on the healthcare system, improve immunization coverage, and strengthen public health resilience.

Ethics

Ethics Committee Approval: For this study, ethics approval was obtained from the Marmara University Faculty of Medicine Clinical Research Ethics Committee (approval number: 09.2024.286, dated: 09.02.2024).

Informed Consent: Informed consent was obtained from all participants.

Footnotes

Authorship Contributions

Concept: H.İ., B.T.B., S.H., F.B.D., Design: H.İ., B.T.B., F.B.D., Data Collection or Processing: H.İ., F.B.D., Y.T., D.K.Ç., H.S., Analysis or Interpretation: H.İ., B.T.B., S.H., F.B.D., Literature Search: H.İ., B.T.B., S.H., F.B.D., Writing: H.İ., B.T.B., S.H., F.B.D.

Conflict of Interest: The authors declared no conflicts of interest.

Financial Disclosure: The authors declared that this study received no financial support.

REFERENCES

1. World Health Organization. Guideline for establishing or improving primary and intermediate vaccine stores [Internet]. Geneva: World Health Organization; 2002 [cited 2025 May 22]. Available from: https://iris.who.int/bitstream/handle/10665/67807/WHO_V-B_02.34_eng.pdf
2. Kumar HNH, Aggarwal A. Cold chain maintenance and vaccine administration practices in hospitals & clinics of Mangalore city - A health system's research. Natl J Community Med. 2013;4:231-235. Available from: https://njcmindia.com/index.php/file/article/view/1502
3. Thielmann A, Puth MT, Weltermann B. Visual inspection of vaccine storage conditions in general practices: a study of 75 vaccine refrigerators. PLoS One. 2019;14:1-13.
4. Yauba S, Kuaban C, Wiysonge CS. Temperature monitoring in the vaccine cold chain in Cameroon. J Vaccines Vaccin. 2018;9:1000384.
5. Bektay MY, Okuyan B, Sancar M, Izzettin FV. Insight into Turkish Community Pharmacists' Services in the First Wave of the COVID-19 Pandemic. Disaster Medicine and Public Health Preparedness. 2022;16(6):2211-2212. https://doi.org/10.1017/dmp.2021.185
6. Braun V, Clarke V. Reflecting on reflexive thematic analysis. Qual Res Sport Exerc Health. 2019;11:589-597.
7. Tong A, Sainsbury P, Craig J. Consolidated criteria for reporting qualitative research (COREQ): a 32-item checklist for interviews and focus groups. Int J Qual Health Care. 2007;19:349-357. https://doi.org/10.1093/intqhc/mzm042
8. Hogue MD, Grabenstein JD, Foster SL. Pharmacist involvement with immunizations: a decade of professional advancement. J Am Pharm Assoc. 2006;46:168-182.
9. Ozdemir N, Kara E, Bayraktar-Ekincioglu A. Knowledge, attitudes, and practices regarding vaccination among community pharmacists. Prim Health Care Res Dev. 2022;23:e38.
10. Papastergiou J, Folkins C, Li W, Zervas J. Community pharmacist-administered influenza immunization improves patient access to vaccination. Can Pharm J (Ott). 2014;147:359-365.
11. Bach AT, Goad JA. The role of community pharmacy-based vaccination in the USA: current practice and future directions. Integr Pharm Res Pract. 2015;4:67-77.
12. Rusic D, Nanasi D, Bozic J. Attitudes of community pharmacy service users towards vaccination programs in pharmacy: a cross-sectional survey-based study in Croatia. Pharmacy. 2022;10:167.
13. Alrasheedy AA, Alharbi AT, Alturaifi HA. Community pharmacists' knowledge, beliefs, and perceived barriers toward vaccination services at community pharmacies: a cross-sectional study from Saudi Arabia. Hum Vaccin Immunother. 2024;20:2314551.
14. Byrne H, Hew H, Mullally T. Vaccination services in community pharmacy practice: a scoping review. Int J Pharm Pract. 2024;32(Suppl 1): i35-i36.
15. Isenor JE, Bowles SK. Evidence for pharmacist vaccination. Can Pharm J (Ott). 2018;151:301-304.
16. Çalışkan Z. Applicability of immunization services in pharmacies in Turkey: evaluation through SWOT analysis. Eurasian J Health Technol Assess. 2021;5:99-123.
17. Sallam M. COVID-19 vaccine hesitancy worldwide: a concise systematic review of vaccine acceptance rates. Vaccines. 2021;9:160.
18. MacDonald NE. Vaccine hesitancy: definition, scope and determinants. Vaccine. 2015;33:4161-4164.
19. Longobardi G, Brunelli L, Piciocchi B. The role of pharmacists in counteracting vaccine hesitancy: effectiveness of the 2019 Carnia

Project in improving adherence to influenza vaccination among target population. Vaccines. 2024;12:331.

20. Kasahun AW, Zewdie A, Mose A. Health professionals' knowledge on vaccine cold chain management and associated factors in Ethiopia: systematic review and meta-analysis. PLoS One. 2023;18:e0293122.
21. Hickler B, Guirguis S, Obregon R. Vaccine Special Issue on vaccine hesitancy. Vaccine. 2015;33:4155-4156.
22. Dadari IK, Zgibor JC. How the use of vaccines outside the cold chain or in controlled temperature chain contributes to improving immunization coverage in low-and middle-income countries (LMICs): a scoping review of the literature. J Glob Health. 2021;11:04052.
23. Kowalczuk A, Wong A, Chung K. Patient perceptions on receiving vaccination services through community pharmacies. Int J Environ Res Public Health. 2022;19:2538.
24. Lan L, Veettil SK, Donaldson D. The impact of pharmacist involvement on immunization uptake and other outcomes: an updated systematic review and meta-analysis. J Am Pharm Assoc (2003). 2022;62:1499-1513.e16.
25. Rahim M, Dom SM, Hamzah MS. Impact of pharmacist interventions on immunisation uptake: a systematic review and meta-analysis. J Pharm Policy Pract. 2024;17:2293441.

2025 Referee Index